Optimisation of Energy Efficiency in Communication Networks

Tao Lin

Submitted in total fulfilment of the requirements of the degree of

Doctor of Philosophy

Department of Electrical and Electronic Engineering
THE UNIVERSITY OF MELBOURNE

August 2015

Produced on archival quality paper

Abstract

The mobile data traffic is experiencing unprecedented growth due to the rapid proliferation of devices such as smart phones and tablets. Improving the efficiency of mobile networks, both in terms of traffic flow and energy consumption, is thus critical for sustaining this growing demand. While the adoption of new technologies such as small cell networks and cognitive radio reduces deployment and operational costs, challenges remain regarding how the data traffic can be efficiently processed and transported over the mobile backhaul network. The first aim of this study is to improve the energy efficiency of mobile backhaul networks, while simultaneously balancing the traffic load on its various backhaul nodes, in order to maintain required service quality. First a multi-objective optimisation problem is formulated, then a distributed algorithm is proposed to solve it. The theoretical analysis and numerical simulations demonstrate the results. It is shown that the traffic diurnal cycle poses notable challenges for operators to plan, design and operate mobile backhaul networks so as to achieve desired energy-performance tradeoffs.

Continuing growth in cloud-based services and global IP traffic necessitates performance improvements in energy consumption, network delay and service availability. Data centres providing cloud services and transport networks have often multiple stakeholders, which makes it difficult to implement centralised traffic management. The second aim of this study is to apply a game-theoretic approach to data traffic management to obtain a distributed and energy-efficient solution, where each edge router is acting as a strategic player. A multi-objective optimisation problem with a-priori user-specific preferences is formulated for each player and a distributed iterative algorithm is proposed to solve the game. The existence of Nash Equilibrium (NE) of the proposed game

is proven followed by the theoretical convergence analysis of the iterative algorithm. The efficiency loss between the strategic game and corresponding global optimisation method is analysed to quantify the impact of selfish behaviour on the overall system performance. Simulation results show notable challenges for operators to plan, design and operate a multimedia content network in order to optimise energy consumption, network delay and load balance over a diurnal cycle.

The third aim of this study is to develop an optimisation framework for energy efficiency of optical core networks using Software Defined Networking (SDN). A general system model is proposed where switch-off/sleep mode is introduced to model the power consumption of individual network devices. A multi-objective optimisation problem is formulated by considering system power consumption, server load balance and transport network latency. To demonstrate the problem, a generic Software Defined Networking model is implemented in the Mininet platform by leveraging the OpenFlow protocol. A core network topology is studied in the Mininet framework with various parameter configurations. The simulation results show network topology, traffic diurnal cycle and user Quality of Service (QoS) requirements pose notable challenges for network plan, design and operation so as to achieve the desired energy-performance tradeoffs.

Declaration

This is to certify that

1. the thesis comprises only my original work towards the PhD,
2. due acknowledgement has been made in the text to all other material used,
3. the thesis is less than 100,000 words in length, exclusive of tables, maps, bibliographies and appendices.

Tao Lin, August 2015

Acknowledgements

This dissertation would not have been possible without the support and the guidance of several individuals who contributed and extended their valuable assistance in the preparation and completion of this work.

First and foremost I would like to thank my supervisors, Associate Professor Tansu Alpcan, Dr. Kerry Hinton and Professor Rod Tucker, for their constant support and guidance throughout my PhD candidature. Their ongoing motivation, assistance and patience make what could have been a very tough 4 years a great learning experience I will never forget. All of my supervisors supported me personally and mentally, which is really appreciated.

I would like to thank Dr. Arun Vishwanath for his assistance, technical expertise and for helping me revise publications.

To all my colleagues and friends at the Institute, Sascha, Fatemeh, Chrispin, Dinuka, Hamid and Olivia, and all other persons that I might not be able to mention individually, hearty thanks to you for your friendships and support over the period of my study.

I am deeply thankful to my wonderful children and my parents for their patience and unconditional support. Most importantly, I would like to acknowledge my beloved life partner, Dr. Hui Wu, for giving me an overwhelming sense of love and standing by my side at every stage of the journey. I honestly couldn't have done any of this without your support. I love all of you.

To Hui, Carina, Annabelle and Levin.

Contents

List of Figures

List of Tables

Chapter 1
Introduction

The exponential growth of Internet traffic continues with emerging and diversified applications such as Video-on-demand streaming, Peer-to-Peer data transferring and social networking. Global Internet Protocol (IP) traffic has quadrupled over the last 5 years and will exceed the zettabyte threshold in the short term future [1–3]. It is forecasted in [2] that IP traffic will increase at a compound annual growth rate (CAGR) of 21% over the next 5 years.

Mobile-connected devices will soon outnumber the population over the planet [4]. According to the estimate of [5], seven trillion wireless devices will be employed to serve seven billion people in the world by 2020. With fast growing connection speeds and high penetration of smart mobile devices, the resulting global mobile data traffic will surpass 15 exabytes per month by 2018. As stated in [2], global mobile data traffic will grow with a CAGR of 61% and will occupy 12% of total IP traffic by 2018. Compared to fixed IP traffic, global mobile data traffic is escalating more than 3 times faster from 2013 to 2018.

Global video traffic such as IPTV and video on demand (VoD) will contribute more than half of the total consumer Internet traffic [2]. End consumers are more likely than before to watch online video clips and multi-media content via mobile-connected devices. By 2018 mobile video traffic will take more than two-thirds of the world's mobile data traffic. It is estimated that 65% of all Internet video traffic will be delivered by content delivery networks (CDN) by 2018 [2].

Machine-to-machine communication (M2M) is an emerging technology that allows devices connected to the Internet to communicate with each other via wired or wireless networks [6]. Considered as an integral part of the Internet of Things (IoT), M2M is a

new paradigm that will play a important role in the near future with a wide range of applications such as industrial/home automation, logistics, Smart Grid, Smart Cities and e-health [7]. According to Gartner [8], the number of M2M devices will increase to 26 billions by 2020 and other reports show even higher estimates such as in [6]. Bandwidth-intensive M2M connections are becoming more prevalent with advanced access technologies such as 4G. It is estimated that global M2M traffic will grow at 43 percent CAGR from 2013 to 2018 [2]. This in turn leads to 2.8% of global IP traffic.

The dramatic growth of wired and wireless IP traffic results in the current communication networks suffering from extensive load congestion and severe service request rejection [9, 10]. In addition, the concern of energy consumption is now drawing both academic and industrial attention to the need for sustainable growth of the future wireless networks [11–13]. As mentioned in [14], the ICT sector alone accounts for 3% of global electricity consumption and 2% global carbon footprint. A large portion of ICT energy consumption and green house emission is related to mobile and wireless network as reported in [12].

1.1 Problem Definition

Energy consumption and carbon footprint of communication networks are expected to become the main "bottleneck" constraining the Internet expansion in reach and capacity. As stated in [15], the energy consumption of the Internet is now widely regarded as an important economic, environmental and social issue. Increasing transmission bit rate, processing speed and switching capacity of the underlying network elements could enhance the network capability to accommodate the increasing data traffic. But it will inevitably result in increased energy consumption of communication networks [16], which leads to unsustainable energy consumption requirements for network equipment. The study [17] demonstrates the effect of data traffic growth on the power and energy efficiency of communication networks. It is shown that historically, network energy efficiency only increases at $10 \sim 15\%$ per year [3]. However, global mobile and backbone data traffic is growing at a faster pace as confirmed by multiple reports [1, 3, 4, 18]. The gap will

be amplified further in the future with the business-as-usual scenario [17], which indicates that further energy-efficient technology advances are required to reduce the power consumption of communication networks and adapt to the future data traffic growth.

To address this pressing matter, a few ICT industrial institutes and organisations such as European Telecommunications Standards Institute (ETSI), Global e-Sustainability Initiative (GeSI) and GreenTouch™ were formed to collect metrics, raise awareness, implement standards and provide solutions to energy efficiency of communication networks. GreenTouch™ is a consortium founded in early 2010 aims to significantly reduce the energy consumption and the carbon footprint of global communication and data networks. Based on historical global Internet traffic volumes and near-term forecasts, the study [3] adopts a semi-empirical hyperbolic function to prepare the long-term Internet traffic projections, which indicate that Internet traffic will be doubling every two years. This means that global data traffic will increase by a factor of 1000 in 20 years. To sustain the future data traffic growth, GreenTouch™ provided a technology roadmap to improve the energy efficiency of communication networks by a factor of 1000 compared to that of 2010. In order to accomplish such ambitious goal, GreenTouch™ delivered the architecture, specifications and technologies for ICT devices, platforms and networks in June 2015.

Achieving such bold objective requires holistic approaches considering every aspect of communication networks and the applied technologies. GreenTouch™ mainly considered the following research challenges and focus areas:

- Mobile access networks
- Fixed-line access networks
- Metro/core networks

It is important to note that improving energy efficiency of communication networks is not simply reducing network power consumption. Many other network performance metrics such as server load balance, network bandwidth and traffic delay Quality of Service (QoS) are of concern for network operators and service providers. It is highly unlike that network operators will only focus on reducing energy consumption of communication networks and ignore other important network performance measures.

Current research on energy efficiency of mobile communication networks is mainly focused on radio access networks, which account for a large proportion of the total energy consumption [12, 19]. Little work is dedicated to improving energy efficiency of mobile backhaul networks. The massive deployment of small cells with macro cell capacity will generate much higher backhaul traffic than the current backhaul traffic [20]. How to distribute backhaul traffic in an energy efficient manner and maintain certain level of service availability for massive small cell deployment is still largely unclear in current literature. This research gap has motivated the study of improving energy efficiency of heterogeneous backhaul networks presented in this dissertation.

To date, network energy optimisation proposals require a centralised controller to operate the whole network by leveraging the global information about all end users in the network [21, 22]. They generally assume end users will follow directions from the centralised controller to achieve the global optimum in terms of system energy consumption. However, implementing a centralised controller is difficult for a large distributed network such as the Internet. Also this assumption ignores the fact that end users are rational and interested in maximising individual payoffs. The discrepancy between the individual optimal solution and the global optimal solution in terms of network energy consumption has not been studied in existing literature. One focus of this dissertation is to explain this gap.

In this dissertation, we focus on improving energy-efficiency of heterogeneous backhaul networks and optical core networks, while considering other network performance metrics such as server load balance, bandwidth assurance and traffic delay QoS. In addition, we highlight the impacts of cloud computing on mobile backhaul networks and optical core networks in terms of energy consumption and service availability. Solutions to network design and operation are proposed in the form of theoretical analysis and optimization algorithms. We also look to understand the emerging network architecture paradigm, i.e. software defined networking (SDN). Simulation results are presented and discussed to reveal the relation between network energy efficiency and other network performance metrics.

We consider three typical communication networks: mobile backhaul networks [Chap-

ter 4], cloud-based metro/core networks [Chapter 5] and SDN-based optical core networks [Chapter 6]. To address energy efficiency and other network performance such as load balance and delay QoS in a system manner, we apply the weighted multi-objective optimisation scheme specified in Section 1.2.1 to those networks. However, we adopt different methods to improve energy efficiency of those networks, while taking into account their performance.

For mobile backhaul networks, network operators are more interested in improving energy efficiency of backhaul networks than mobile service users. Mobile service users are unable to choose how their traffic to be routed and processed. It is rather network operator's responsibility to plan, design and operate backhaul networks in an energy efficient manner. However, for mobile network operators, centralised solutions such as mixed integer programming are becoming difficult to scale up for massive small cell deployment. Therefore, in Chapter 4, we propose a scalable distributed algorithm from network operators point of view to improve energy efficiency of backhaul networks, while considering Serving Gateway (S-GW) load balance.

In Chapter 5, we consider cloud-based metro/core networks where the underlying infrastructure is generally not owned by a single party. In contrast to mobile backhaul networks specified in Chapter 4, regional Internet service providers (ISPs) located in the edge of the metro/core networks are network users. It is their own interest to distribute the traffic over the cloud-based metro/core networks in an energy efficient manner, while maintaining a certain level of QoS. In addition, network users are sharing the underlying networking and cloud infrastructure. Each user has different traffic distribution strategy in terms of energy consumption and QoS. The optimisation frame proposed in Chapter 4 is not suitable to handle this situation. Considering the non-cooperative behaviour of network end users, we apply the non-cooperative theory specified in Section 1.2.2.2 to cloud-based metro/core networks in Chapter 5.

SDN is the main topic discussed in Chapter 6 for energy efficiency of optical core networks. Core network operators are the interesting parties concern about the energy consumption of the network. By leveraging the emerging networking technology, it is possible to have a logically centralised SDN controller managing the whole network.

With global knowledge of network states such as topology and traffic, core network operators can implement sophisticated network functions in the SDN controller only so as to improve network energy efficiency while consider other network performance requirements. To demonstrate the agility of the SDN structure, we implement a centralised optimisation algorithm in the SDN controller and emulate the system in Mininet specified in Section 1.2.3.3. In contrast to the non-cooperative game solution adopted in Chapter 5, the centralised optimisation algorithm used in Chapter 6 is able to provide the global optimal solution.

This dissertation addresses the following challenges and problems:

1. What is the impact of heterogeneous backhaul technologies on energy consumption of future mobile backhaul networks with small cell deployment? [Chapter 4]

2. What is the optimisation strategy to improve energy efficiency of mobile backhaul networks while maintaining a balanced traffic load over network elements? [Chapter 4]

3. How much energy can be saved in network systems by introducing switching-off operation modes to network elements? [Chapter 4]

4. How can diurnal characteristic of data traffic be used to reduce energy consumption of communication networks? [Chapter 5]

5. What is the efficiency loss in terms of energy consumption and load balance for the whole network system when end users interact in a non-cooperative environment? [Chapter 5]

6. What is the relationship between network energy consumption and other network performance requirements such as server load balance and network service QoS? [Chapter 5]

7. What is the impact of energy-proportional traffic processing on optimising energy consumption of communication networks? [Chapter 5]

8. How can software defined networking facilitate improving optical core network energy efficiency? [Chapter 6]

9. What are the challenges for operators in network design and operation to achieve multiple optimisation objectives including improving energy efficiency? [Chapter 6]

1.2 Methodologies and Approaches

1.2.1 A Brief Introduction of Optimisation

Multiple reports [1, 3, 4, 8] show that global IP traffic is escalating in an unprecedent way, which in turn demands more network capacity and bandwidth to support the traffic growth. However, communication network resources are not unlimited, neither radio spectrum nor optical lightpaths. Efficient network resource allocation and utilisation are vital for network operators to reduce capital expenditures (CAPEX) and operational expenditure (OPEX), while providing networking services to users with desired QoS. Thus, it is naturally expected that a number of problems arising in communication network plan, design and operation to fit in the framework optimisation.

There has been a long history of applying optimisation and control methods to solve various communication networks problems. The study [23] mainly focuses on communication network design in two different areas: multi-access communications and network routing, in which optimisation and control theory can facilitate formulating, studying and solving complex communication network problems. The authors also indicate that the field of communication networks offers a rich selection of applications such as flow control and traffic scheduling for optimisation theory.

Initially communication network optimisation focuses on solving problems such as resource allocation, system throughput, communication delay, traffic congestion, network reliability and service availability [24–29]. It is observed that the growth of network throughput and bandwidth is accompanied with fast increases of network traffic and the resultant energy consumption [1, 3]. The study [17] shows increasing gap between the improvement of network energy efficiency and the growth rate of global traffic. Developing optimisation frameworks to reduce energy consumption is thus critical to satisfy the growing demands for data traffic and network services.

In this dissertation, we aim to propose an optimisation framework of improving energy efficiency of communication networks. Other system performance optimisation requirements such as server load balancing and network delay QoS are also taken into account. Given the fact that network equipment has limited traffic processing capacity, we need to introduce network capacity constraints for the proposed optimisation problem, such that the aggregated traffic on each network element can not exceed the desired threshold such as the maximum traffic processing capacity. In addition, we want to enforce the input traffic flow conservation such that no traffic will be dropped if the network has enough capacity to accommodate all input traffic. To serve this purpose, we first introduce a general definition for an optimisation problem as below:

Definition 1.1. *A general optimisation problem can be expressed as the following form:*

$$\textit{minimise } f(\mathbf{d}) \tag{1.1}$$

$$\textit{subject to } g_n(\mathbf{d}) \leq b_n, \quad n = 1, \cdots, N \tag{1.2}$$

$$h_j(\mathbf{d}) = 0, \quad j = 1, \cdots, J \tag{1.3}$$

where

- $\mathbf{d} = [\mathbf{d}_1, \cdots, \mathbf{d}_R]^T$ *denotes a vector of optimisation variables.*
- $f : \mathbf{d} \longrightarrow \Re$ *denotes an objective function.*
- $g_n : \mathbf{d} \longrightarrow \Re$ *denotes a function for an inequality constraints.*
- $h_j : \mathbf{d} \longrightarrow 0$ *denotes a function for an equality constraints.*
- $b_1, \cdots, b_N$ *are constants for the corresponding constraint functions.*

Many network optimisation problems aim to find an optimal value or vector from a finite set of discrete values, which are often formulated as integer programming problems. Serving as one of the standard tools and methods specified in a vast literature, integer and mixed integer programming (MIP) nowadays is extensively applied to solve various kinds of communication network design and routing problems, such as shortest path routing [30], network planning [31] and power-aware traffic distribution [21]. The

study [30] applies integer programming optimisation to solve a shortest path routing problem, in which end-to-end routing paths comprise binary arc routing variables. In [31], the authors adopts mixed integer linear programming (MILP) models and methods to solve both the access and backbone network design problem, given various technical and administrational constraints such as hardware configurations, node locations and traffic demands. Driven by the objective of improving energy-efficiency, the study [21] develops a MILP mode to minimise the energy consumption of an IP over WDM network, and the simulation results show significant energy consumption reduction.

The mixed integer problem is a branch of the optimisation problem modeled in Definition 1.1. Specifically, some decision variables $\mathbf{d}_r$, $r \in \{1, \cdots, R\}$, defined in Definition 1.1 are constrained to be integer values such that $\mathbf{d}_r \in \mathbb{Z}$ with $\mathbb{Z}$ denoting the set of integers. For mixed integer linear programming problems, the constraint functions g_n and h_j in Eq. (1.3) are linear. As demonstrated in [32], the combinatory nature of mixed integer programming makes an optimisation problem non-convex, and therefore NP-hard to solve. Generally the branch-and-bound algorithm is applied to solve mixed integer problems. However this method is not well-suited for solving large systems and performs poorly on finding optimal solutions [33].

Convex optimisation, as another subfield of optimisation, is also widely used in the design and analysis of communication networks. In contrast to integer programming, convex optimisation aims to minimise convex objective function over convex sets [34]. It is generally agreed that solving convex problems is computationally easier than combinatory problems due to the convexity property that local minimum leads to global minimum [34]. The challenge of using convex optimisation methods is to identify and formulate the problem in a convex manner. Once the optimisation problem is formulated in a convex form, the structure of the solution is often identified by leveraging existing efficient algorithms. The tutorial [35] surveys basic concepts and main techniques in convex optimization in communication networks. Several studies [36–38] have utilised convex optimisation methods to improve energy-efficiency of various communication systems such as sensor networks and wireless networks.

The definition of a convex optimization problem is very much like the general for-

mation in Definition 1.1, where the object function f and constraint functions g_n, h_j, are convex. The original convex problem in the form of Definition 1.1 is also called the primal optimisation problem with f_0^* denoted the optimal value of the object function f. By augmenting the objective with a weighted sum of constraints, the primal optimisation problem can be transferred to a Lagrangian function [34].

$$\mathcal{L}(\mathbf{d}, \gamma, \boldsymbol{\lambda}) = f(\mathbf{d}) + \sum_{n=1}^{N} \gamma_n g_n(\mathbf{d}) + \sum_{j=1}^{J} \boldsymbol{\lambda}_j h_j(\mathbf{d}) \tag{1.4}$$

where $\gamma \in \Re^N$ and $\boldsymbol{\lambda} \in \Re^J$ denote the Lagrangian multipliers (dual variables) for constraints in Eq. (1.2) and (1.3) respectively. The study [39] indicates that convex optimization has highly useful Lagrange duality properties leading to decomposability structures, which can facilitate solving the primal problem. Define the dual fuction for Eq. (1.4) as

$$\mathcal{D}(\gamma, \boldsymbol{\lambda}) = \inf_{\mathbf{d} \in \Re^R} \mathcal{L}(\mathbf{d}, \gamma, \boldsymbol{\lambda}) \tag{1.5}$$

As demonstrated in [34], $f(\mathbf{d}) \geq \mathcal{L}(\mathbf{d}, \gamma, \boldsymbol{\lambda})$ for any primal feasible vector $\mathbf{d}$ and any dual feasible vector $(\gamma, \boldsymbol{\lambda})$. The largest lower bound for $f(\mathbf{d})$ can be found by solving the following dual optimization problem:

$$\text{maximise } \mathcal{D}(\gamma, \boldsymbol{\lambda}) \tag{1.6}$$

$$\text{subject to } \gamma \geq 0 \tag{1.7}$$

$$\boldsymbol{\lambda} \in \Re^J \tag{1.8}$$

Let u^* be the optimal value for $\mathcal{D}(\gamma, \boldsymbol{\lambda})$. As illustrated in [34], for a convex problem, the dualty gap $f_0^* - u^* = 0$ if the equality constraints in (1.3) are linear, the inequality constraints in (1.2) are affine with some contrstaints hold strict inequality, if the Slater's condition [34] holds. Then the solution to the primal problem in Eq. (1.1) is equivalent to the solution to the dual problem in Eq. (1.6).

The tutorial [39] shows the importance of the decomposability structures in network utility maximisation (NUM), which may lead to distributed algorithms that converge to the global optimum. For large-scale networks, distributed solutions are more appealing

in that a centralised solution is generally unreliable, non-scalable. The authors of [39] further demonstrate various decomposition methods for primal or dual network utility optimisation problems such that a large problem is decomposed into distributively solvable subproblems. With appropriate signalling mechanisms and local optimisation algorithms, the decomposed subproblems are able to collectively achieve the global optimum.

In fact, many studies prior to [39] had applied the distributed NUM method to solve complex networking problems. The seminal work [24] decomposes the rate control system problem for a large-scale broadband network into a network problem and local user problems. Each network user informs the network the committed total amount of payment, and the network decides the traffic allocation for each user. By iteratively solving the network problem and local user problems, the system can achieve the global optimum that maximises the sum of all users' utility. The study [40] also proposes a different distributed approach to optimise the network traffic control by solving the decomposed dual problem with a gradient algorithm [34, 41] finding the optimal link prices (Lagrangian multipliers) maximising the joint optimisation problem. In contrast to [24], this work assumes that network users decide their rate of charge for routing a data traffic unit and comply to the resultant payment and bandwidth allocation.

Communication network design and operation generally requires simultaneous optimisation of multiple, often conflicting objectives such as system throughput, service availability, network energy consumption, bandwidth and QoS. It is rare that network operators only focus on a single network performance metric. Many previous works such as [21, 27, 42] apply the single-objective optimisation mechanism to solve such problems by transforming all but one objective into constraints.

Multi-objective optimisation (MOO) is the framework that consolidates and relates seemingly different terminology and methods [43]. The aim of multi-objective optimisation is to find a vector of decision variables $\mathbf{d}$ (specified in Definition 1.1) which satisfies constraints and optimises a vector function whose elements represent individual objective functions. The definition of a multi-objective optimisation problem follows the general optimisation problem in Definition 1.1 with same constraints expression in Eq. (1.3)

and Eq. (1.2). In stead of have a single objective function f in Eq. (1.1), a multi-objective optimisation problem needs to optimise a set of objective functions expressed as,

$$\text{minimise } \mathbb{F}(\mathbf{d}) = [f_1(\mathbf{d}), \cdots, f_M(\mathbf{d})] \tag{1.9}$$

where $f_m(\mathbf{d})$ denotes the m-th objective function with $m = 1, \cdots, M$. In contrast to single objective optimisation, there is generally no single global solution to the multi-objective problem specified in Eq. (1.9). Instead of treating all objectives equally, the authors of [43] also propose another solution concept for multi-objective optimisation problems that applies customized weights to each individual objectives expressed as:

$$\text{minimise } \mathbb{F}_\omega(\mathbf{d}) = \sum_{m=1}^{M} \omega_m f_m(\mathbf{d}) \tag{1.10}$$

where weighting factor $\omega_m \in \Re$ represents a priori user-specific preference for objective function m.

In summary, increasing data traffic and heterogeneous technologies result in complex communication networks. Network planning, design and operation require solving a diversity of optimisation problems. These optimisation problems can vary substantially in terms of optimisation objectives, the underlying network infrastructure and the adopted networking technologies. In particular, optimising energy-efficiency of communication networks is becoming important to support the increasing demands for data traffic and network services. There is a growing needs for theoretical frameworks for optimising communication network performance in a holistic and energy efficient manner.

In this dissertation, we adopt the aforementioned convex optimisation, distributed network utility maximisation and multi-object optimisation described in Chapter 4 to solve a joint optimisation problem for system power consumption and server load balance in a distributed manner. In Chapter 5, we also apply convex optimisation and multi-object optimisation to optimise network performance in terms of energy consumption and data centre load balance. In Chapter 6, a mixed integer programming solver is implemented in a controller to solve a joint optimisation problem trading off network energy consumption and data centre load balance under user-defined delay QoS.

1.2.2 Game Theory

Game theory as a mathematical framework is the methodology used to study the competing and cooperative interactions between rational decision-makers [44]. This mathematical discipline was pioneered by several scholars such as von Neumann, Morgenstern [45] and Nash [46–48] decades ago. Initially developed to study economics problems, game theory has been successfully applied in a wide variety of domains such as political science, computer science, biology and communication networking. Following the seminal work of [45], research work in different domains has flourished.

Traditional optimisation theory discussed in Section 1.2.1 generally assume a single centralised decision maker. Having the global view of the whole system, this centralised decision maker is able to operate or control the system in a global optimal manner. It is assumed that every entity in the system will behave the way the centralised decision maker expects so as to achieve the global optimal result. However, such an assumption may not reflect the real environment in which it is difficult to implement a centralised controller for a large system. In addition, individual entities may not have the global view of the system and may not comply to the global optimisation objective due to their selfish nature. A typical example is the Prisoners' Dilemma illustrated in Example 1.6.

In contrast, game theory admits the rational self-interest of individual entities in the system. Instead of assuming a single centralised decision maker, game theory treats each entity as a decision maker or a game player. Each game player has certain knowledge of the system and other players. To maximise individual payoffs, they choose to cooperate or compete with each other. In that sense, a centralised optimiser is able to provide the best solution but it may be impossible to achieve. Game theory to some extent provides a feasible solution, which may not be global optimal due to incomplete system knowledge and selfish behaviour.

1.2.2.1 Basic Concepts of Game Theory

In order to explain the concepts and principles of game theory, the definition of a game is given as below [44]:

Definition 1.2. *A game is defined as a formal description of strategic interactions between a group of players, who will make rational decisions by considering individual interests, constraints and impacts from other players' decision.*

There are mainly three elements in a game [44, 49–53]:

- The rational decision makers (game players)
- The strategies or actions they can adopt
- The preferences they hold in order to maximise their payoff

Note there are at least two game players in a game and each has more than one strategy or action available, otherwise the game is rather trivial.

Definition 1.3. *A strategy is a complete contingent plan of actions for a decision maker to choose in every possible circumstance of the game in which the player is required to move [54].*

Definition 1.4. *The set of feasible strategies available to a player is defined as the strategy space for that player.*

The outcome of the game will be determined by the combined decisions made by all game players. Each game player has certain knowledge of the consequence of the game under the decisions profile and will not take irrational strategies or actions to sacrifice his/her own payoff. If game players have full information about other players' previous movement at every point of the game, they play a game with *perfect information*. In contrast, in a game with *imperfect information*, game players do not hold all information about the previous actions taken by other players. In addition, a game with *complete information* indicates that all game players share the same common knowledge such as the payoffs and possible strategies of all players. If some players are not fully aware of those information, a game with *incomplete information* will be played. The detail descriptions of those games can be found in [44, 49–54] and references therein.

The goal of game theory is to formulate, construct and explain strategic decision making between individual game players. Interaction is the key to understand how rational or self-interest driven individuals (or government, corporations, etc) choose actions to

fulfil their own objectives. It is generally unrealistic to assume a global coordinator to directly control the behaviour of each individual, although the claim is quite debatable. The decision/action chosen by an individual agent is usually subject to many factors and constraints. Individual objectives are of primary concern for rational decision makers. However, the outcomes of individual decisions are usually affected by strategies/actions adopted by other agents within the same environment. The so-called "interdependence" [54] applies such that the decision made by an individual has negative or positive impacts on the wellbeing of others, while each individual needs to consider the actions taken by other agents and choose his/her own best strategy accordingly. For example in a competitive market such as the telecommunication industry comprising multiple Internet Service Providers (ISPs), the market size is usually limited and consumer demands are subject to many factors. If a firm launches an aggressive business activity such as drastic price reduction to promote new services or products, he/she must evaluate the possible responses of the potential competitors in order to maximise the profit.

Individual rationality is one of the most important assumptions in game theory, and game theory is often interpreted as a theory of rational choice [45]. In previous literature such as [44, 45, 49, 54, 55], it is a common assumption that game players have capacities typically denoted as rationality. It means that rational decision makers have consistent and complete preferences for all possible outcomes, and they have full knowledge of those preferences. Rationality is not only applied to single human actors, it is often considered for non-human entities such as firms and government agents or any combination of those. In different areas and disciplines such as psychology and political science, rationality may have different meanings. Literally, rationality refers the state of being thoughtful and reasonable based on facts and logical deduction [55]. In game theory, rationality has a specific and narrower definition and generally implies that, if a decision maker has well-defined strategies or actions over a set of outcome, this agent always pursues the one leading to the most preferable outcome from that individual's point of view. Therefore, a rational decision maker is generally self-interested and motivated by maximising his/her own payoff after some processes of optimisation. Given the opponents's behaviour or actions, a rational individual is able to form expectation of unknowns, prob-

abilistically derive the results from feasible strategies and make intelligent decisions on choosing appropriate actions [49].

Rationality is a vague assumption without quantitatively defining the preferences of game players. In economics, rationality often indicates that game players seek to maximise their monetary gains by interacting with other players. However, this assumption does not consider other objectives such as social wellbeing and fairness that game players may want to achieve. In some cases, game players are highly motivated by multiple factors instead of a single incentive as explained in [54]. Therefore, it is important to precisely describe the game players' preferences by jointly considering different and sometimes conflicting objectives. Based on the nature of a decision maker's objective, a utility function can be adopted to specify the preference or payoff for a rational decision maker. Ideally those functions should be constructed to reflect the decision makers' attitude towards a collection of factors. Then the rationality of an agent can simply be expressed by maximising the utility function [54].

Based on the characteristics of interactions, i.e. cooperation or competition, game theory can be categorised into two main branches: cooperative and noncooperative game theory. The concept of cooperative and non-cooperative game theory was briefly mentioned by von Neumann and Morgenstern in [45]. Later on, it was Nash who made significant contributions on general game theory by specifying the distinguish between those two branches in his work [46–48, 56]. Inspired by Nash's pioneering work, further investigations were conducted to expand the theoretical framework on cooperative and non-cooperative games.

1.2.2.2 Non-cooperative Games

Non-cooperative game theory provides a framework to study the behaviour of *rational* decision makers, or players involved in an interactive environment [48, 51, 52, 54]. Each game player is able to undertake independent actions/strategies to optimise their individual objectives, which could fully or partially conflict with other players [50–52, 54]. The outcome of the game is jointly determined by the action or strategy profile consisting of multiple decisions adopted by individual game players. The heterogeneous nature

of individual interests could lead to different impacts on the well-being of each player.

In contrast to cooperative games, non-cooperative games do not assume enforceable binding agreements between the decision makers. The notation of "non-cooperative" is rather a technical term and the framework of non-cooperative game does not rule out the cooperation between game players [52–54]. In non-cooperative games players may communicate and make decision in a group, but any cooperation must be self-enforcing without involving third parties to enforce the process. During the game process, each player acts as an autonomous decision maker driven by maximising his/her own payoff. Possible agreements between game players are not formally contracted and will be followed only if doing so is aligned to individual interests.

Non-cooperative game theory examines independent decision making processes of individual rational game players in a competitive environment. As demonstrated in [49–54, 57], non-cooperative game theory is widely used to model the interaction between intelligent and rational individuals aiming to optimise their own objectives in a defined procedure. The main feature of non-cooperative games is that individual incentives [49, 54] are the dominant factors influencing the decisions and actions chosen by rational game players. This indicates that non-cooperative game players only care about individual payoffs in the game and have no interests in wellbeing of other players. Independent decision making is another key assumption for *selfish* game players in non-cooperative games such that all of the players' actions are treated as individual actions [54]. However, this assumption does not exclude the possibility that the action taken by one player can affect the decisions adopted by other players. In non-cooperative games, each player understands that maximising individual payoffs depends not only on his/her own decision but also on other players' decisions. Therefore, individual players need to consider other players' reasoning and assume that other players will act rationally in the same way [54].

One important branch of non-cooperative game is the game in normal (strategic) form [44, 51], which is usually represented by a matrix such as the one shown in Table 1.1 for "The Prisoners' Dilemma". As specified in [51], the details of players' movements are abstracted from the non-cooperative game in normal/strategic form. It is assumed that all decision makers will take simultaneous play in a non-cooperative game with

normal/strategic form. Note individual strategy spaces define all possible actions each player can adopt. Hence, the resulting strategy profile set determines every feasible outcome of the non-cooperative game, which is evaluated by all players with individual payoffs. A non-cooperative game with normal-form representation is defined as,

Definition 1.5. *A normal-form non-cooperative game is defined as a tuple* $\langle \mathcal{N}, \{\mathbf{x}_n\}_{n\in\mathcal{N}}, \{U_n : \vec{\mathbf{x}} \longrightarrow \Re\}_{n\in\mathcal{N}}\rangle$*, where:*

- $\mathcal{N} = \{1, \cdots, N\}$ *denotes a finite non-empty set of players, indexed by* n*.*
- *Each player* $n \in \mathcal{N}$ *has a non-empty set* $\mathbf{X}_n$ *of strategies to choose and* $\mathbf{x}_n \in \mathbf{X}_n$ *is the strategy adopted by the player in the game.*
- $U_n : \vec{\mathbf{x}} \longrightarrow \Re$ *is the utility (cost) function for player* n*.* $\vec{\mathbf{x}} = [\mathbf{x}_1, \cdots, \mathbf{x}_N]$ *denotes the strategy profile determined by all players. Let* $\tilde{n}$ *denote the fact that this term does not include any term with index* n*. For player* n*,* $\vec{\mathbf{x}} = \mathbf{x}_n \cup \vec{\mathbf{x}}_{\tilde{n}}$ *with* $\vec{\mathbf{x}}_{\tilde{n}} = [\mathbf{x}_1, \cdots, \mathbf{x}_{n-1}, \mathbf{x}_{n+1}, \cdots, \mathbf{x}_N]$ *and* $\vec{\mathbf{x}}_{\tilde{n}} \in \vec{\mathbf{X}}_{\tilde{n}} = \times_{\acute{n}\neq n}\mathbf{X}_{\acute{n}}$ *(Cartesian product of the strategy sets).*

In a non-cooperative game with normal form, each player will choose a feasible strategy based on the knowledge of other players such that individual payoff is maximised. If each user is certain about which strategy to be selected with probability 1, we define that strategy a *pure* strategy [49–51]. For a game with *pure* strategies, the outcome of the game is deterministic as each player chooses only one strategy making the resulting strategy profile unique. However, in some situations, game players are not certain about the course of action other players will take. In stead of choosing one strategy, each player would rather randomise his/her choice over a set of *good* strategies according to some probability distributions. This is the so-called *mixed* strategy [49–51] comprising multiple *pure* strategies associated with a probability distribution which defines how frequently a strategy will be played for a game player. This dissertation mainly focuses on non-cooperative games with *pure* strategies. Detail explanations and solutions to games with *mixed* strategies can be found in [49–54]. Unless specified separately, games with *pure* strategies are assumed in the rest of this dissertation.

It is arguable that predicting outcomes of non-cooperative games is mainly based on the understanding of specific game structures such as relations between the players

and individual payoff functions. A description of a game is generally unable to provide deterministic information about the actual strategies adopted by game players. Solution techniques, on the contrary, abstract from particular game features and provide general principles to yield rational outcomes independent of specific games [54]. The theory describes the mapping from particular classes of games to potential strategies adopted by players, and consequently the results of those games. In other words, game solution techniques can provide general recommendations to rational decision makers on how to behave in abstracted games and explain why certain game results persist if decision makers act rationally.

Rationality is a key assumption for non-cooperative game solution techniques such that a perfectly rational player can play prudent strategies against other perfectly rational players. In such games, each player is self-aware with clear knowledge of feasible strategies to select in the game and his/her own preference towards the game outcome [51]. Through some cognitive processes [54], a game player will form a belief about other players. Based on this belief, self-interest driven game players will choose certain strategies to maximise individual payoffs. Furthermore, all players share the common understanding that each player will reason and behave in the same way. Each player is sophisticated enough to have the knowledge that one player's action will impact on other players' payoff in some degree. Therefore, by reasoning from other players' perspectives, all game players will try to estimate other players' possible actions and response with rational decisions. Based on this assumption, there are some commonly used solution techniques for non-cooperative games such as dominated strategies and Nash Equilibrium (NE) as specified in [51–54].

Finding solutions for non-cooperative games with dominated strategies is not difficult. If a rational game player has dominated strategies, this player would not adopt those strategies under any circumstances. This is because the player can always deviate from those strategies to obtain a better payoff no matter which strategy the opponent player will choose. As a consequence, this player will have less strategies to choose since dominated strategies are excluded. Furthermore, other rational players also bear the same information and conclude that this player will not play dominated strategies.

Therefore, other players can downsize their strategy set as well by eliminating strategies associated with those dominated strategies. This process could iterate until the resulting candidate strategy profiles comprise no dominated strategies. A classic example of non-cooperative games with dominated strategies is the Prisoners' Dilemma demonstrated in Example 1.1.

Definition 1.6. *In a normal-form game* $\langle \mathcal{N}, \{\mathbf{x}_n\}_{n\in\mathcal{N}}, \{U_n : \vec{\mathbf{x}} \longrightarrow \Re\}_{n\in\mathcal{N}}\rangle$*, strategy* $\mathbf{x}_n \in \mathbf{X}_n$ *of player n is* ***strictly dominated*** *if for all other strategies* $\acute{\mathbf{x}}_n \in \mathbf{X}_n$

$$U_n(\mathbf{x}_n, \vec{\mathbf{x}}_{\tilde{n}}) < U_n(\acute{\mathbf{x}}_n, \vec{\mathbf{x}}_{\tilde{n}}),\ for\ all\ \vec{\mathbf{x}}_{\tilde{n}} \in \vec{\mathbf{X}}_{\tilde{n}}$$

The strategy $\mathbf{x}_n \in \mathbf{X}_n$ *is* ***weakly dominated*** *for all other strategies* $\acute{\mathbf{x}}_n \in \mathbf{X}_n$ *if*

$$U_n(\mathbf{x}_n, \vec{\mathbf{x}}_{\tilde{n}}) \leq U_n(\acute{\mathbf{x}}_n, \vec{\mathbf{x}}_{\tilde{n}}),\ for\ all\ \vec{\mathbf{x}}_{\tilde{n}} \in \vec{\mathbf{X}}_{\tilde{n}},\ and$$

$$U_n(\mathbf{x}_n, \vec{\mathbf{x}}_{\tilde{n}}) < U_n(\acute{\mathbf{x}}_n, \vec{\mathbf{x}}_{\tilde{n}}),\ for\ some\ \vec{\mathbf{x}}_{\tilde{n}} \in \vec{\mathbf{X}}_{\tilde{n}}$$

Example 1.1 (The Prisoners' Dilemma)**.** *Two suspects are arrested for a crime and isolated in different rooms. The judge believes they are guilty but could not find evidence to convict them. There are two options, i.e. cooperate or defect, available to those two suspects to select. And each suspect knows they are given the same option set. Table 1.1 illustrates the matrix representation of the Prisoners' Dilemma for* 2 *players. Each entity* $(-a, -b)$ *represents a and b years sentence for suspect* 1 *and* 2 *respectively. If they both cooperate (keep silent), they will be both prosecuted with one year sentence represented as* -1 *payoff. In contrast, if they both defect (confess), each of them will be prisoned for two years. If one suspect defect and the other suspect confess, the confessor will be set free while the latter will receive maximum punishment of three-year sentence. This is a typical non-cooperative game in normal form, which is solvable by eliminating dominated strategies. Suspect* 1 *will evaluate the possible outcomes of choosing different strategies. No matter which strategy suspect* 2 *will choose, suspect* 1 *is always better off by choosing "defect" than "cooperate", which means "cooperate" is a strictly dominated strategy. On the other hand, suspect* 2 *will do the same reasoning and choose the "defect" option. As a consequence, both suspects will choose defect and receive two-year sentence.*

Table 1.1: Prisoners' Dilemma with two players

	Suspect 2 cooperates (C)	Suspect 2 defects (D)
Suspect 1 cooperates (C)	$(-1,-1)$	$(-3,0)$
Suspect 1 defects (D)	$(0,-3)$	$(-2,-2)$

Best response [44] is another realisation of solution concepts for non-cooperative games. Rational game players will refrain from using dominated strategies and adopt un-dominated strategies in non-cooperative games. However, some non-cooperative games have more than one un-dominated strategies or even no dominated strategy such as "the battle of sexes" game demonstrated in the literature [49, 51, 54]. As a consequence, it is difficult to anticipate how those non-cooperative games will be played on the basis of dominated strategy criterion. Suppose game players can form expectations of other players by learning or observing their behaviour. Based on this knowledge, a rational game player will choose a strategy so as to produces the most favourable outcome for himself/herself. This is so called *best response* (*best reply*) describing the rationality of intelligent game players.

Definition 1.7. *For game player n, the best response against the strategy profile $\vec{\mathbf{x}}_{\tilde{n}}$ of other players is the strategy $\mathbf{x}_n^* \in \mathbf{X}_n$ such that*

$$U_n(\mathbf{x}_n^*, \vec{\mathbf{x}}_{\tilde{n}}) \geq U_n(\mathbf{x}_n, \vec{\mathbf{x}}_{\tilde{n}}),\ for\ all\ \mathbf{x}_n \in \mathbf{X}_n$$

The concept of mutual *best response* is the foundation of Nash equilibrium for non-cooperative games introduced by Nash in his early works [46, 48, 56]. The equilibrium embodies the idea that all players' beliefs and behaviours are consistent, that is to say that each player can reason how his/her opponents would act by putting his/her own feet in other's shoes. This is a stronger hypothesis than the implication of *common knowledge* [51]. The rationality concept does not entirely exclude strategy uncertainty of individual players. Rather it accounts for a self-enforcing agreement instead of a binding agreement between players [51]. By *best responding* to other players' *best strategies*, all players could coordinate on a unique strategy profile, which is a solution to non-cooperative games commonly noted as Nash equilibrium. More formally, the Nash equilibrium of a pure-strategy non-cooperative game is defined as

Definition 1.8. *A strategy profile* $\vec{\mathbf{x}}^* = [\mathbf{x}_1^*, \cdots, \mathbf{x}_N^*]$ *is a Nash equilibrium if every player's strategy is the* best response *to other players' strategy such that*

$$U_n(\mathbf{x}_n^*, \vec{\mathbf{x}}_{\tilde{n}}^*) \geq U_n(\mathbf{x}_n, \vec{\mathbf{x}}_{\tilde{n}}^*), \ for\ all\ \mathbf{x}_n \in \mathbf{X}_n\ and\ n \in \mathcal{N}$$

In other words, if each game player has chosen the Nash equilibrium strategy, no player has an incentive to unilaterally deviate from that equilibrium strategy. A pure-strategy non-cooperative game can admit zero, one or multiple Nash equilibria [51–53]. Kakutani's fixed point theorem [58] has been widely used to show the existence of Nash equilibrium following the proof in [46]. The detail descriptions of the existence of Nash equilibrium in non-cooperative games can be found in [49–51, 53, 59].

Nash equilibrium implies coordination to some extent because it converges to a single strategy profile for all players in a non-cooperative game. Such *congruity* [54] however does not always ensure a Nash equilibrium solution is global optimal. It is specified in [60] that Nash equilibrium of games with smooth payoff functions are generally inefficient. From a global view point instead of individual view point, there may exist some strategy profiles resulting better outcomes than that of the Nash equilibrium. In other words, the global optimal solution with a centralized controller could outperform the Nash equilibrium solution driven by rational behaviour of selfish game players [53].

To demonstrate the concept of Nash equilibrium, we refer to the Prisoners's Dilemma illustrated in Table 1.1 and Example 1.1. This is a classic non-cooperative game with a single Nash equilibrium, i.e. the $[D, D]$ strategy profile in Table 1.1. It is not difficult to show that the strategy profile $[C, C]$ is not the Nash equilibrium. Assume suspect 2 knows that suspect 1 decides to cooperate (selects the C strategy), suspect 2 will deviate from the C strategy because the D strategy (confess) is the *best response* for suspect 2 against the C strategy chosen by suspect 1. Instead of receiving 1-year sentence, suspect 2 can be set free if the strategy profile $[C, D]$ is adopted. Obviously, suspect 1 is intelligent enough not to apply the strategy profile $[C, D]$. If suspect 1 knows that suspect 2 will choose the D strategy, suspect 1 will best response with the D strategy, which leads to 2-year sentence instead of 3-year sentence for suspect 1. Likewise it is easy to show that the strategy profile $[D, C]$ is not stable as well. This simple deduction proves that the Prisoners's

Dilemma with two players has only one Nash equilibrium.

As for efficiency, the Nash equilibrium of the Prisoners's Dilemma, i.e. the $[D, D]$ strategy profile in Table 1.1 with payoffs $(-2, -2)$, is not global optimal. It is clear that both suspects are better off if they choose to cooperate (strategy C) with payoffs $(-1, -1)$. However, as described above, the $[C, C]$ strategy profile is not stable in a non-cooperative environment. Selfish game players can always achieve better payoffs by deviating from the global optimal strategy profile.

The seminal work [61] introduces the term Price of Anarchy (PoA) to measure the efficiency loss between the worst game solution and the global optimal solution due to selfish behaviour of individual game players.

Definition 1.9. *The price of anarchy of a game* $\langle \mathcal{N}, \{\mathbf{x}_n\}_{n\in\mathcal{N}}, \{U_n : \vec{\mathbf{x}} \longrightarrow \Re\}_{n\in\mathcal{N}} \rangle$ *is defined as*

$$\pi = \frac{\sum_{n=1}^{N} U_n(\vec{\mathbf{x}}^g)}{\sum_{n=1}^{N} U_n(\vec{\mathbf{x}}^*)}$$

where $\vec{\mathbf{x}}^g$ *is the global optimal solution and* $\vec{\mathbf{x}}^*$ *denotes the worst Nash equilibria.* [1]

Take the the Prisoners's Dilemma for example. We add 3 to payoffs in Table 1.1 such that all payoffs are non-negative. Therefore, the NE solution $[D, D]$ leads to payoff $(1, 1)$ and the global optimal solution $[C, C]$ results in payoff $(2, 2)$. By using Definition 1.9, we show the PoA for the Prisoners's Dilemma is 2.

In summary, a NE is a rationalisable strategy profile comprising iteratively undominated strategies. It embodies the concept of self-enforcing agreement and congruity over all game players. Due to the game structure, a non-cooperative game may have multiple or zero Nash equilibria. The outcome of a Nash equilibrium could be socially inefficient from a global view point. Exploring those important properties have generated a significant body of research in non-cooperative game theory.

In Chapter 5, we apply non-cooperative game theory to model the rational behaviour of individual users in a cloud-based communication network. The concept of NE is adopted to demonstrate the solution of the proposed non-cooperative game in which end users aim to optimise individual objectives in term of energy consumption and traf-

[1] For cost minimisation, the PoA is the ratio of the worst Nash equilibria over the global optimal solution.

fic load balance over allocated data entres. We use the concept of PoA to demonstrate the inefficiency loss between the game solution and the global optimal solution in terms of network energy consumption and data centre load balance.

1.2.3 Software Defined Networking

The Internet as a communications network is now the largest infrastructure to provide connections between institutions, business and customers. Communication networks facilitate new business models and applications on a domestic and international scale. As a consequence, communication networks are becoming a strategic asset for service providers, enterprise users and individual customers [62]. However, the underlying networks are being pushed to their limits due to the exponential growth of users, versatile applications and devices connected to the networks [63]. This in turn creates an incentive for innovations in design, deploy and manage modern communication networks.

Until recently, the fundamental architecture for the underlying networks for packet switching and routing remained relatively unchanged in terms of control plane and data (forwarding) plane. In order to treat each packet appropriately, packet-switched network devices such as routers and switches must be able to distinguish between data plane and control plane packets. Guided by this principle, the majority of network equipment is still built in an orthodox fashion by integrating control plane and data plane within devices [64]. The control plane in general is responsible for processing control packets and making switching or routing decision for incoming data packets. The data plane is in charge of data packet forwarding based on direction from the control plane.

1.2.3.1 The Rise of Software Defined Network (SDN)

The Internet has evolved into a sophisticated global infrastructure in terms of coverage and scale. Further development and expanding of this modern communication network are subject to many physical constraints and theoretical limitations such as shown in [65]. In addition, traditional network architectures are often blamed for not meeting new requirements of customers using today's Internet [66–68]. Different customers and

stakeholders bear variant and some times conflicting interests and objectives. Individual consumers care more about the quality of experience of using the Internet in terms of network performance and the associated cost. Enterprise users put more focus on how to create new value and revenues by squeezing the most from networks, whether owned or rented from third parties. On the other hand, network operators and service providers are more concerned about the exploding demand for mobility and bandwidth. Escalating operational cost and deflated revenue drive network operators to take more radical actions on network management and IP traffic control. However, many previous attempts found it hard to balance the tradeoff due to limitations of current network architectures and technologies. As summarised in [69], the advances of communication networks is lagging behind for supporting current network traffic and emerging cloud services.

With the current packet delivery paradigm the network layer is becoming the "narrow waist" of today's Internet [67]. As the core of the Internet, the network layer in the OSI hierarchy is responsible for transferring datagrams from a source to a destination through one or multiple networks [67]. Major communication networks are built around the network layer with protocols and functionalities implemented above or below this layer. The primary design requirement for the network layer is to provide best effort packet delivery over the underlying transmission media. Traditional packet processing relies on the connectionless IP addressing mechanism by which each data unit is individually addressed and routed based on self-contained information. The end-to-end design principle [70] for IP protocols requires no application specific functionalities embedded in the network layer. Rather, functions for completeness and correctness are relegated to upper layer protocols managed by end hosts [68]. As a consequence, the network layer is only required to support simple lightweight IP packet routing, but it is also incapable of distinguishing packets for different upper layer applications [67].

SDN is an emerging architecture where network control plane and data plane are decoupled to facilitates designing, building and managing networks through abstraction of lower level functionality [71]. The study [71] claims that by leveraging SDN, the current static network can evolve into an extensible service delivery platform capable of responding rapidly to changing business and customer requirements.

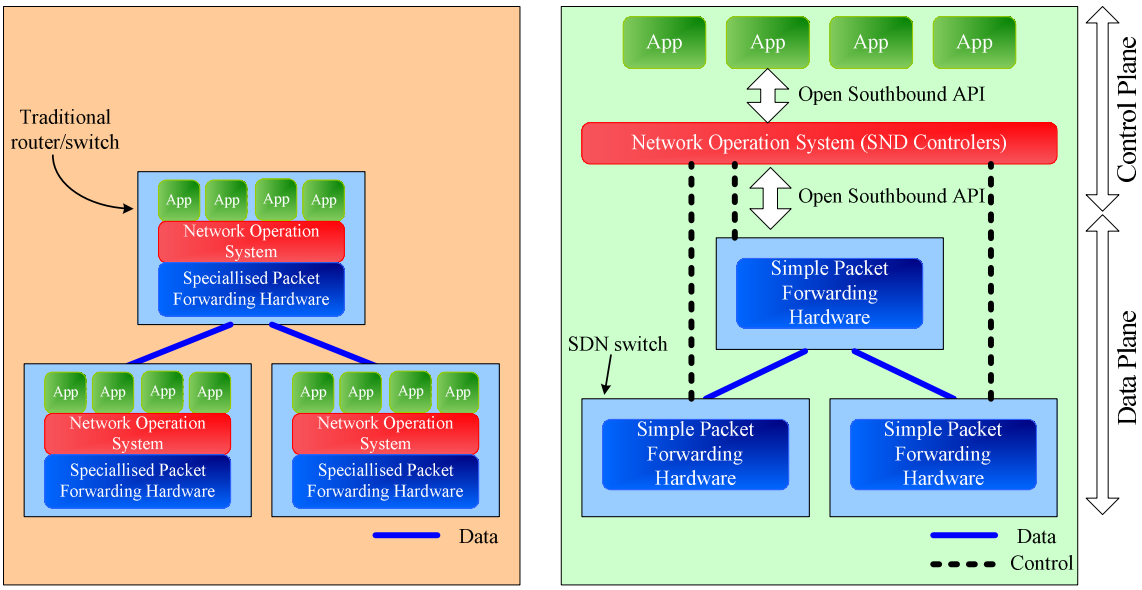

Figure 1.1: Traditional networking architecture Vs. SDN architecture

Fig. 1.1 compares the traditional networking architecture with coupled data/control planes and the SDN architecture with separated data/control plane. Traditional network equipment such as router and switch implements both control plane and data plane functionalities such that each equipment acts as an autonomous system. By adopting specific routing protocols, the control plane of a single network equipment gathers routing information from other related network devices to form routing tables. The data plane examines the incoming packets, refers to address look-up tables, and decides data transferring between different ports.

In contrast, the SDN approach removes control plane intelligence from all networking devices. The control logic is moved to an external SDN controller, which can run on commodity servers. As a consequence, the implementation of the network equipment is rather simple such that only simple packet forwarding functionality is required to implemented in software or hardware. The resulting data plane device is usually called SDN forwarding device as shown in Fig. 1.1. By receiving flow table contents from the controller, the generic SDN forwarding device is able to realise customised networking

functionalities such as switching, routing and firewall.

Residing in the so-called management plane, network applications implement customised control-logic, which will be transferred into commands and installed in the data plane. SDN network applications support traditional networking processions such as switching and routing. Also the SDN architecture allows novel networking functionalities such as traffic-aware load balancing [72], end-to-end QoS enforcement [73] and seamless mobility management [74]. The study [75] categorised a variety of SDN applications into five groups: traffic engineering, mobility and wireless, measurement and monitoring, security and dependability and data center networking.

In summary, SDN provides an alternative solution to manage the entire network in an efficient and agile manner. The centralised control mechanism enables simple and less error-prone network configuration. By leveraging the new architecture with decoupled control/data planes, network application developers can implement sophisticated networking functions, services without knowing the details of lower-level devices. With the global network information, the centralised controller facilitates optimisation of existing network applications, services, and infrastructures. The resulting SDN architecture enables network service providers to rapidly adopt to changing business needs with scalable and innovative solutions. In addition, the abstracted structure helps network service providers gain unprecedented programmability, improved automation and fast control on networks. As reported in [75], SDN has obtained significant traction in both academia and industry such that major industrial players fund Open Networking Foundation (OFN) [76] to promote the adoption of SDN through open standard development.

1.2.3.2 OpenFlow: One Enabler of SDN

OpenFlow is one realisation of SDN protocols to facilitate the communication between the Controller and the data plane abstraction. OpenFlow provides a compromise solution to address those requirements by isolating experiment and production networks [77]. OpenFlow is designed to support remote controllers on determining forwarding path for network packets through networked devices [77]. Initially OpenFlow was developed for Ethernet switches in IP packet domain. A new generic and extended opti-

cal OpenFlow specification was proposed in [78] to support emerging optical transport technologies. By leveraging the unified control plane abstraction, network operators can seamlessly integrate packet networks and optical circuit networks allowing smooth deployment of sophisticated network functions cross heterogeneous domains [78, 79]. The current OpenFlow specification [80] defines the components and the required functions for an OpenFlow switch, and the message structures for OpenFlow switch protocol (with new set of properties for optical ports). Fig. 1.2 illustrates the main components of a flow entry as specified in [80].

As described in [77], an OpenFlow switch comprises 3 elements: a flow table to store forwarding instructions, a secure communication channel connecting the switch to a remote controller and the OpenFlow protocol defined to be an open and standard application programming interface (API). Based on the current specification [80], an OpenFlow switch can have multiple flow tables, each containing multiple flow entries. Fig. 1.2 illustrates the main components of a flow entry as specified in [80]. The OpenFlow channel is able to run over TCP secured by encryption protocol such as Security Socket Layer (SSL). Through the OpenFlow channel, a controller can configure the connected switches, receive event information or packets from the switches and send packets back to switches. Details of OpenFlow channel connections and protocol message structures can be found in [80].

Ingress packets are pipeline processed through a chain of flow tables attached with an empty action set as described in the specification [80]. In a flow table, a packet will be matched against the flow entries in the order of priority, which is shown in Fig. 1.2. Once the packet is matched, the defined instruction will be applied to the packet and the action set is updated. If required by the instruction, the packet and the associated action set can be sent to the next flow table for further processing. If the instruction does not contain a "*Goto-Table*" instruction or no more flow table is present, the pipeline processing will stop. At the end of pipeline processing, packet actions such as *Output*, *Drop* and *Push-Tag/Pop-Tag* in the action set will be executed.

OpenFlow is the first standard SDN southbound interface for control and forwarding layers. As a key enabler of SND, OpenFlow allows direct access of low-level forwarding

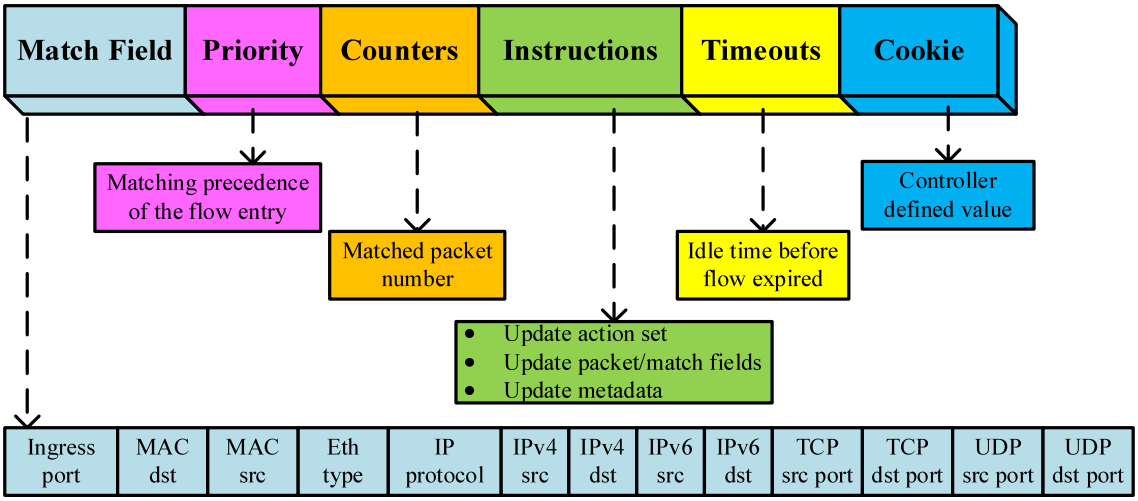

src: source dst: destination

Figure 1.2: OpenFlow entry.

devices and flexible data traffic handling. While originated from Ethernet-based networks, OpenFlow is now extending to more broad application areas such as optical networks [78]. OpenFlow is now wildly adopted by major network equipment vendors to support SDN migration in the short future [71].

1.2.3.3 Network Emulator: Mininet

SDN is becoming a plausible technology for network design, deployment and operation. This paradigm is gaining significant interest from both academic and industrial communities. However many challenges for SDN such as scalability, reliability and security still impede it's industrial adoption at large scale. New SDN-based applications and configurations need thorough testing and evaluation before being deployed in production networks. Meanwhile, network researchers demand suitable test and evaluation tools to experiment new ideas and protocols for SDN in a cost-efficient manner. The tradition prototyping methods are generally classified in 2 groups, testbeds and simulators, each has its own merits and constraints [81]. For testing and evaluation fidelity, using hardware testbeds could generate reliable results. However, building such physical environments is typically not feasible for a broad section of the research community. A

traditional simulator, on the other hand, is cheaper to run but lack of fidelity [82].

The Mininet open-source network emulator is designed to support research, development, prototyping, testing SDN systems on a standard PC platform [81]. It can run unmodified code interactively on virtual hardware, providing prototyping convenience and realism at low cost. A virtual software-defined network can be created in Mininet on-the-fly, which consists of an OpenFlow controller, multiple OpenFlow-enabled Ethernet switches, multiple host and ethernet links connecting those elements. By leveraging the OpenFlow protocol, the emulated switches can support highly flexible SDN with customised network topologies. The authors of [82] demonstrated that Mininet can be used to reproduce published results by running networks on a single PC, using lightweight OS virtualisation. Those properties make Mininet a simple, cost-effective and efficient network testbed for developing OpenFlow applications.

In Chapter 6, the SDN architecture described above is adopted to model a core network in a Mininet platform hosted in a Ubuntu virtual machine. By leveraging the OpenFlow protocol discussed in this chapter, a centralised controller is implemented to facilitate traffic distribution in an energy efficient manner. With the decoupled data plane and control plane, the proposed SDN model is able to run customised networking functions with real networking protocols in the Mininet platform.

1.3 Contributions of the Dissertation

In this section the original contributions of the dissertation are listed and explained in detail.

The main results of Chapter 4 are:

- A general system model is developed for next generation mobile backhaul networks that allows the performance of heterogeneous backhaul technologies to be evaluated and compared.
- The system model encompasses an optimisation framework along with a distributed algorithm to optimise both network power consumption and load balancing over network elements.

The main results of Chapter 5 are:

- A strategic game approach is proposed to optimise the system performance with multiple objectives, including a-priori user-specific performance preferences and a special emphasis on energy savings.
- The impact on network behaviour arising from multi-objective optimisation of players on the network is studied through simulations.
- With sufficient network provisioning and moderate objectives, the simulation results show that the power consumption of the proposed game solution is close to the global solution.
- User specific nonlinear multi-objective cost functions and asymmetrical resources allocation for game players lead to inefficient resources usage in terms of energy and traffic load for the game solution compared to the global optimal solution.

The main results of Chapter 6 are:

- The system model encompasses an multi-objective optimisation framework to optimise both network power consumption and balancing of load over generic network elements with defined QoS requirements.
- A SDN-based platform is implemented in Mininet, which enables demonstration of customised network functions such as statistical switching, multi-path routing and QoS-energy-aware traffic distribution in a systematic manner.
- The Mininet simulation results show that unintended individual stringent QoS requirements could introduce unfair network resource allocation and result in system power consumption and server load balance performance degradation.

1.4 Outline of the Dissertation

The chapters in this dissertation are organized in the following structure.

Chapter 2 provides a literature review on improving energy efficiency of communication networks. First we highlight the challenge of energy consumption and greenhouse gas emission to sustain the data traffic growth for Next Generation Networks [83]. We further categorise important studies into three broad topics pertaining to energy efficiency of communication networks: power-awareness design in heterogeneous backhaul networks, network optimisation with non-cooperative game theory and energy efficiency in optical core networks. Significant findings of these studies and their limitations are discussed. We also evaluate technological and methodological differences between similar work.

Chapter 3 presents a general system model for cloud-based communication networks discussed in the rest of this dissertation. We apply Graph theory to describe network topologies with matrices built upon network elements, routes, source and destination nodes. To facilitate data traffic analysis, a fluid flow model model is adopted to to describe the average macroscopic behaviour of network traffic. We also introduce a generic power consumption model for heterogeneous network elements.

Chapter 4 proposes a multi-objective optimisation framework for energy efficiency and load balance of heterogeneous backhaul networks. We highlight the challenges in terms of traffic flow and energy consumption for next generation wireless backhaul networks with massive deployment of small cells and rapid growth of wireless data traffic. This chapter presents a distributed algorithm to energy efficiently route traffic over a heterogenous backhaul network while main a certain level of load balance over network elements. We apply theoretical convergence analysis to the algorithm and use numerical simulations to demonstrate the results.

Chapter 5 extends the multi-objective network optimisation framework by considering the multi-ownership of the underlying infrastructure. Non-cooperative game theory is adopted to data traffic management in a cloud-based network to obtain a distributed and energy-efficient solution, where each edge router is acting as a strategic player. In addition, we also aim to optimise weighted inter-datacentre load balance and weighted transport network delay with a-priori user-specific preferences. After proving the existence and uniqueness of NE of the proposed game, we analyse the convergence of the

proposed algorithm. This chapter also describes the efficiency loss between the proposed game solution and the global optimal solution due to rational behaviour of individual game players. The following simulation results show notable challenges to plan, design and operate a multimedia content network in a non-cooperative environment, which essentially reflects the real world.

Chapter 6 addresses the power consumption minimisation problem of optical core networks by using SDN. By leveraging the centralised SDN controller, we propose a joint algorithm optimising system power consumption and traffic load balance under user defined traffic QoS requirements. To demonstrate the optimisation problem, we build a generic SDN model in the Mininet platform hosted by a Ubuntu virtual machine. By leveraging the OpenFlow protocol, we study a core network topology with different parameter configurations by running real networking protocols in the Mininet platform. The simulation results show impacts of network topology, traffic diurnal cycle, and user defined QoS requirements on network power consumption.

Chapter 7 concludes the main findings of this dissertation and highlights future research directions.

1.5 Publications

- T. Lin, T. Alpcan, and K. Hinton, "An energy-efficiency framework in optical communication networks using software defined networking," submitted to *Optical Communications and Networking, IEEE/OSA Journal of*, 2015.

- T. Lin, T. Alpcan, and K. Hinton, "A game-theoretic analysis of energy efficiency and performance for cloud computing in communication networks," *Systems Journal, IEEE*, vol. PP, no. 99, pp. 1–12, 2015.

- T. Lin, T. Alpcan, K. Hinton, and A. Vishwanath, "A distributed multi-objective optimisation framework for energy efficiency in mobile backhaul networks," accepted by *Multi-Conference on Systems and Control, 2015 IEEE Conference on*, Sydney, Australia, September 2015.

- T. Lin, T. Alpcan, K. Hinton, and A. Vishwanath, "A multi-objective optimisation approach for energy efficiency of backhaul traffic in mobile networks," in *Proceedings of the 2015 ACM Sixth International Conference on Future Energy Systems*. Bangalore, India: ACM, July 2015, pp. 203–204.

- T. Lin, T. Alpcan, and K. Hinton, "Energy efficiency games for backhaul traffic in wireless networks," in *Signals, Systems and Computers (ASILOMAR), 2012 Conference Record of the Forty Sixth Asilomar Conference on*, Pacific Grove, CA, USA, November 2012, pp. 666–670.

Chapter 2
State of The Art Review

2.1 Introduction

While it is widely agreed that Information and Communications Technologies (ICT) are able to provide solutions to reduce overall energy consumption and greenhouse gas (GHG) emission [18, 84, 85], ICT industry itself accounts for a non-negligible portion of global electricity consumption and carbon footprint. As reported in [14, 86], the global ICT ecosystem consumes 2% $\sim$ 3% of the world's annual electricity generation. With the escalation of electricity consumption, the resulting carbon emission from the ICT industry also mounts and is responsible for 2% $\sim$ 2.5% global greenhouse gas emissions [14, 87]. The study [18] shows that the annual GHG emissions are projected to increase to 12% by 2020 for the business-as-usual model in 2011. In particular, the energy consumption of ICT communication networks is increasing rapidly, with an annual growth rate 10% as reported in [86]. The increasing trend of energy consumption and greenhouse emission is more likely to continue with the rapid growth of data traffic in communication networks [85, 88]. Managing the supply of electricity to communication networks, and treating the resulting heat dissipation is likely to become a formidable engineering challenge [89].

This dissertation addresses some challenges and problems such as optimising network traffic distribution, coordination conflicting network performance requirements and adopting emerging SDN architectures to improve energy efficiency of communication networks. Energy efficiency of mobile backhaul networks, optical core networks and software defined networks is the main focus in this work. We aim to provide insights

on planing, designing and operating of communication networks in an energy efficient manner, combined with other network performance requirements such as server load balancing, network bandwidth and traffic delay QoS.

The rest of the chapter is structured as follows. The next section reviews related work on energy efficiency of heterogeneous backhaul networks. Section 2.3 discusses relevant literature on network optimisation using non-cooperative game theory. In Section 2.4, previous work on energy efficiency of optical core networks is analysed followed by discussion on emerging SDN technologies.

2.2 Heterogeneous Backhaul Networks

New mobile broadband services are adding exponentially to the growth of backhaul traffic [20]. Mobile operators are now facing the challenges of the explosion of mobile backhaul traffic, the ongoing technology evolution and the associated energy consumption [90]. New RAN technologies such as HSPA+ and LTE require very large "backhaul pipes". As stated in [91] mobile service providers should plan for more than 100 Mbps backhaul capacity per site. However, the peak data rate for LTE-Advanced will exceed 1 Gbps and 500 Mbps for DL and UL respectively in the near future [92]. In addition, the increasing demand for coverage and capability requires the deployment of more advanced base stations, which in turn leads to more backhaul traffic. It is expected that all-IP packet traffic will be the trend for next-generation networks [91]. Therefore, as largely agreed [20, 90, 91], the legacy networks will migrate to the IP/MPLS architecture. The resulting heterogeneous network deployment of 2/3/4G will incur more challenges of managing backhaul networks.

Furthermore the massive deployment of small cells will make the situation worse. The move to smaller cells to augment existing macro mobile networks is widely viewed as a potential solution to the RAN congestion problem. However it also directly creates a new challenge: backhaul [93]. Driven by increasing demand for mobile data, backhaul requirements for small cells are expected to approach macro cell capacity requirements [94] in the years to come. This means the backhaul traffic to be processed will not be just

doubled. Given the massive deployment of small cells in the near future, the resulting backhaul traffic could be tens or even hundred times higher than the current backhaul traffic [93, 94].

All these challenges lead to a bottleneck for next-generation wireless networks. How to distribute and process the escalating mobile backhaul traffic intelligently and efficiently are now important topics for both industry and academia. Without addressing this issue, mobile backhaul networks will be unable to accommodate the required traffic although the advanced RAN technologies such as 4G can provide such large bandwidth.

The first goal of this dissertation is to identify the potential energy consumption bottleneck for next-generation wireless networks. Many research works on energy efficiency of cellular networks in the literature are focused on RANs as shown in [12, 95, 96]. This is because the energy consumption of BSs dominates the total energy consumption of the current cellular networks as reported in [19]. However, this situation could change for next-generation cellular networks where massive numbers of small cells will be deployed. As specified in [20, 93], the backhaul traffic for next-generation network could grow exponentially leading to a significant increase of the energy consumption for backhaul and core networks. Given relatively low energy consumption of small BSs and RRHs such as lightRadio™"Cube" [97], the proportion of energy consumption for wireless core networks (CN) could significantly increase to dominate the total energy consumption of the system. The corresponding investigation of energy consumption could create a new view of next-generation cellular networks with small cell deployments and reveal new research areas.

The modeling of cellular heterogeneous networks is an important objective of this dissertation. For simplicity, but without losing generality, a high level LTE cellular network architecture comprising the CN and the RAN as described in [98] will be adopted in this dissertation. We propose a general wireless cloud framework by leveraging the virtualisation technology. A mesh network structure will be modeled to fully explore multi-paths between the RAN and the CN. Unlike the stochastic queuing model used in [99, 100], we establish a fluid-flow model [101, 102] to emulate the transportation of mobile backhaul traffic.

In this dissertation, we propose a framework to formulate joint optimisation problems. A multi-objective optimisation scheme with a-priori user-specific performance preferences [43] is adopted to explore independent and possibility conflicting system requirements. A generic weighted sum scheme is implemented to provide flexible controls over different optimisation objectives. Previous works on traffic scheduling are mainly focused on the total system response time based on queuing theory such as in [99, 100]. However, little work has been done to jointly consider both load balancing and energy efficiency for the traffic scheduling between CNs and RANs. In this dissertation, optimisation objectives of system power consumption and traffic load balancing are applied to optimise the mobile backhaul traffic allocation. We develop a distributed optimisation algorithm for mobile data traffic distribution. System performance is examined and compared using numerical simulations. The simulation results analyses provide insights of how to improve the energy efficiency and maintain the service availability in cellular networks. In addition, we also investigate the convergence of the proposed algorithm to show it's stability.

2.3 Communication Network Optimisation with Non-cooperative Game Theory

In recent years, game theoretical techniques have gained prominence in wireless and communication networks although they originate from the economic and biology domains. Studying strategic interactions between self-interested participants is the common factor that ties those different disciplines. The essence of game theory makes it very suitable for modeling situations where game players have to take specific actions or strategies that can have mutual or possibly conflicting consequences [44]. Large-scale communication networks like cellular networks and core networks comprise multiple heterogeneous and autonomous entities. The associated complicated interrelationships make it difficult to access the centralised information. Traditional network optimisation methods often struggle to deal with such sophisticated problems with a single administrative domain and control objective [103]. In many communication networks, the players have to choose

strategies with agreements to share common resources with multiple constrains in a preferred distributed manner. This situation effectively resembles the non-cooperative game described in Section 1.2.2.2, in which a number of *rational* decision makers with potential conflicting interests try to maximise their own payoff or alternatively minimise the corresponding costs, in a way that all actors perform the optimisation in the same manner.

Non-cooperative games have been widely studied in communication networks for power control, spectrum assignment, network selection, service provisioning, traffic routing and flow control with Nash equilibrium (NE specified in Definition 1.8 of Section 1.2.2.2) as the relevant solution concept [57]. NE is in fact a static concept that represents a viable strategy profile agreed by all game players. It does not address how the equilibrium will be reached or which one of several possible equilibria will be chosen for the non-cooperative game. The work [44] shows that the existence of a mixed-strategy [1] NE is guaranteed for a finite [2] norm-form game, in which game players move simultaneously and receive the payoffs resulted from combinations of actions played [44, 51]. However, the existence of a pure-strategy NE is subject to more constraints of the corresponding payoff or cost functions [44]. There are ample studies [52, 53, 57, 104] focused on establishing NE for the non-cooperative games used to model interactions in communications networks.

Applying non-cooperative game theory to optimise uplink power control in wireless systems is a typical example as summarised in [52]. The work [104] presents a framework of distributed and market-based uplink power control for a single cell CDMA system using non-cooperative game theory. The existence of a unique NE is demonstrated with a user cost function representing the difference of a charge function based on the transmission power and a utility function based on the signal-to-interference ratio (SIR). Another study [105] considers a multicell wireless system and investigates the distributed power control in the same framework of non-cooperative games. The effects of different pricing based distributed power control mechanisms are studied. The non-cooperative game outcomes show inefficient NE for the whole system, that the centralised global optimal solution can yield higher user utilities with lower uplink power allocation for each user.

[1] mixed-strategy and pure-strategy are defined in Section 1.2.2.2

[2] A game with a finite number of players, each player has a finite set of strategies.

Modern communication networks are generally heterogeneous and decentralised such as the Internet. Analysing such large systems requires a rich theoretical framework such as game models and algorithms to tackle the challenges faced by current and future communication networks. In [99], the authors outlined a general distributed computing system as a collection of computing resources shared by customers. A non-cooperative game was formulated such that each customer as a game player aims to minimise the total job execution time of the required workload. The *best-response* concept defined in Definition 1.7 is adopted to derive an optimal solution for each game player, which leads to a NE for the whole load distribution scheme. However the corresponding game theoretical model is restricted to a simple static grid computing system. The authors of [100] further extend the work to a cloud system consisting additional storage and communication resources. In [100] the proposed semi-static scheme is capable of responding to system status changes during runtime with limited information exchanges. In addition, communication delays of transport networks are taken into account for the proposed non-cooperative load distribution scheme.

The efficiency of NE is another key research topic for non-cooperative games in communication networks. As stated in [106], highly distributed and complex communication networks such as the Internet are becoming increasingly dependent on the interactions of intelligent end users and applications with autonomous operation capability. A highly dynamic and rapid changing system generally does not have a central authority that plans, designs and operates the underlying networks [52]. It is rather difficult or even impossible to coordinate a large number of self-interest driven end users or applications with local and partial information so as to achieve the global optimum in terms of the sum of payoffs over all participants [53].

Non-cooperative game theory provides alternative approaches to solve optimisation problems in highly distributed communication networks. If the game solution is close to the global optimal solution, it indicates that there is no need to develop a centralised controller responding network performance optimisation in a global scale. On the other hand, further investigations are required if the gap between the game solution and the global optimal solution is significant. The centralised optimisation approach could be

more attractive if the performance gap between the game solution and the global optimal solution outweigh the cost of implementing a centralised controller. Therefore understanding the performance gap in terms of Price of Anarchy (PoA) in Definition 1.9 is becoming important for network protocols design and network operation.

Several studies [61, 107–109] exist in the literature show that NE solutions for non-cooperative routing games are generally inefficient in terms of network delay. A typical example is the Prisoners' Dilemma specified in Section 1.2.2.2, where the NE results in inferior outcomes for all game players. The seminal work [61] conducts a detailed analysis of the efficiency of NE for a simple network topology comprising L parallel links connecting a source-destination pair. Network users would rationally select a signal link with a probability to route their traffic so as to minimise the associated delay. The main outcome of this work is to demonstrate the ratio of the latency cost for the worst NE over the latency cost for the global optimal solution. This ratio represents the concept of the PoA described in Definition 1.9, which is extensively studied in the following research work.

The effect of a lack of coordination among rational players in a non-cooperative routing game is further investigated in the study of [107]. Compared to [61], this work considers pure strategies only but extends the system model to accommodate multiple source-destination pairs. Instead of choosing a single path, each end user is assigned a set of possible routes over which they distribute the associated traffic to attain a given average data rate. Unlike the simple linear mapping adopted in [61], network edge latency is represented by a non-negative, non-decreasing and continuous function of the carried traffic flow. By replacing the abstracted cost function with an affine cost function, the authors of [107] prove the PoA of the modeled network is at most $4/3$. If only continuous and non-decreasing link latency functions are assumed, this study shows that the PoA may be unbounded. Another important outcome of this work is that, given continuous and non-decreasing cost function, the total latency of a data flow at NE is no more than the latency incurred by optimally routing twice the amount of data traffic.

The authors of [108] show that the existence of PoA is independent of the underlying network topology. It is shown that, with different latency cost functions, a network com-

prising only two parallel links could have a PoA larger than 1.0. Therefore, for network operators, simplifying network topologies may not improve the PoA incurred by *selfish* routing decisions adopt by network users. The concept of PoA is further investigated in [109, 110] for network congestion games considering a linear latency function with respect to the carried traffic on a network node. Given linear cost functions for all network facilities, both works conclude that the PoA is tightly bounded by a constant for the given game.

Although there is a rich literature on game theoretical analysis of data traffic routing and distribution for Internet-like communications networks, most existing research is restricted to investigating the delay-related network performance and ignore the energy efficiency of the system. For example, previous works [99, 100] regarding non-cooperative traffic scheduling mainly focus on the total system response time based on queuing theory. However, few publications have considered optimising energy consumption in a data network where end users' interactions are modelled as a non-cooperative game. In addition, the majority of research work [107–110] only take into account various delay cost functions when investigating the PoA of routing games and flow control games. To the best of our knowledge, there is no work on analysing the PoA of a network system when considering the energy consumption performance.

In this dissertation, we propose a general non-cooperative game framework for analysing energy efficiency and network performance for cloud computing in communication networks. Cloud computing is gaining importance in multimedia content delivery and other Internet applications. Many key industry players such as Amazon, Google, Apple and Microsoft have been providing cloud services to business and individual customers. The aim of cloud computing is to deliver computing and storage services hosted on hardware and software platforms such as data centres connected via telecommunication networks [111]. Many previous works on energy efficient cloud computing mainly focused on data centre servers and storages such as CPU utilisation, workload scheduling and migration as shown in [112]. Recently the authors of [113] highlighted the impact of the energy consumption of transport networks in a cloud environment. The study indicates that both academia and industry may have underestimated the energy consumption of cloud

computing. Many proclaimed "green" clouds could in fact be "dirty" under certain circumstances [113] if the energy consumption of transport networks is taken into account.

We propose a general system model for cloud-based communication networks. In contrast to the work [114] that focuses on a segment of a cloud system such as data centres, we endeavor to provide end-to-end solutions to energy-efficient traffic distribution in cloud systems, where energy consumption of data centres and transport networks are explicitly taken into account. Although improving energy efficiency of cloud systems is of paramount importance, cloud service providers are unlikely to optimise the system energy consumption only without also considering other system performance requirements. However, as pointed in [115], it is rather difficult to find a holistic approach to balance heterogeneous and even conflicting objectives. In this study, we propose a multi-objective optimisation framework for cloud computing in communication networks considering system performance parameters such as system energy consumption, server load balancing and transport network delay.

Considering the potential multi-ownership of a cloud infrastructure, we apply non-cooperative game theory to model the interactive traffic distribution and routing for multiple end users. The network resources such as servers, routers/switches and network links can be shared or exclusively allocated to end users. Each end user aims to *selfishly* optimise her/his own cost, which represents the combination of energy consumption, server load balance and transport network delay with his/her individual preference. Instead of assuming a centralised controlling mechanism, we propose a distributed algorithm by which each end user iteratively *best-responds* to opponents' data traffic distribution decision. Further, in contrast to the classic elastic traffic distribution studied in [24, 107, 109], a bandwidth constraint is introduced to assure all users' end-to-end bandwidth QoS requirement for any feasible solution. By relaxing the network resource capacity constraint and the bandwidth guarantee constraint, we show the proposed non-cooperative game admits a unique NE. To solve the game, an iterative gradient method is proposed followed by the continuous-time Lyapunov stability analysis. We calculate the PoA to investigate the efficiency loss between the proposed non-cooperative game solution and the global optimal solution. In the proposed multi-objective optimisation

framework, we not only investigate the efficiency loss of the joint objective function as specified in [107, 109], but also extend the PoA analysis to individual optimisation objectives such as system energy consumption, server load balance and transport network delay.

2.4 Energy Efficiency in Optical Core Networks with SDN

To sustain the traffic growth and fuel emerging Internet services, next-generation core networks require a major evolution to improve capacity, configurability and reliability [116]. Adopting optical technologies is widely agreed by the communication network community as a dominant approach to provide energy-efficient and cost-effective solutions to next-generation core networks [117, 118]. With the initial adoption of the optical long-haul network technology, core networks were temporally relieved from being strained in terms of capacity and QoS [116]. However, the advances of wavelength-division multiplexing (WDM) technology enable edge nodes to provide higher bandwidth to accommodate more traffic-demanding network applications [116]. As a consequence, much more data traffic will need to traverse core networks. Core networks will again become the bandwidth and operational bottleneck for the future data traffic growth [116].

The proliferation of multimedia data traffic and emergent cloud services result in far more energy consumption of core networks [3, 119]. Although several studies such as [120] claim that moving to the cloud reduce energy consumption and carbon emission, the underlying cloud infrastructure consumes a huge amount of energy. Data centres are main components of the Internet infrastructure and recent reports [2, 3] show that inter-data-centre traffic is escalating swiftly over core networks. As reported in [121], data centres consumes a large portion of electricity used by cloud applications. The study [122] conducted by Greenpeace alleges that the electricity demand of the cloud exceeds the fifth largest national demand over the world.

Many studies such as [16, 116, 123, 124] have been devoted to the energy-efficiency improvement of core networks. However, until recently, the impact of data centre traf-

fic and emerging cloud services on core networks have been largely ignored. The study [125] proposes a power consumption model for an Internet-like optical network, which comprises a video distribution network (VDN) providing multimedia severities to end customers. However the interaction between the core network and the video distribution network is not clearly specified. A more recent study [126] presents an optical cloud infrastructure including a wide-area optical network. The optimisation objective of this work is merely to minimise the total energy consumption of the system. The study [119] focuses on the energy efficiency of public cloud for content delivery over non-bypass IP/WDM core networks. In contrast to [126], this study considers more detailed conditions for core network and cloud infrastructure/service such as flow conservation constraint, link capacity constraint, core router ports aggregation, content popularity and location information.

Given the current overview of energy efficiency of core networks [116, 124, 125], there is definitely a need for a new network architecture to address the increasing power consumption of core networks. SDN is an approach breaks the vertical integration of control plane and data plane bundled inside the physical network equipment. The centralised control plane is able to gather information from different subnetworks such as optical core network and the access networks [71]. By leveraging the global information of the underlying infrastructure, SDN based networks enable energy efficient networking over a wider area while maintain QoS of different types of traffic as demonstrated in [127]. The study [128] proposes a network-wide power manager *ElasticTree* for data centres build on OpenFlow switches. By exploring the centralised network information provided by the SDN architecture, *ElasticTree* can save up to 50% of network energy, while maintaining the ability to handle normal traffic. The study [129] indicates that Openflow can enable energy-efficiency improving strategies to be deployed in carrier grade networks. However, the current Openflow protocol needs extra control messages to support the advanced power management in the switches. Later the authors of [130] designed an energy-aware traffic routing algorithm for core networks and the simulation results indicate notable energy saving by adopting the SDN technology.

Traditional core network devices are built with vendor-specific control protocols, which

make autonomous traffic forwarding decisions. Introducing new network functionalities usually requires great effort on device-by-device configuration. Such undesirable practices are time consuming and subject to human errors. Avoiding manual configuration of individual network devices, the centralised SDN control mechanism facilitates less error-prone network re-configurations and automation. This can significantly reduce the time and cost of deploying new network applications and services. Although the Generalized Multiprotocol Label Switching (GMPLS) technology also claims to support control and Data plane separation, it implements a new middle layer on individual network devices such as routers and switches to facilitate routing, traffic engineering (TE), and path computing [131]. As GMPLS evolves, it requires changes in existing protocols such as Resource Reservation Protocol (RSVP) and Link Management Protocol (LMP) [131], which leads to protocol updates for all GMPLS network devices. Such overlay structure is difficult to improve network wide stability and convergence due to fast and frequent network state changes [132, 133]. In contrast, SDN enforces control and data plane abstraction. Control plane functions are implemented in a logically centralised controller while the underlying data plane devices can be built on generic hardware platforms [71]. By consolidating control plane functions into a logically centralised controller, SDN provides flexional control plane programmability to facilitate network wide optimisation in terms of data throughput, traffic distribution and network energy efficiency, which is difficult to realise in a global optimal manner for traditional core network architectures [71, 133].

In this dissertation, an optimisation framework is proposed to distribute real-time traffic across an optical communication network in an energy efficient manner encompassing large data centres. Previous studies [22, 119, 126] assume the power consumption of core network elements are independent of the carried traffic. However, this is not entirely true as the authors of [134] show that the power consumption of a core network router is related to the carried traffic. Furthermore, with the advances of new technologies, the network equipment will become more energy-proportional, which results in increasingly energy-proportional core networks and data centres as described in [135, 136]. We apply a general power consumption model specified in Chapter 3 to an optical core

network with large data centres. By choosing a proper scaling factor β in Eq. (3.6) representing the ratio of the idle power consumption over the maximal power consumption, the power consumption of a core network elements or a data centre can be expressed in a general form as shown in Eq. (3.6).

We develop a multi-objective optimisation scheme for core networks with a-priori user-specific performance preferences on the associated network power consumption and load balance over virtual server nodes (data centres). Many works such as [21, 22] generally do not consider individual preferences on different network performance requirements. However, it is rather common that end users or network service providers have different emphasis on the various optimisation goals. Some may focus more on the energy consumption while others may concern more about the network service availability. In contrast to [21, 22], we formulate a joint traffic routing problem with user defined weights on network power consumption and inter-data-centre load balance. To address Quality of Experience (QoE) for end customers, traffic latency policy is enforced by applying user defined network delay constraints to the traffic to be distributed.

Furthermore, we adopt the emerging SDN architecture to model the propose core network. The resulting network data plane design is simple leading to standard and vendor-agonistic network devices. All the routing and switching intelligence is offloaded to the control plane in the external controller. The underlying network devices only need to do simple actions such as forwarding and dropping packets based on instructions from the control plane [77]. By leveraging the programmability of the SDN control plane, underlying "dumb" network devices are able to perform customised network functions such as routing, flow based switching and firewall [77]. This in turn simplifies the network policy enforcement, network automation and traffic engineering. New SDN advances such as in [78, 79] promote IP and optical convergence and help operators to reduce the CAPEX and OPEX of core networks.

We implement a SDN-based platform in Mininet [81], which facilitates cost-efficient and accurate network emulation for the proposed network. By leveraging the SDN technology and OpenFlow protocol [77], we have developed customised network functions such as statistical switching, multi-path routing, anycast routing and QoS-energy-aware

traffic distribution on a Mininet platform to support the proposed multi-objective core network optimisation with special focus on energy efficiency. Unlike traditional simulation tools such NS-2 and Matlab, the Mininet platform uses real networking protocols such as ARP, ICMP and TCP on virtual hardware. As a consequence, the fidelity of Mininet emulation is guaranteed to some extent, and the new network function prototype can be easily transferred to the SDN-compliant hardware platform. In addition, the resulting Mininet platform is light and can be implemented in a standard PC or a virtual machine [81]. Compared to a real testbed such as the one specified in [78], the Mininet platform is easy to setup and enables cost-efficient network function evaluation.

Chapter 3
System Model

3.1 Introduction

The explosive growth of IP networks, the proliferation of the Internet in particular, has been witnessed for the past decades. The trend is likely to continue over years to come. Nowadays, communication networking is so ubiquitous and expansive that virtually exists everywhere. The concept of ubiquitous networking promotes capabilities for exchanging information and provisioning services anytime, anywhere provided the underlying infrastructure such as communication networks and hardware platforms are available. Ubiquitous communication does not distinguish between wireline and wireless access technologies and makes our world more closely connected. From business perspectives, it erases many previous distinctions between home customers, mobile users and enterpriser users by providing seamless network access on demand.

However, ubiquitous communication results in complex and heterogeneous systems with different technologies and characteristics. Heterogeneous networking plays an important role in facilitating information dissemination, communication unification and application convergence. Many recent networking and communication technologies such as content delivery networks, wireless mesh networks, mobile ad hoc networks and machine-to-machine networks have been deployed to provide domain-specific applications and services. The heterogeneity of networks, devices and applications brings challenges to integrate different network technologies into a unified platform. In addition, it is more likely that new network technologies and applications will surface in the near future. Customising new services to a specific network or technology is not desirable.

It is challenging to analyse modern communication networks which comprise heterogeneous network elements. Further, the difficulty increases as the underlying networks become larger and more complex. The rest of this chapter will be devoted to constructing a top level network system model and a generic power consumption model for network elements.

3.2 Notation

To unify the symbol notation, a common naming rule is introduced. In this dissertation, all vectors are denoted by lowercase bold characters with $\mathbf{a}_i$ denoting the i-th element of vector $\mathbf{a}$. Unless specified elsewhere, a vector is structured in a column form. Bold-faced capital characters denote matrices with $\mathbf{A}_i$ representing the i-th row and $\mathbf{A}_{i,j}$ is the element of the i-th row and the j-th column of matrix $\mathbf{A}$ respectively. Term $\mathbf{A}_i\mathbf{a}$ stands for the inner product of the row vector $\mathbf{A}_i$ and the column vector $\mathbf{a}$. Notation $\mathbf{A}^T$ denotes the transpose of matrix $\mathbf{A}$. Term $(\mathbf{a})_{\text{diag}}$ denotes the diagonal matrix built from vector $\mathbf{a}$.

3.3 General Network Model

Modern communication networks are usually complex systems, such as the Internet, including heterogeneous components like routers, servers, links and etc. Delivering data traffic from senders to receivers is the functionality provided by all networks. Each network needs to integrate different technologies, protocols, software and hardware to successfully transfer information. It is nearly impossible to model a large-scale network, comprising many heterogeneous sub-systems, in every aspect. Using abstraction is a common way to reduce the difficulty of modeling complex communications networks. A typical example is the classical 7-layer Open Systems Interconnection model (OSI) [137], which uses abstraction layers to characterise and standardize the internal functions of a communication system. Details of the underlying entities are categorised and summarised with simplified representations. Instead of using different notations and terminologies, a few key characteristics such as bandwidth, delay and power consumption can

be adopted to describe individual elements within communication networks.

A communication network can be defined as a collection of terminal nodes, links and intermediate nodes, which use communication protocols to exchange data [138]. There are many communication network models to describe information exchange between network nodes. Some models are technology driven such as the wireless network and the wireline network [139], and some are application oriented such as the public switched telephone network (PSTN) [140] and the data centre network [141]. Based on the geographical classification criterion, there are local area networks (LANs), as well as wide area networks (WANs) [142]. Different communities adopt different network models to support their own purpose, either technology oriented or domain specific. However, modern communication networks are generally hybrid systems comprising heterogeneous sub-networks with different technologies, topologies and communication protocols [138]. Without proper abstraction, it is difficult to describe and analyse large-scale networks by using a specific network model.

One objective of this dissertation is to build a general system model for cloud-based communication networks. To construct a system model for communication networks, a set of domain generic terms needs to be defined to describe the system. To serve this purpose, an abstraction approach is adopted to model cloud-based communication networks represented by

- network topology defining the network layout and relations between network elements
- network traffic characteristics such as transmission rate, source/destination and traffic volume
- power consumption of network elements such as servers, switches, routers, links (wireless and wireline)

Fig. 3.1 shows a general communication network model used in this dissertation. The rest of this chapter will describe this model in terms of network topology, network traffic and power consumption for network elements.

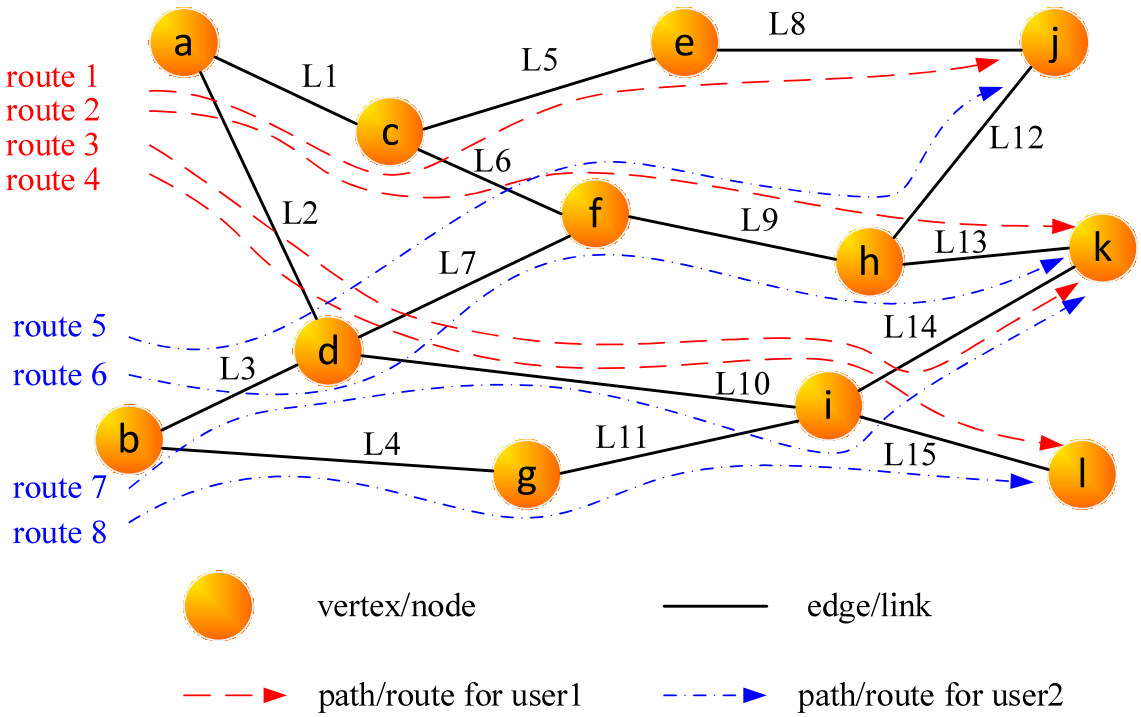

Figure 3.1: General network model

3.3.1 Network Topology

Network topology examines relationships and interconnections of network elements. Communication network topology can be physical or logical. Physical Topology describes the physical layout of switches, servers and links in the network; while logical topology focuses on the pattern of data traffic flow between network elements. The physical representation and the logical representation of a network topology may not be identical. The logical topology describes the way that data flows pass through the network. In general, network protocols and applications determine the logical topology, which can be dynamically created and reconfigured.

Fig. 3.2 illustrates some basic network topologies for communication networks. Each topology has its own advantages and disadvantages, and is usually adopted in different domains to meet specific requirements. For example, the bus topology is often used in local area networks, where each node is connected to a single cable. This topology is easy to deploy for small networks with low cost but subject to traffic congestion. Due to the centralised nature, star topology offers operation and maintenance convenience but

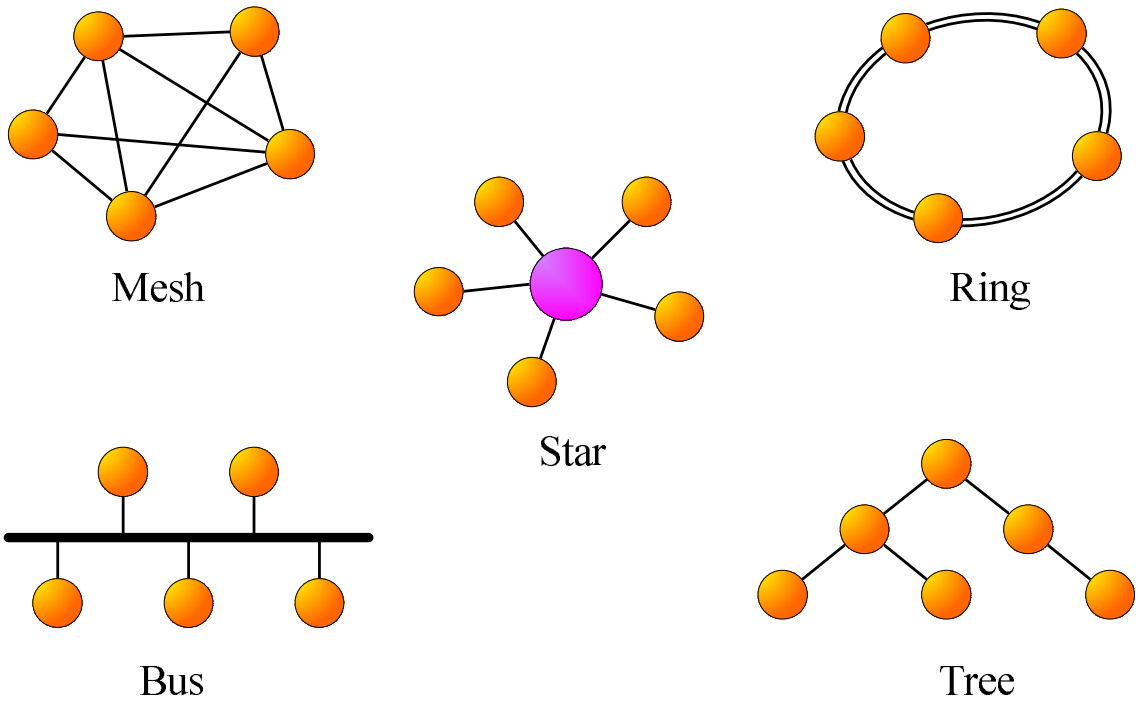

Figure 3.2: Basic network topologies

is vulnerable to single point failure. The detail description of the topologies shown in Fig. 3.2 can be found in [143].

As demonstrated in previous works such as [144], Graph theory is a field in mathematics that can be used to describe the communication network topology. Large communication networks, such as the Internet, usually have multiple topologies such as rings, trees and mesh shown in Fig. 3.2. Graph theory is a tool that allows us to describe large communication infrastructures in a concise and precise way [144]. A network can be conceptually represented by a graph that consists of a collection of vertices (nodes) connected by edges (links). Using conventional notations, a graph can be defined as follow,

Definition 3.1. *A graph is a mathematical structure denoted as* $\mathbb{G} := (\mathbb{V}, \mathbb{E})$*, where* $\mathbb{V}$ *denotes a set of vertices and* $\mathbb{E}$ *denotes a set of edges in graph* $\mathbb{G}$*. An edge* $e \in \mathbb{E}$ *is defined as* $e := \langle v, u \rangle$ *with* $v, u \in \mathbb{V}$*. In this case vertices* v *and* u *are said to be adjacent and edge* e *is said to be incident to* v *and* u*.*

Note an edge in a graph connects exactly two vertices. If those two vertices are the same, the edge will form a loop, which will not be discussed in this dissertation. On

the other hand, two adjacent vertices can have multiple edges. It is common in real networks for two nodes have parallel links for data exchange. For simplicity, only one edge between two adjacent vertices is considered in this dissertation. In Fig. 3.1, labeled circles $a \sim l$ represent vertices and $L1 \sim L16$ represent edges.

The graph representation of network topologies can provide insights to understand communication networks. A graph can be expressed in different ways. The visual demonstration by drawing circles connected by lines merely provides intuitive interpretation. Such representation seldom leads to meaningful insights to understand the associated communication networks. Also the visual representation is not feasible for displaying large communication networks such as the Internet.

In contrast, mathematical expressions can be used to describe complex graphs in a compact and precise way. The adjacent matrix and incidence matrix shown in [144] are common ways to define a graph. The adjacent matrix $\mathbf{N}$ for a graph with n vertices is a $n \times n$ symmetric matrix with $\mathbf{N}_{i_v,j_u} = 1$ if $e = \langle v, u \rangle \in \mathbb{E}$ or 0 otherwise. Terms i_v and j_u denote the row/column index for vertices v and u respectively. The incidence matrix on the other hand indicates the relationship between vertices and edges. There are n rows and m columns in an incidence matrix $\mathbf{M}$, where m denotes the number of edges. If edge e connects vertex v, $\mathbf{M}_{i_v,j_e} = 1$ or 0 otherwise. Term j_e denotes the column index for edge e. Each entity of the adjacent matrix $\mathbf{N}$ and the incidence matrix $\mathbf{M}$ only has binary values (0 or 1). In communication networks, notations for vertex and node are treated equally. Also an edge and a link both indicate the same network entity. For notation consistency, node/link in stead of vertex/edge will be used in the rest of this disseration.

The adjacent matrix and the incidence matrix representation hold some important properties, which can be used to topologically model communication networks and mathematically solve network problems such as Dijkstra's algorithm [145] and Minimal Spanning Tree (MST) algorithm [146]. However, the graph representation using the adjacent matrix and the incidence matrix mainly focuses on the connectivity of neighboring nodes. It does not explicitly show how traffic transverses the network from a source node to a sink node. In addition, the associated hop-by-hop routing mechanism does not display the relationships between the aggregated traffic and the underlying network elements

such as routers, servers and links.

Networking technologies such as multi-path routing [147] and anycast routing [148] require end-to-end representations of network topologies. Traditional network routing schemes largely focus on finding the "optimal" route to deliver all traffic from a source to a destination [147]. It is reported in [149] that flexible data traffic splitting over multiple end-to-end paths could improve the efficiency and robustness of large communication networks such as the Internet. In addition, Anycast [148] is a communication paradigm addressing IP traffic distribution from a single source to a group of receivers sharing the same destination address. Unlike the traditional hop-by-hop datagram communication, anycast applies the *flow-oriented* communication mechanism to express the *one-to-nearest* routing strategy [150]. The classical adjacent matrix or incidence matrix representation focusing on the "neighborhood" relationship is not suitable to describe those multiple end-to-end connections.

In this dissertation, path/route based matrices are used to express the relation between nodes, links and the carried data traffic. For the rest of this dissertation, path and route will be used interchangeably. A route can be defined as follow,

Definition 3.2. *A route (v, u) is an sequence of distinct nodes and links, representing a continuous traversal from source node v to sink node u.*

For example, route 1 in Fig. 3.1 can be represented by a sequence of network elements $\{a, L1, c, L5, e, L9, j\}$, which includes both nodes and links.

Consider a network has N network elements (including nodes and links) and R defined routes. The author of [24] showed that a network topology can be expressed by a N-by-R matrix $\mathbf{A}$ with

$$\mathbf{A}_{n,r} = \begin{cases} 1 & \text{if route } r \text{ includes network element } n \\ 0 & \text{otherwise} \end{cases} \tag{3.1}$$

Table 3.1 illustrates the 0-1 network element/route matrix defined in Eq. (3.1) for network topology shown in Fig. 3.1.

The binary matrix $\mathbf{A}$ defined in Eq. (3.1) demonstrates the mapping of routes on net-

Table 3.1: Network element/route matrix **A**

	*route*1	*route*2	*route*3	*route*4	*route*5	*route*6	*route*7	*route*8
a	1	1	1	1	0	0	0	0
b	0	0	0	0	1	1	1	1
c	1	1	0	0	0	0	0	0
d	0	0	1	1	1	1	1	0
e	1	0	0	0	0	0	0	0
f	0	1	0	0	1	1	0	0
g	0	0	0	0	0	0	0	1
h	0	1	0	0	1	1	0	0
i	0	0	1	1	0	0	1	1
j	1	0	0	0	1	0	0	0
k	0	1	1	0	0	1	1	0
l	0	0	0	1	0	0	0	1
*L*1	1	1	1	0	0	0	0	0
*L*2	0	0	1	1	0	0	0	0
*L*3	0	0	1	0	1	1	1	0
*L*4	0	0	1	0	0	0	0	1
*L*5	1	0	1	0	0	0	0	0
*L*6	0	1	1	0	0	0	0	0
*L*7	0	0	1	0	1	1	0	0
*L*8	1	0	1	0	0	0	0	0
*L*9	0	1	1	0	1	1	0	0
*L*10	0	0	1	1	0	0	1	0
*L*11	0	0	1	0	0	0	0	1
*L*12	0	0	1	0	1	0	0	0
*L*13	0	1	1	0	0	1	0	0
*L*14	0	0	1	0	0	0	1	0
*L*15	0	0	0	1	0	0	0	1

work elements. However, it does not directly show sources of those routes. As shown in Fig. 3.1, there are 2 source nodes (node *a* and node *b*) which initiate 8 routes leading to 3 sink nodes. Each source node distributes its input traffic over the allocated routes towards the corresponding sink nodes. Considering a network with J source nodes, we use a $J \times R$ routing matrix

$$\mathbf{B}^{\mathrm{rt}}_{j,r} = \begin{cases} 1 & \text{if route } r \text{ is originated from network node } j \\ 0 & \text{otherwise} \end{cases} \tag{3.2}$$

Table 3.2: Network source/route matrix $\mathbf{B}^{\text{rt}}$

	*route*1	*route*2	*route*3	*route*4	*route*5	*route*6	*route*7	*route*8
a	1	1	1	1	0	0	0	0
b	0	0	0	0	1	1	1	1

to represent the mapping between source nodes and all feasible routes. Fig. 3.2 illustrates the 0-1 source/route matrix defined in Eq. (3.2) for the network topology shown in Fig. 3.1. Note $\mathbf{B}^{\text{rt}}$ is a sub-matrix of $\mathbf{A}$. From $\mathbf{B}^{\text{rt}}$ and $\mathbf{A}$, we can derive a binary J-by-N source/element mapping matrix

$$\mathbf{B}^{\text{res}} = \begin{bmatrix} \mathbf{B}^{\text{res}}_{1,1} & \cdots & \mathbf{B}^{\text{res}}_{1,N} \\ \vdots & \ddots & \vdots \\ \mathbf{B}^{\text{res}}_{J,1} & \cdots & \mathbf{B}^{\text{res}}_{J,N} \end{bmatrix} = \left(\mathbf{B}^{\text{rt}}\mathbf{A}^T > 0\right) \tag{3.3}$$

where $\mathbf{B}^{\text{res}}_{j,n} = 1$ indicates there is a route linking source node j and network element n. Operation $>$ is an element-wise Boolean process such that a positive matrix entity is mapped to 1 and 0 otherwise.

One obstacle of with using the element-route matrix in Eq. (3.1) is the size of the matrix. Without dimension reduction, the total number of entities in the matrix is $N \times R$. This matrix representation of network topologies is not efficient to handle networks with large number of network elements and routes. Note for large network topologies it is less likely that each network element will carry many routes and each route will traverse many network elements. This indicates that the element-route matrix is more likely to be sparse for those topologies. Then one possible solution is to use the concept of "edge list" described in [144] to efficiently store the matrix for further processing. Ignoring the detail implementation, we use the element-route matrix specified in Eq. (3.1) to describe network topologies in the rest of this dissertation.

3.3.2 Network Traffic

Modern communication networks such as the Internet are marked by the exploding volume of data traffic, the unprecedented data traffic variations and the wide variety of net-

work applications. Attaining accurate estimation of network performance is crucial to successfully deploy network services [151]. The key to success in designing and operating complex communication networks lines in detailed understanding of network traffic characteristics. To better accommodate network services and applications, it is vital to analyse the interaction between network topologies and the carried data traffic.

Previous studies such as [152] have proposed different models to facilitate network traffic analysis. The Poisson queuing model pioneered by Erlang [153] is one of the most widely used traffic model in literatures. In the classical Poisson traffic model, random packet arrival is assumed with a mean arrival rate and the packet inter-arrival times are exponentially distributed. Poisson models are memoryless such that the current status of a Poisson process is independent of the previous status of the process. The exhibited mathematical properties make Poisson models suitable for analysing traffic in traditional telephony networks [152].

In order to design and operate complex communication networks, it is of critical importance to understand the corresponding traffic pattern and traffic volume. Traditional discrete-event packet-based approaches assume that the arrival of a single data packet is a separate event [152]. Those methods have advantages in revealing the microscopic interactions between individual packets, and are predominantly adopted in traffic queuing analyses and traffic congestion control [151, 152, 154]. However, due to the inherent computational complexity, the packet based model does not scale well as the number of network nodes increases [155]. In addition, the study of [152] has shown that Poisson-based models cannot capture all network traffic characteristics.

Fluid flow model as an alternative approach has been adopted in previous works [101, 102, 156–159] to describe the average macroscopic behaviour of networks. Traffic of data networks is different to that of telephonic networks in that the time scale of flow dynamics is much longer than the time scale of the packet level [102]. In fluid-based models, network traffic is represented as continuous packet streams with a finite flow/stream rate. Therefore incoming discrete packets can be modeled as continuous data flows with rates varying with time. Fig 3.3 illustrates the relation between discrete packets and fluid flows. Note data packets are grouped in chunks of data such that all packets in a data

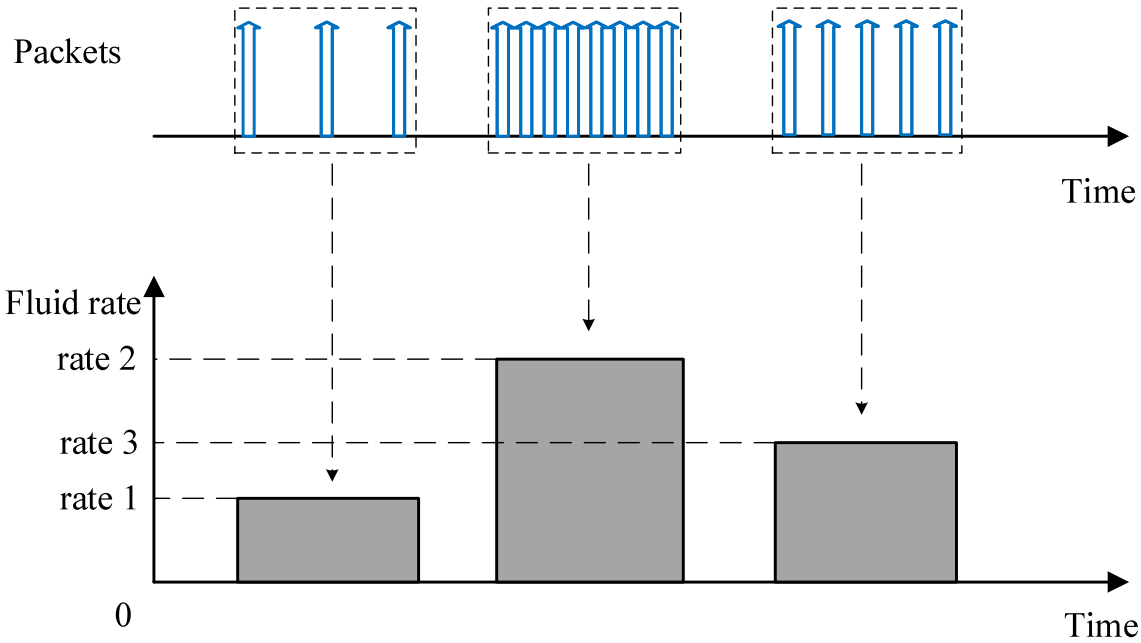

Figure 3.3: Fluid stream from discrete packets

chuck will have the same transmission rate. As a consequence, the fluid model is deterministic and thus unable to directly investigate the effects of random arrivals as well as packet level information such as jitter [159, 160]. However, it is reported in [159] that fluid-based models can predict the behaviour of large networks with reasonable accuracy and high efficiency. The continuous nature of the fluid model also makes it suitable for network congestion control and analysis [161]. By abstracting out the small time-scale variations in the packet arrival stream, the fluid mode only needs to track the traffic rate change due to queueing, multiplexing and data generation [158].

In this dissertation, network data traffic is modeled as fluid flows with different transmission rate. Consider the network topology in Fig. 3.1. Assume at time t traffic sources $j \in \{1, \cdots, J\}$, generate an aggregated data traffic with a data rate $\mathbf{d}_j^{\text{in}}(t)$ such that traffic generated by all sources nodes can be expressed a vector $\mathbf{d}^{\text{in}}(t) = [\mathbf{d}_1^{\text{in}}(t), \cdots, \mathbf{d}_J^{\text{in}}(t)]^T$. Without losing generality, the time t will be omitted in the following sections unless specified otherwise. Each input traffic $\mathbf{d}_j^{\text{in}}$ will be split into multiple sub-flows with each sub-flow mounted on a available route r determined by the binary matrix $\mathbf{B}^{\text{rt}}$ defined in

Eq. (3.2) such that

$$\mathbf{d}_j^{\text{in}} = \sum_{r=1}^{R} \mathbf{B}_{j,r}^{\text{rt}} \mathbf{d}_r \tag{3.4}$$

where traffic $\mathbf{d}_r$ denotes the sub-flow carried by route r such that the traffic on all routes can be expressed as a vector $\mathbf{d} = [\mathbf{d}_1, \cdots, \mathbf{d}_R]^T$. Given the element-route matrix $\mathbf{A}$ specified in Eq. (3.1) and the traffic vector $\mathbf{d}$, the aggregated traffic load on network element n can be expressed as,

$$\mathbf{d}_n^{\text{res}} = \sum_{r=1}^{R} \mathbf{A}_{n,r} \mathbf{d}_r \tag{3.5}$$

Then all aggregated traffic on network elements can be expressed as a vector $\mathbf{d}^{\text{res}} = [\mathbf{d}_1^{\text{res}}, \cdots, \mathbf{d}_N^{\text{res}}]^T$.

3.3.3 Network Element Power Consumption Model

The issue of energy consumption is now drawing the attention of the ICT industry to the sustainable growth of communication and data networks [3]. Network operators in particular have a strong motivation to reduce the operational expenditure (OPEX) associated with the ever growing network power consumption [11]. Modern communication networks encompass many heterogeneous network elements such as switches, routers, optical cross-connects (OXCs) and optical transceivers. It is becoming increasingly important to understand the cumulative power consumption of the various network elements so as to improve the energy efficiency of communication networks.

Describing energy consumption of network elements requires a benchmark model with a sufficient level of accuracy. Network equipment is more likely made from different vendors with a range of proprietary functionalities. Network equipment is generally complex and comprising different components. For instance, a core network router comprises a main chassis, multiple line cards, memories, processors and cooling components. As shown in [162], there are various factors contributing the total power consumption of a switch/router such as,

- Power consumption of the base chassis
- Number of line cards plugged in the chassis

- Number active ports in the line card and the corresponding configuration
- Power consumption of ternary content-addressable memory (TCAM)
- Data traffic characteristics such as packet size and inter-packet delay

As network equipment becomes more energy-proportional, the power consumption of packet processing equipment is more related to the carried IP traffic [162]. Currently data sheets for network devices merely specify the required power supply. This vale alone does not reflect the true power consumption of network equipment under various operational conditions. In some cases, the difference between the maximal power consumption and the operational power consumption can be as much as 70% of the maximal rated power consumption as reported in [162]. It is indicated in [134, 162, 163] the energy consumption of switches/routers varies under different traffic load and line cards/ports configurations. It is worth noting that the number of active line cards and ports is also related to the traffic load to some extent. For example, consider a switch with 2 line cards each having 10 Gbps switching capacity. If the input traffic is 5 Gbps, it is possible to active only one line card to accommodate the traffic load. If the input traffic grows to 15 Gbps, it is more likely that both line cards need to be energized to handle the increased traffic load.

The power consumption of circuit switching related network elements may have little or no relationship to the carried traffic. Optical links are typical network elements with power consumption independent of the carried traffic as reported in [164]. By using advanced photonic technologies such as Micro Electrical Mechanical System (MEMS), the photonic-switching-based optical cross connect (OXC) is more energy efficient than the electrical-switching-based digital cross connect (DXC) as shown in [165]. The corresponding power consumption depends on the internal fabrication, O/E/O conversion and the number of ports.

In this dissertation, a general affine function is proposed to model the power consumption of a network element $n = 1, \cdots, N$ as shown in Fig. 3.4,

$$P_n = \beta_n P_n^{\max} + (1 - \beta_n) \frac{\mathbf{d}_n^{\text{res}}}{\mathbf{C}_n} P_n^{\max} = \bar{P}_n + \hat{P}_n \tag{3.6}$$

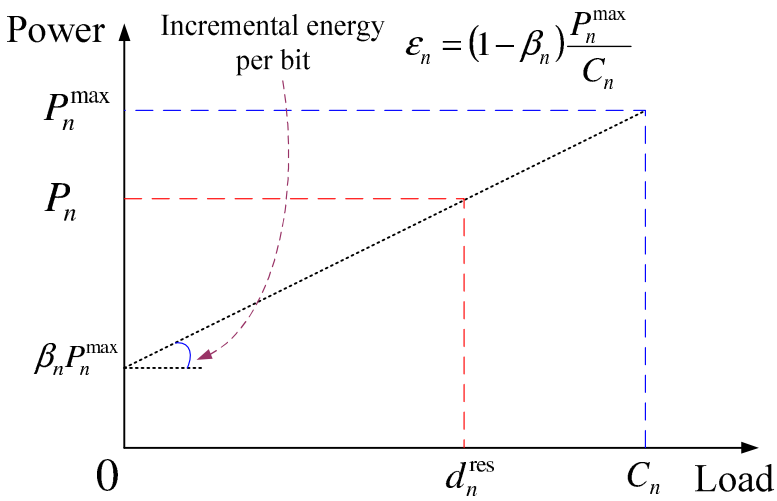

Figure 3.4: General power vs. traffic load model for network element

where β_n is a scaling factor, $P_n^{\max}$ represents the maximal power consumption of the element in Watts with full load $\mathbf{d}_n^{\text{res}} = \mathbf{C}_n$ and $\bar{P}_n = \beta_n P_n^{\max}$ denotes the idle power consumption with zero load. The slope $\mathcal{E}_n$ (nJ/b) expressed as

$$\mathcal{E}_n = (1-\beta_n)\frac{P_n^{\max}}{\mathbf{C}_n} \tag{3.7}$$

denotes the incremental energy per bit [166]. Consider the aggregated traffic load on network element n with $\mathbf{d}_n^{\text{res}} = \mathbf{A}_n\mathbf{d}$. The corresponding incremental power consumption can be expressed as

$$\hat{P}_n = (1-\beta_n)\frac{\mathbf{A}_n\mathbf{d}}{\mathbf{C}_n}P_n^{\max}. \tag{3.8}$$

Using different scaling factors β_n, the model specified in Eq. (3.6) can be used to describe the power consumption for both packet processing related network elements and circuit switching related network elements. Choosing $\beta_n = 1$, the resulting power consumption for network element n only comprises the idle power consumption $\bar{P}_n$. The model with this configuration is suitable to describe the power consumption of circuit switching related network elements such as optical links and OXCs [167]. As β_n reduces to zero the network element becomes energy-proportional [168]. Idle power consumption $\bar{P}_n$ incurs when $\beta_n > 0$. With this configuration, Eq. (3.6) can be used to model the

power consumption of packet processing related network elements such as routers and switches.

The idle power consumption $\beta_n P_n^{\max}$ for network equipment n in Eq. (3.6) is independent of the traffic load $\mathbf{d}_n^{\text{res}}$. If the network element only carries traffic from a single user or a single service, one could claim that the idle power is consumed by that user or service. With data traffic from multiple sources, we modify the idle power consumption modeled by Eq. (3.6) to distribute the idle power over the different sources.

One approach is to divide the idle power over all sources such that traffic from each source accounts for an equal share of the idle power. Then for user j, the allocation of idle power of network element n is given by

$$\bar{P}_{n,j} = \mathbf{B}_{j,n}^{\text{res}} \frac{\bar{P}_n}{\sum_{l=1}^{J} \mathbf{B}_{l,n}^{\text{res}}} \tag{3.9}$$

However, such idle power allocation is independent of the traffic from each source, and may be considered unfair for unequal traffic from difference sources. In addition, the mapping $\mathbf{B}_{j,n}^{\text{res}}, j = 1, \cdots, J$ needs to be known apriori in order to derive the portion of the idle power allocated to each resource. Therefore, this method seems not to be the ideal approach to study the effective power consumption of traffic from different sources on a network element.

To provide fair allocation of the idle power, a power consumption approximation model modifying Eq. (3.6) is proposed in this dissertation as shown in Fig. 3.5. To improve network service availability and avoid traffic overloading on a individual network equipment, network operators are reluctant to operate each network equipment at full capacity. For example, the CPU utilisation ratio for CISCO routers is recommended to set at 60% of the maximal capacity [169]. In this dissertation, we introduce a network element capacity utilisation ratio $\rho_n^{\text{res}} = \frac{\mathbf{d}_n^{\text{res}}}{\mathbf{C}_n}$ to approximate the idle power consumption $\bar{P}_n$ for network element n. Note this ratio can be predefined based on the network operator's preference or it can be measured dynamically based on the aggregated traffic. The

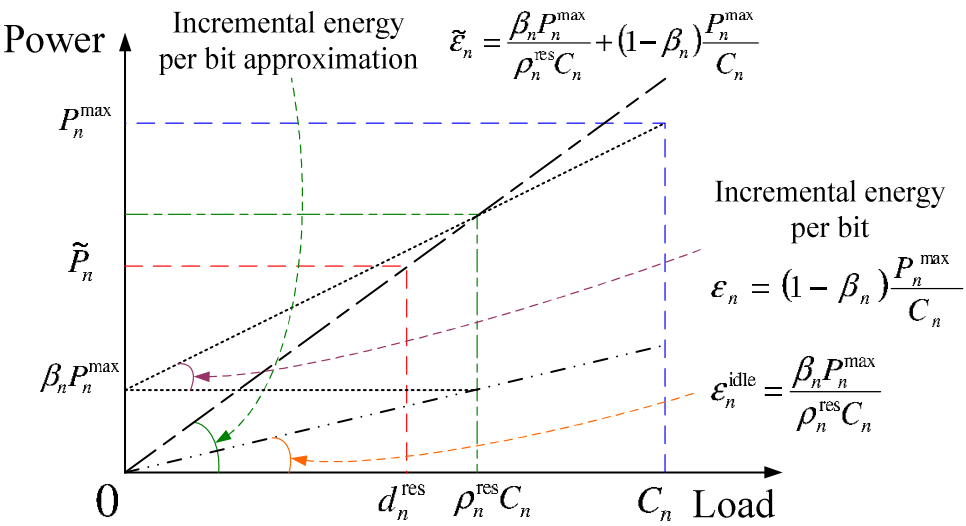

Figure 3.5: General power vs. traffic load approximation model for network element

power consumption in Eq. (3.6) is replaced by

$$\tilde{P}_n = \tilde{\mathcal{E}}_n \mathbf{d}_n^{\text{res}} = (\mathcal{E}_n^{\text{idle}} + \mathcal{E}_n)\mathbf{d}_n^{\text{res}} \tag{3.10}$$

where the slope $\tilde{\mathcal{E}}_n$ denotes the effective incremental energy per bit as shown in Fig. 3.5, and comprises two items $\mathcal{E}_n^{\text{idle}}$ and $\mathcal{E}_n$. Term $\mathcal{E}_n$ is the incremental energy per bit defined in Eq. (3.7). The slope $\mathcal{E}_n^{\text{idle}}$ is the energy per bit for the idle power based on the capacity utilisation ratio ρ_n^{res} with

$$\mathcal{E}_n^{\text{idle}} = \frac{\beta_n P_n^{\max}}{\rho_n^{\text{res}} \mathbf{C}_n} \tag{3.11}$$

By introducing the capacity utilisation ratio ρ_n^{res}, the power consumption including the idle power for network element n can be decomposed over all sources such that

$$\tilde{P}_n = \sum_{j=1}^{J} \mathbf{B}_{j,n}^{\text{res}} (\mathcal{E}_n^{\text{idle}} + \mathcal{E}_n)\mathbf{d}_j^{\text{in}} \tag{3.12}$$

where $\mathbf{B}_{j,n}^{\text{res}} \mathcal{E}_n^{\text{idle}} \mathbf{d}_j^{\text{in}}$ denotes the corresponding share of idle power consumption due to traffic from source j.

3.4 Summary

A graph theory based representation of network topologies has been adopted in this dissertation to mathematically describe complex communication networks. The generic vertex-edge (node-link) and path (route) notations are used to represent networks in a concise manner. Unlike the adjacent matrix and the incidence matrix described in [144], an element-route matrix shown in Eq. (3.1) is adopted in this dissertation to describe communication network topologies. This matrix can explicitly show how traffic traverses the network from a source node to a destination node in a flow-oriented fashion. This expression also facilitates expressing the aggregated traffic on individual network element.

A fluid flow model has been adopted in this dissertation to characterise the data traffic carried by communication networks. This model aggregates groups of data packets into continuous data streams. Although the packet-level information is lost by such aggregation, this approximation allows the fluid model to scale over large networks [101] where packet-based models usually do not. In this dissertation, network traffic is modeled as fluid such that different traffic flows carried by a network element can be aggregated in an additive way. This traffic load representation will be applied in the following chapters to investigate network power consumption, server load balance and network latency.

A general power consumption model for network elements has been proposed in this dissertation to account for the idle power when the element is energised and the incremental power associated with the carried traffic. By choosing the appropriate value for β this model can be used to model the power consumption for both packet-processing based network elements and circuit-processing based network elements. We will use this model in Chapter 6.

By introducing the network element capacity utilisation ratio ρ^{res}, the proposed power consumption model distributes the idle power allocation over traffic from different sources. This model will facilitate network element power consumption decomposition in order to study the contrition of individual traffic to the power consumption of a network element. This power consumption model will be used in Chapter 4 and Chapter 5.

Chapter 4

A Distributed Optimisation Framework for Energy Efficiency of Backhaul Traffic in Mobile Networks

4.1 Introduction

In this chapter, we present a detailed analysis of improving the energy efficiency of mobile backhaul networks, while considering load balance over Serving Gateways (S-GWs). In the previous chapter we have developed a network topology model based on graph theory and a general power consumption model for network elements. A fluid flow model described in Section 3.3.2 is applied in this chapter to investigate backhaul network power consumption and S-GWs load balance. As explained in Section 1.1, the distributed optimisation framework specified in Section 1.2.1 is chosen to improve the energy efficiency of backhaul networks. We aim to address challenges $1 \sim 3$ in 1.1 and provide possible solutions to those problems. To better explain those challenges, we start with the motivation to improve energy efficiency of mobile backhaul networks.

Global mobile data traffic is projected to increase nearly 11-fold between 2013 and 2018 [4] as global IP traffic enters an estimated 1.4 zettabytes per year in 2017. Improving the efficiency of mobile networks – in terms of energy consumption and traffic flow – is key to sustaining the growing traffic demand [3], because it is recognised that Base Stations (BS) have high per-bit energy consumption [170], and dramatic growth in wireless IP traffic can lead to severe network congestion and service request rejection rates [10].

Prior work on energy efficiency of mobile networks is focused on Radio Access Net-

works (RAN) because the energy consumption of base stations dominate the total energy consumption of current mobile networks [19]. However, this situation could change for next-generation mobile networks where large numbers of small cells [171] will be deployed to meet the increasing demand for coverage and capacity. The move to smaller cells to augment existing macro mobile networks is widely viewed as a potential solution to the RAN congestion problem. But it also creates a new one: that of backhaul capacity [93]. Driven by increasing demand for mobile data, backhaul requirements for small cells are expected to approach macro cell capacity requirements in the years to come [93].

New RAN technologies such as LTE demand very large "backhaul pipes", requiring mobile service providers to plan for more than 100 Mbit/s backhaul capacity per site [91]. By addressing the limitations of the traditional RANs, China Mobile has promoted C-RAN [172], a new concept of implementation and deployment of RAN with a "cloud" architecture, which introduces significant backhaul traffic. Innovations such as small base stations, Remote Radio Head (RRH) such as the lightRadio™"Cube" [97] and the GreenTouch consortium's "road-map" [3] means that the proportion of energy consumption for backhaul will increase significantly relative to the total energy consumption of the system.

In this chapter, we propose an optimisation framework for distributing traffic across a mobile backhaul network in an energy efficient manner. A multi-objective optimisation scheme is developed to explore independent, and possibly conflicting, system requirements. We implement a generic weighted-sum scheme to provide flexible controls over different optimisation objectives. Previous work on traffic distribution has mainly focused on the total system response time, based on queuing theory such as in [100]. However, little work has been done to jointly consider both load balancing and energy efficiency for traffic distribution in mobile backhaul networks.

Our optimisation objectives of system power consumption and traffic load balancing are applied to evaluate the allocation of traffic in the mobile backhaul. Centralised solutions such as mixed integer programming [21] are usually NP-hard and difficult to scale [32, 33]. We develop a distributed algorithm for mobile data traffic distribution, which requires no centralised information and has the benefit of distributing the computational

load over the network. In contrast to the game theoretical solution described in Chapter 5, we propose a distributed optimisation solution discussed in Section 1.2.1 to improve energy efficiency of mobile backhaul networks in this chapter. The primary reason is that mobile network operators manage backhaul networks and data traffic processing resources. Mobile service end users are not able to control how their traffic is routed and processed over backhaul networks. Generally, there is no direct interaction between end users. It is mobile network operators' interest to distribute data traffic in an energy efficient manner because they are directly responsible for the resulting operational cost in terms of energy consumption. Therefore, as mentioned in Section 1.1, we do not adopt the game theoretical solution in this chapter to solve the problem in Section 4.3. Given the proposed distributed algorithm, system performance for several optimisation scenarios is examined and compared using numerical simulations. The simulation results provide insights into improving the energy efficiency and maintaining the desired service quality in mobile networks.

The rest of this chapter is organised as follows. In Section 4.2, we introduce the system model. The multi-objective optimisation framework is developed in Section 4.3. The distributed approach for solving the optimisation is presented in Section 4.4 and its stability analysis is conducted in Section 4.5. The detailed simulation results are described in Section 4.7 and this chapter is concluded in Section 4.8.

4.2 System Model

In this chapter, we consider a general system model, which consists of J evolved NodeBs (eNodeB), M virtualised intermediate multiplexing/aggregation (MUX) nodes and I virtualised Serving Gateway (S-GW) nodes in the RAN, the backhaul network and the core network respectively. In Fig. 4.1, we show the set of MUX nodes and the set of S-GW nodes located in the Backhaul Network (BN) and Evolved Packet Core (EPC) respectively. For simplicity we consider zero buffer size for both S-GW nodes and MUX nodes. The network has L links connecting eNodeBs and S-GWs via MUX nodes. Table 4.1 summaries the notation used in this chapter. The system has in total $N = I + M + L$

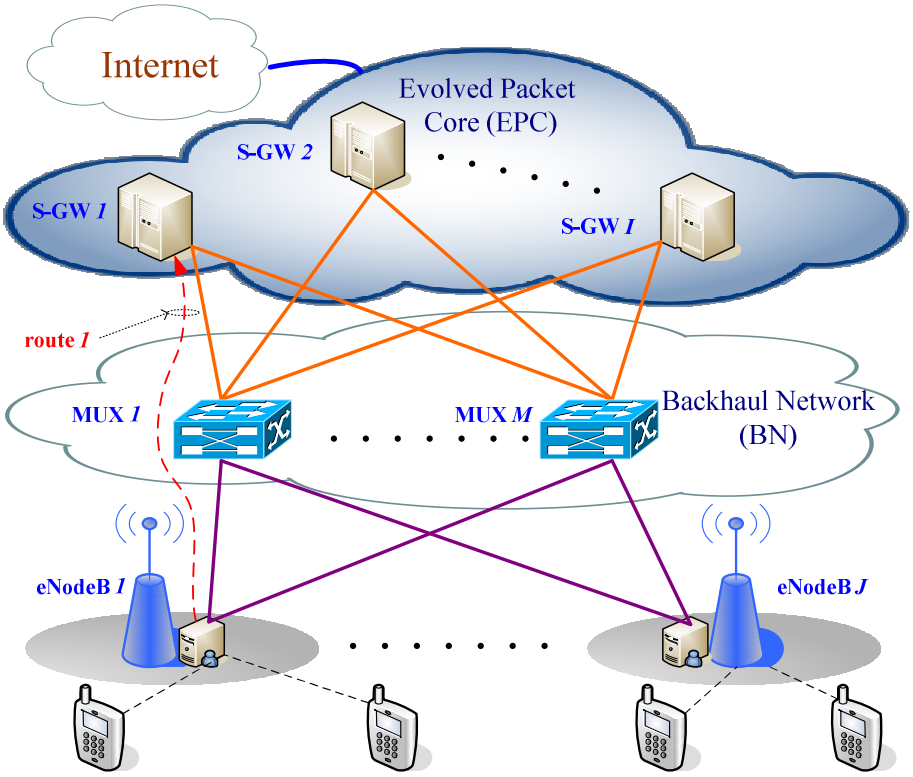

Figure 4.1: System model for mobile backhaul networks with 2 eNodeB, 2 MUX and 3 S-GW nodes.

resources for eNodeBs [1] to share. Each *resource* is characterised by the maximum data traffic processing capacity $\mathbf{C}_n$ with $n = 1, \cdots, N$. At time t eNodeB $j = 1, \cdots, J$, generates aggregated data traffic with data rate $\mathbf{d}_j^{\text{in}}(t)$ such that all traffic generated by eNodeBs can be expressed as a vector $\mathbf{d}^{\text{in}}(t) = [\mathbf{d}_1^{\text{in}}(t), \cdots, \mathbf{d}_J^{\text{in}}(t)]^T$. Note the aggregated data traffic from each S-GW is slowly changing over a diurnal cycle. We assume $\mathbf{d}^{\text{in}}(t)$ is fixed during a short period. For simplicity we omit the time index notation t for the rest of the chapter. Let $r = 1, \cdots, R$ be the index of predefined routes each carrying average traffic $\mathbf{d}_r$ from a eNodeB to a S-GW such that the traffic on all routes can be expressed as a vector $\mathbf{d} = [\mathbf{d}_1, \cdots, \mathbf{d}_R]^T$. Fig. 4.1 illustrates the route 1 from eNodeB 1 to S-GW 1 via MUX 1. Each eNodeB then distributes its traffic $\mathbf{d}_j^{\text{in}}$ over a subset of Ω_R to the designated S-GWs. We use the $J \times R$ routing matrix $\mathbf{B}^{\text{rt}}$ defined in Eq. (3.2) of Section 3.3.1 to illustrate the mapping between eNodeBs j and routes such that $\mathbf{B}_{j,r}^{\text{rt}} = 1$ indicates eNodeB can dispatch

[1] In [98], each eNodeB can connect to its neighbour eNodeB via its X2 interface to share traffic load. For simplicity we ignore the X2 interface in this chapter.

Table 4.1: Term Notation

Term	Explanation
J	Number of eNodeB nodes
M	Number of MUX nodes
I	Number of S-GW nodes
L	Number of links connecting nodes
N	Number of resources including S-GWs, MUXs and links with $N = I + M + L$
R	Number of routes from eNodeBs to S-GWs
$\mathbf{C}$	Vector of network *resource* maximum capacity $\mathbf{C}_n$ for all S-GWs, MUX nodes and links
Ω_R	Set of routes indexed by $r = 1, \cdots, R$ with each carrying traffic $\mathbf{d}_r$
$\mathbf{B}^{\text{rt}}$	0-1 matrix mapping R routes to J eNodeBs
$\mathbf{A}$	0-1 matrix mapping R routes to N *resources* with sub-matrices $\mathbf{A}^{\text{sgw}}$ and $\mathbf{A}^{\text{mux}}$
$\mathbf{d}^{\text{in}}$	Vector of input traffic with the entity $\mathbf{d}_j^{\text{in}}$ as the traffic generated by eNodeB j
$\mathbf{d}$	Vector of traffic $\mathbf{d}_r$ carried by route $r = \{1, \cdots, R\}$
$\mathbf{d}^{\text{res}}$	Vector of aggregated traffic $\mathbf{d}_n^{\text{res}}$ on *resource* $n = 1, \cdots, N$ with sub-vectors $\mathbf{d}^{\text{sgw}}$ and $\mathbf{d}^{\text{mux}}$

traffic via route r while $\mathbf{B}_{j,r}^{\text{rt}} = 0$ indicates otherwise. This in turn indicates $\mathbf{d}^{\text{in}} = \mathbf{B}^{\text{rt}}\mathbf{d}$. In addition, the topology of the system in Fig. 4.1 can be represented by the $N \times R$ matrix $\mathbf{A}$ defined in Eq. (3.1) of Section 3.3.1. Let $\mathbf{d}_n^{\text{res}}$ be the aggregated traffic at *resource* n such that all aggregated traffic on S-GW nodes, MUX nodes and links can be expressed as a vector $\mathbf{d}^{\text{res}} = [\mathbf{d}_1^{\text{res}}, \cdots, \mathbf{d}_N^{\text{res}}]^T$. The relationship between the aggregated traffic on each *resource* and the traffic on each route can be expressed as $\mathbf{d}^{\text{res}} = \mathbf{A}\mathbf{d}$.

4.3 Problem Formulation

Guided by the network utility maximisation (NUM) problem in [24], we formulate a traffic distribution problem in order to find the optimal traffic for each eNodeB to dispatch over the predefined routes through the BN to EPC such that the associated cost function is minimised. We propose a joint cost function where two potentially conflicting objectives are considered: (1) total system power consumption minimisation and (2) system

traffic load balancing. We assume a fixed number of network elements including S-GWs, MUXs and backhaul links are provisioned. How many network elements will be energised depends on the traffic carried and the energy-saving/load-balance criteria.

4.3.1 Power Consumption Objective

Today, network equipment is always turned on, even if the carried traffic is nearly zero [173]. Given the traffic diurnal cycle, the author of [174] proposed a system-wide solution such that the inactive network equipment carrying no data traffic can be completely switched off to improve the system energy efficiency. We use P_n defined in Eq. (3.6) of Section 3.3.3 to model the power consumption of network element $n = 1, \cdots, N$. Optimising the total power consumption $\sum_{n=1}^{N} P_n$ including each equipment's idle power shown in (3.6) is classified as a mixed-integer programming problem [21, 22], which is NP-hard [32]. We apply Eq. (3.10) of Section 3.3.3 to model the power consumption of a network equipment such that the idle power of a network element can be approximately amortised over different traffic flows carried by the element. Therefore, the normalised system power consumption approximation can be expressed as,

$$\tilde{P}_{\text{sys}}(\mathbf{d}) = \frac{\sum_{n=1}^{N} \tilde{P}_n}{P^{\max}} \tag{4.1}$$

where $\tilde{P}_n$ denotes the power consumption approximation defined in Eq. (3.10).

4.3.2 Load Balance Objective

Load Balancing (LB) is one of the important features of Self-Organising Networks (SON) for LTE as indicated in [175]. Unbalanced traffic load can cause throughput degradation and result in suboptimal utilisation of network resources. In this chapter, the load balancing objective addresses the traffic throughput of the various EPC and MUX nodes. Let $T = \sum_{j=1}^{J} \mathbf{d}_j^{\text{in}}$ be the total traffic generated by all eNodeBs. Assume all traffic shall be forwarded in the BN and processed in the EPC, which leads to a system throughput $\sum_{i=1}^{I} \mathbf{d}_i^{\text{sgw}} = T$. Let $\mathbf{C}_{\text{sys}}^{\text{sgw}} = \sum_{i=1}^{I} \mathbf{C}_i^{\text{sgw}}$ and $\mathbf{C}_{\text{sys}}^{\text{mux}} = \sum_{m=1}^{M} \mathbf{C}_m^{\text{mux}}$ denote the total processing capability of the S-GWs and MUXs respectively. Define the load balanced condition over

all S-GWs in the EPC and all MUX nodes in BN respectively as,

$$\eta_1^{\text{sgw}} = \eta_2^{\text{sgw}} = \cdots = \eta_I^{\text{sgw}} = \frac{T}{\mathbf{C}_{\text{sys}}^{\text{sgw}}} \tag{4.2}$$

$$\eta_1^{mux} = \eta_2^{mux} = \cdots = \eta_M^{mux} = \frac{T}{\mathbf{C}_{\text{sys}}^{\text{mux}}} \tag{4.3}$$

where $\eta_i^{\text{sgw}} = \frac{\mathbf{A}_i^{\text{sgw}}\mathbf{d}}{\mathbf{C}_i^{\text{sgw}}}$ and $\eta_m^{mux} = \frac{\mathbf{A}_m^{\text{mux}}\mathbf{d}}{\mathbf{C}_m^{\text{mux}}}$ denotes the normalised load for S-GW i and MUX m respectively. The load balancing condition is defined by using the normalised utilisation rather than the absolute throughput traffic to provide a simple mathematical condition that automatically accounts for network elements with different maximum capacities. To address complex networks in which h is the number of hops averaged across all routes in the network, the load balance condition in (4.3) is replaced by $\frac{hT}{\mathbf{C}_{\text{sys}}^{\text{mux}}}$ [125].

However, maintaining the load balanced condition illustrated in (4.2) and (4.3) is not easy for a large-scale system. In order to handle this challenge, we propose an alternative implementation of load balancing by introducing a normalised load balancing variance over S-GW and MUX nodes as,

$$S(\mathbf{d}) = \frac{1}{\hat{S}I}\sum_{i=1}^{I}\left(\frac{\mathbf{A}_i^{\text{sgw}}\mathbf{d}}{\mathbf{C}_i^{\text{sgw}}} - \frac{T}{\mathbf{C}_{\text{sys}}^{\text{sgw}}}\right)^2 + \frac{1}{\hat{S}M}\sum_{m=1}^{M}\left(\frac{\mathbf{A}_m^{\text{mux}}\mathbf{d}}{\mathbf{C}_m^{\text{mux}}} - \frac{hT}{\mathbf{C}_{\text{sys}}^{\text{mux}}}\right)^2 \tag{4.4}$$

where $\hat{S}$ denotes the upper bound [2] of the load balancing variance for both S-GW and MUX nodes. $\sigma^{\text{sgw}} = \left[\frac{1}{\hat{S}I}\sum_{i=1}^{I}\left(\frac{\mathbf{A}_i^{\text{sgw}}\mathbf{d}}{\mathbf{C}_i^{\text{sgw}}} - \frac{T}{\mathbf{C}_{\text{sys}}^{\text{sgw}}}\right)^2\right]^{\frac{1}{2}}$ and $\sigma^{\text{mux}} = \left[\frac{1}{\hat{S}M}\sum_{m=1}^{M}\left(\frac{\mathbf{A}_m^{\text{mux}}\mathbf{d}}{\mathbf{C}_m^{\text{mux}}} - \frac{hT}{\mathbf{C}_{\text{sys}}^{\text{mux}}}\right)^2\right]^{\frac{1}{2}}$ denote the corresponding normalised standard deviation (STD). Minimising the load balancing variance leads to (4.2) and (4.3).

4.3.3 Multi-objective Optimisation

Given fixed input traffic $\mathbf{d}^{\text{in}}$, the objective of minimising the system power consumption tends to direct data traffic $\mathbf{d}$ to the more energy efficient S-GWs via energy efficient links while the objective of minimising the load balancing variance tends to distribute data

[2] The extreme case that all traffic directed to only one S-GW via only one MUX with each having a capacity the same as the total traffic.

traffic $\mathbf{d}$ over all S-GW and MUX nodes. To compromise between the two objectives in (4.1) and (4.4), we apply the weighted sum method to construct the joint problem :

$$\min_{\mathbf{d}} U(\mathbf{d}) = \min_{\mathbf{d}} \left((1-\omega)\tilde{P}_{\text{sys}}(\mathbf{d}) + \omega S(\mathbf{d})\right) \tag{4.5}$$

$$\text{subject to } \mathbf{B}^{\text{rt}}\mathbf{d} = \mathbf{d}^{\text{in}} \tag{4.6}$$

$$\mathbf{A}\mathbf{d} \leq \mathbf{C} \tag{4.7}$$

$$0 \leq \mathbf{d} \tag{4.8}$$

where $0 \leq \omega \leq 1$ denotes the weight between power consumption and load balancing. The first constraint (4.6) indicates the input traffic flow conservation, the constraint (4.7) indicates that the aggregated traffic on each *resource* shall not exceed its corresponding packet processing capacity, and the constraint (4.8) indicates non-negative traffic on each route.

Theorem 4.1. *The joint optimisation problem* (4.5) *with the associated constraints in* (4.6), (4.7) *and* (4.8) *is a convex optimisation problem.*

Proof. Let $\tilde{\mathbf{e}} = \left[\frac{(1-\beta_1)}{\mathbf{C}_1 P^{\max}} P_1^{\max}, \cdots, \frac{(1-\beta_N)}{\mathbf{C}_N P^{\max}} P_N^{\max}\right]$ be the normalised slope (incremental energy per bit) vector for all *resources* in the system. Then the normalised total incremental power consumption of the system as (4.1) can be expressed as

$$\tilde{P}_{\text{sys}}(\mathbf{d}) = \tilde{\mathbf{e}}\mathbf{A}\mathbf{d} \tag{4.9}$$

Let $\mathbf{A}^I$ (sub-matrix of $\mathbf{A}$) be the I-by-R matrix representing the route allocation for all the S-GWs. The aggregated traffic vector $\mathbf{d}^{\text{sgw}} = [\mathbf{d}_1^{\text{res}}, \cdots, \mathbf{d}_I^{\text{res}}]^T$ over all S-GWs can be expressed as

$$\mathbf{d}_i^{\text{sgw}} = \sum_{r=1}^{R} \mathbf{A}_{i,r}^I \mathbf{d}_r, \; i = 1, \cdots, I \tag{4.10}$$

Define the M-by-R matrix $\mathbf{A}^M$ as sub-matrix of $\mathbf{A}$ illustrating the route allocation for all the MUXs. The aggregated traffic vector $\mathbf{d}^{\text{mux}} = [\mathbf{d}_1^{\text{mux}}, \cdots, \mathbf{d}_M^{\text{mux}}]^T$ over all MUXs can be expressed as

$$\mathbf{d}_m^{\text{mux}} = \sum_{r=1}^{R} \mathbf{A}_{m,r}^M \mathbf{d}_r, \; m = 1, \cdots, M \tag{4.11}$$

To show the convexty of the load balancing variance $S(\mathbf{d})$ in a matrix form, we decouple the system throughput T over all S-GWs and MUXs respectively. Note $T = \mathbf{d}_i^{\text{sgw}} + \sum_{k \neq i} \mathbf{d}_k^{\text{sgw}}$ and $T = \frac{\mathbf{d}_m^{\text{mux}} + \sum_{l \neq m} \mathbf{d}_l^{\text{mux}}}{h}$. The load balancing variance in (4.4) can be expressed as

$$\begin{aligned} S(\mathbf{d}) &= \frac{1}{\hat{S}I} \sum_{i=1}^{I} \left(\left(\frac{1}{\mathbf{C}_i^{\text{sgw}}} - \frac{1}{\mathbf{C}_{\text{sys}}^{\text{sgw}}} \right) \mathbf{d}_i^{\text{sgw}} - \frac{1}{\mathbf{C}_{\text{sys}}^{\text{sgw}}} \sum_{k \neq i} \mathbf{d}_k^{\text{sgw}} \right)^2 \\ &+ \frac{1}{\hat{S}M} \sum_{m=1}^{M} \left(\left(\frac{1}{\mathbf{C}_m^{\text{mux}}} - \frac{1}{\mathbf{C}_{\text{sys}}^{\text{mux}}} \right) \mathbf{d}_m^{\text{mux}} - \frac{1}{\mathbf{C}_{\text{sys}}^{\text{mux}}} \sum_{l \neq m} \mathbf{d}_l^{\text{mux}} \right)^2 \\ &= \frac{1}{\hat{S}I} (\mathbf{d}^{\text{sgw}})^T (\mathbf{Q}^{\text{sgw}})^2 \mathbf{d}^{\text{sgw}} + \frac{1}{\hat{S}M} (\mathbf{d}^{\text{mux}})^T (\mathbf{Q}^{\text{mux}})^2 \mathbf{d}^{\text{mux}} \\ &= (\mathbf{d})^T \tilde{\mathbf{Q}} \mathbf{d} \end{aligned} \tag{4.12}$$

where $\tilde{\mathbf{Q}} = \frac{1}{\hat{S}I} \left(\mathbf{A}^I\right)^T (\mathbf{Q}^{\text{sgw}})^2 \mathbf{A}^I + \frac{1}{\hat{S}M} \left(\mathbf{A}^M\right)^T (\mathbf{Q}^{\text{mux}})^2 \mathbf{A}^M$. The I-by-I symmetric matrix $\mathbf{Q}^{\text{sgw}}$ can be expressed as

$$\mathbf{Q}^{\text{sgw}} = \begin{bmatrix} \frac{1}{\mathbf{C}_1^{\text{sgw}}} - \frac{1}{\mathbf{C}_{\text{sys}}^{\text{sgw}}} & \frac{-1}{\mathbf{C}_{\text{sys}}^{\text{sgw}}} & \cdots & \frac{-1}{\mathbf{C}_{\text{sys}}^{\text{sgw}}} \\ \frac{-1}{\mathbf{C}_{\text{sys}}^{\text{sgw}}} & \frac{1}{\mathbf{C}_2^{\text{sgw}}} - \frac{1}{\mathbf{C}_{\text{sys}}^{\text{sgw}}} & \cdots & \vdots \\ \vdots & \vdots & \ddots & \frac{-1}{\mathbf{C}_{\text{sys}}^{\text{sgw}}} \\ \frac{-1}{\mathbf{C}_{\text{sys}}^{\text{sgw}}} & \cdots & \frac{-1}{\mathbf{C}_{\text{sys}}^{\text{sgw}}} & \frac{1}{\mathbf{C}_I^{\text{sgw}}} - \frac{1}{\mathbf{C}_{\text{sys}}^{\text{sgw}}} \end{bmatrix}$$

and the M-by-M symmetric matrix $\mathbf{Q}^{\text{mux}}$ has the same structure such that diagonal elements equal

$$\left[\frac{1}{\mathbf{C}_1^{\text{mux}}} - \frac{1}{\mathbf{C}_{\text{sys}}^{\text{mux}}}, \cdots, \frac{1}{\mathbf{C}_M^{\text{mux}}} - \frac{1}{\mathbf{C}_{\text{sys}}^{\text{mux}}} \right]$$

and off-diagonal elements equal $\frac{-1}{\mathbf{C}_{\text{sys}}^{\text{mux}}}$. Then the joint optimisation function in (4.5) is equivalent to

$$U(\mathbf{d}) = (1 - \omega) \tilde{\mathbf{e}} \mathbf{A} \mathbf{d} + \omega (\mathbf{d})^T \tilde{\mathbf{Q}} \mathbf{d} \tag{4.13}$$

Because $\omega \geq 0$ and $\tilde{\mathbf{Q}}$ is positive semi-definite such that $\tilde{\mathbf{Q}} \succeq 0$, it is clear that the second order derivative $\nabla^2 (U(\mathbf{d})) = 2\omega \tilde{\mathbf{Q}} \succeq 0$. In addition, all constraints in (4.6), (4.7) and (4.8)

are linear. This in turn indicates the optimisation problem (4.5) is a convex problem such that the first order KKT condition [176] is sufficient and necessary for optimisation. □

We form the equivalent Lagrangian for (4.5), (4.6), (4.7), (4.7) and (4.8) as

$$\mathcal{L}(\mathbf{d}, \boldsymbol{\lambda}, \boldsymbol{\gamma}, \boldsymbol{\xi}) = U(\mathbf{d}) + \boldsymbol{\lambda}^T \left(\mathbf{d}^{\text{in}} - \mathbf{B}^{\text{rt}}\mathbf{d}\right) + \boldsymbol{\gamma}^T (\mathbf{A}\mathbf{d} - \mathbf{C}) - \boldsymbol{\xi}^T \mathbf{d} \tag{4.14}$$

where $\boldsymbol{\lambda} = [\lambda_1, \cdots, \lambda_J]^T \geq 0$, $\boldsymbol{\gamma} = [\gamma_1, \cdots, \gamma_N]^T \geq 0$ and $\boldsymbol{\xi} = [\xi_1, \cdots, \xi_R]^T \geq 0$ are the Lagrangian multiplier vectors regarding the constraints in (4.6), (4.7) and (4.8) respectively. Since $U(\mathbf{d})$ is unitless, let $\mathbf{d}$ and $\mathbf{d}^{\text{in}}$ have unit of bit/time=1/time, then the Lagrangian multipliers have the unit of time. Note given fixed $\mathbf{d}$, $\mathcal{L}(\boldsymbol{\lambda}, \boldsymbol{\gamma}, \boldsymbol{\xi})$ is a linear function of $\boldsymbol{\lambda}$, $\boldsymbol{\gamma}$ and $\boldsymbol{\xi}$. Therefore, $\mathcal{L}(\boldsymbol{\lambda}, \boldsymbol{\gamma}, \boldsymbol{\xi})$ is concave for it's arguments.

4.4 Distributed Approach

In this section we present a decentralised approach to solve the optimisation problem in (4.5) with constraints (4.6)∼(4.8). The centralised approach requires a central node to process all information sent from each network node to solve (4.5)∼(4.8) as a single problem and then inform each node of any required action resulting from the solution. This approach provides an unsuitable solution for large-scale systems because a centralised approach does not scale to such systems [32, 33]. Therefore, a decentralised algorithm for the optimisation problem is more likely to scale with network size because less information processing and system synchronisation overhead is required. There are different ways of decomposing a Network Utility Maximization (NUM) problem as demonstrated in [39]. In this chapter, we want to show the impacts of eNodeBs' preference on the optimisation problem in (4.5). Therefore, we express $U(\mathbf{d})$ in terms of $\mathbf{d}$ as a sum over eNodeB $j = 1, \cdots, J$, which is explained in the next section.

4.4.1 Objective Function Decomposition

Inspired by the prime decomposition method in [39], we re-cast Eq. (4.5) into decentralised form. Note each route can only be allocated to one eNodeB such that $\sum_{j=1}^{J} \mathbf{B}^{\text{rt}}_{j,r} =$

$1, \forall r = 1, \cdots, R$. The cost function $U(\mathbf{d})$ in (4.5) can be expressed as

$$\begin{aligned} U(\mathbf{d}) &= (1-\omega)\sum_{n=1}^{N}\sum_{r=1}^{R}\left(\frac{\tilde{\mathcal{E}}_n \mathbf{A}_{n,r}\mathbf{d}_r}{\mathbf{C}_n P^{\max}} P_n^{\max}\right) + \frac{\omega}{\hat{S}I}\sum_{i=1}^{I}\left(\sum_{r=1}^{R}\frac{\mathbf{A}_{i,r}^{\mathrm{sgw}}\mathbf{d}_r}{\mathbf{C}_i^{\mathrm{sgw}}} - \frac{T}{\mathbf{C}_{\mathrm{sys}}^{\mathrm{sgw}}}\right)^2 \\ &\quad + \frac{\omega}{\hat{S}M}\sum_{m=1}^{M}\left(\sum_{r=1}^{R}\frac{\mathbf{A}_{m,r}^{\mathrm{mux}}\mathbf{d}_r}{\mathbf{C}_m^{\mathrm{mux}}} - \frac{hT}{\mathbf{C}_{\mathrm{sys}}^{\mathrm{mux}}}\right)^2 \\ &= (1-\omega)\sum_{n=1}^{N}\sum_{j=1}^{J}\sum_{r=1}^{R}\left(\frac{\mathbf{B}_{j,r}^{\mathrm{rt}}\tilde{\mathcal{E}}_n \mathbf{A}_{n,r}\mathbf{d}_r}{\mathbf{C}_n P^{\max}} P_n^{\max}\right) + \frac{\omega}{\hat{S}I}\sum_{i=1}^{I}\left(\sum_{j=1}^{J}\sum_{r=1}^{R}\frac{\mathbf{B}_{j,r}^{\mathrm{rt}}\mathbf{A}_{i,r}^{\mathrm{sgw}}\mathbf{d}_r}{\mathbf{C}_i^{\mathrm{sgw}}} - \frac{T}{\mathbf{C}_{\mathrm{sys}}^{\mathrm{sgw}}}\right)^2 \\ &\quad + \frac{\omega}{\hat{S}M}\sum_{m=1}^{M}\left(\sum_{j=1}^{J}\sum_{r=1}^{R}\frac{\mathbf{B}_{j,r}^{\mathrm{rt}}\mathbf{A}_{m,r}^{\mathrm{mux}}\mathbf{d}_r}{\mathbf{C}_m^{\mathrm{mux}}} - \frac{hT}{\mathbf{C}_{\mathrm{sys}}^{\mathrm{mux}}}\right)^2. \end{aligned} \tag{4.15}$$

where the slope $\tilde{\mathcal{E}}_n$ denotes the effective incremental energy per bit defined in Eq. (3.10). The sum of the traffic that eNodeB j directs to S-GW i and MUX m over all possible routes are given separatively by

$$s_{j\to i}^{\mathrm{sgw}} = \sum_{r=1}^{R}\mathbf{B}_{j,r}^{\mathrm{rt}}\mathbf{A}_{i,r}^{\mathrm{sgw}}\mathbf{d}_r \text{ and } s_{j\to m}^{\mathrm{mux}} = \sum_{r=1}^{R}\mathbf{B}_{j,r}^{\mathrm{rt}}\mathbf{A}_{m,r}^{\mathrm{mux}}\mathbf{d}_r.$$

Further, we note that the total traffic incident upon S-GW i and MUX m, are given by $\mathbf{d}_i^{\mathrm{sgw}} = \sum_{j=1}^{J} s_{j\to i}^{\mathrm{sgw}}$ and $\mathbf{d}_m^{\mathrm{mux}} = \sum_{j=1}^{J} s_{j\to m}^{\mathrm{mux}}$ separately. The weighted load balancing variance as the second term of (4.15) can be expressed as

$$\begin{aligned} \omega S &= \frac{\omega}{\hat{S}I}\sum_{i=1}^{I}\left(\frac{1}{\mathbf{C}_i^{\mathrm{sgw}}}\sum_{j=1}^{J}s_{j\to i}^{\mathrm{sgw}} - \frac{T}{\mathbf{C}_{\mathrm{sys}}^{\mathrm{sgw}}}\right)^2 + \frac{\omega}{\hat{S}M}\sum_{m=1}^{M}\left(\frac{1}{\mathbf{C}_m^{\mathrm{mux}}}\sum_{j=1}^{J}s_{j\to m}^{\mathrm{mux}} - \frac{hT}{\mathbf{C}_{\mathrm{sys}}^{\mathrm{mux}}}\right)^2 \\ &= \sum_{j=1}^{J}S_j + \frac{\omega}{\hat{S}}\left(\left(\frac{T}{\mathbf{C}_{\mathrm{sys}}^{\mathrm{sgw}}}\right)^2 + \left(\frac{hT}{\mathbf{C}_{\mathrm{sys}}^{\mathrm{mux}}}\right)^2\right) \end{aligned} \tag{4.16}$$

with

$$\begin{aligned} S_j &= \frac{\omega}{\hat{S}I}\sum_{i=1}^{I}\left(\left(\frac{s_{j\to i}^{\mathrm{sgw}}}{\mathbf{C}_i^{\mathrm{sgw}}}\right)^2 + 2\frac{s_{j\to i}^{\mathrm{sgw}}}{\mathbf{C}_i^{\mathrm{sgw}}}\sum_{h\neq j}^{J}\frac{s_{h\to i}^{\mathrm{sgw}}}{\mathbf{C}_i^{\mathrm{sgw}}} + \frac{\theta_{\tilde{j}\to i}^{\mathrm{sgw}}}{(\mathbf{C}_i^{\mathrm{sgw}})^2}\right) - \frac{2\omega T}{\hat{S}I\mathbf{C}_{\mathrm{sys}}^{\mathrm{sgw}}}\sum_{i=1}^{I}\frac{s_{j\to i}^{\mathrm{sgw}}}{\mathbf{C}_i^{\mathrm{sgw}}} \\ &\quad + \frac{\omega}{\hat{S}M}\sum_{m=1}^{M}\left(\left(\frac{s_{j\to m}^{\mathrm{mux}}}{\mathbf{C}_m^{\mathrm{mux}}}\right)^2 + 2\frac{s_{j\to m}^{\mathrm{mux}}}{\mathbf{C}_m^{\mathrm{mux}}}\sum_{h\neq j}^{J}\frac{s_{h\to m}^{\mathrm{mux}}}{\mathbf{C}_m^{\mathrm{mux}}} + \frac{\theta_{\tilde{j}\to m}^{\mathrm{mux}}}{(\mathbf{C}_m^{\mathrm{mux}})^2}\right) - \frac{2\omega T}{\hat{S}M\mathbf{C}_{\mathrm{sys}}^{\mathrm{mux}}}\sum_{m=1}^{M}\frac{s_{j\to m}^{\mathrm{mux}}}{\mathbf{C}_m^{\mathrm{mux}}} \end{aligned}$$

where [3] $\theta^{\text{sgw}}_{\tilde{j}\to i}$ and $\theta^{\text{mux}}_{\tilde{j}\to m}$ denote the combination of items other than $s^{\text{sgw}}_{j\to i}$ and $s^{\text{mux}}_{j\to m}$ for a given j respectively such that

$$\theta^{\text{sgw}}_{\tilde{j}\to i} = \begin{cases} 0 & \text{if } J=1 \\ \left(s^{\text{sgw}}_{\tilde{j}\to i}\right)^2 - \mathbf{d}^{\text{sgw}}_i s^{\text{sgw}}_{\tilde{j}\to i} & \text{if } J=2 \\ s^{\text{sgw}}_{|j+1|_I\to i} s^{\text{sgw}}_{|j|_I\to i} & \\ +s^{\text{sgw}}_{|j|_I\to i}\sum_{h\neq j,|j|_I}^{J} s^{\text{sgw}}_{h\to i} & \text{if } J>2 \end{cases} \quad \theta^{\text{mux}}_{\tilde{j}\to m} = \begin{cases} 0 & \text{if } J=1 \\ \left(s^{\text{mux}}_{\tilde{j}\to m}\right)^2 - \mathbf{d}^{\text{mux}}_m s^{\text{mux}}_{\tilde{j}\to m} & \text{if } J=2 \\ s^{\text{mux}}_{|j+1|_M\to m} s^{\text{mux}}_{|j|_M\to m} & \\ +s^{\text{mux}}_{|j|_M\to m}\sum_{h\neq j,|j|_M}^{J} s^{\text{mux}}_{h\to m} & \text{if } J>2 \end{cases}$$

where $|x|_y = x \; mod \; y + 1$. Taking (4.16) into (4.15), we have the decomposed cost function across all eNodeBs as shown below,

$$U(\mathbf{d}) = \sum_{j=1}^{J} U_j(\mathbf{d}) + \frac{\omega}{\hat{S}}\left(\left(\frac{T}{\mathbf{C}^{\text{sgw}}_{\text{sys}}}\right)^2 + \left(\frac{hT}{\mathbf{C}^{\text{mux}}_{\text{sys}}}\right)^2\right) \tag{4.17}$$

Using this we can express the centralised cost function as a sum of J decentralised functions with $U_j(\mathbf{d})$ denotes the individual cost function for eNodeB j expressed as

$$\begin{aligned} U_j(\mathbf{d}) = (1-\omega)\sum_{n=1}^{N}\sum_{r=1}^{R}&\left((1-\beta_n)\frac{\mathbf{B}^{\text{rt}}_{j,r}\tilde{\mathcal{E}}_n\mathbf{A}_{n,r}\mathbf{d}_r}{\mathbf{C}_n P^{\max}}P^{\max}_n\right) \\ &+\frac{\omega}{\hat{S}I}\sum_{i=1}^{I}\frac{\theta^{\text{sgw}}_{\tilde{j}\to i}}{\left(\mathbf{C}^{\text{sgw}}_i\right)^2} + \frac{\omega}{\hat{S}M}\sum_{m=1}^{M}\frac{\theta^{\text{mux}}_{\tilde{j}\to m}}{\left(\mathbf{C}^{\text{mux}}_m\right)^2} \\ &+\frac{\omega}{\hat{S}I}\sum_{i=1}^{I}\left(\sum_{r=1}^{R}\frac{\mathbf{B}^{\text{rt}}_{j,r}\mathbf{A}^{\text{sgw}}_{i,r}\mathbf{d}_r}{\mathbf{C}^{\text{sgw}}_i}\right)^2 - \frac{2\omega T}{\hat{S}I\mathbf{C}^{\text{sgw}}_{\text{sys}}}\sum_{i=1}^{I}\sum_{r=1}^{R}\frac{\mathbf{B}^{\text{rt}}_{j,r}\mathbf{A}^{\text{sgw}}_{i,r}\mathbf{d}_r}{\mathbf{C}^{\text{sgw}}_i} \\ &+\frac{2\omega}{\hat{S}I}\sum_{i=1}^{I}\left(\sum_{r=1}^{R}\frac{\mathbf{B}^{\text{rt}}_{j,r}\mathbf{A}^{\text{sgw}}_{i,r}\mathbf{d}_r}{\mathbf{C}^{\text{sgw}}_i}\sum_{h\neq j}^{J}\sum_{r=1}^{R}\frac{\mathbf{B}^{\text{rt}}_{h,r}\mathbf{A}^{\text{sgw}}_{i,r}\mathbf{d}_r}{\mathbf{C}^{\text{sgw}}_i}\right) \\ &+\frac{\omega}{\hat{S}M}\sum_{m=1}^{M}\left(\sum_{r=1}^{R}\frac{\mathbf{B}^{\text{rt}}_{j,r}\mathbf{A}^{\text{mux}}_{m,r}\mathbf{d}_r}{\mathbf{C}^{\text{mux}}_m}\right)^2 - \frac{2\omega T}{\hat{S}M\mathbf{C}^{\text{mux}}_{\text{sys}}}\sum_{m=1}^{M}\sum_{r=1}^{R}\frac{\mathbf{B}^{\text{rt}}_{j,r}\mathbf{A}^{\text{mux}}_{m,r}\mathbf{d}_r}{\mathbf{C}^{\text{mux}}_m} \\ &+\frac{2\omega}{\hat{S}M}\sum_{m=1}^{M}\left(\sum_{r=1}^{R}\frac{\mathbf{B}^{\text{rt}}_{j,r}\mathbf{A}^{\text{mux}}_{m,r}\mathbf{d}_r}{\mathbf{C}^{\text{mux}}_m}\sum_{h\neq j}^{J}\sum_{r=1}^{R}\frac{\mathbf{B}^{\text{rt}}_{h,r}\mathbf{A}^{\text{mux}}_{m,r}\mathbf{d}_r}{\mathbf{C}^{\text{mux}}_m}\right) \end{aligned} \tag{4.18}$$

[3]Term $\tilde{j}$ denotes the fact that this term dose not include $s^{\text{sgw}}_{j\to i}$ or $s^{\text{mux}}_{j\to m}$ for a given j.

The cost function $U(\mathbf{d})$ in (4.5) can be decoupled over all eNodeBs as shown in (4.17). Following the decomposition rule [39], the corresponding Lagrangian in (4.14) can be reformulated as

$$\begin{aligned}\mathcal{L}(\mathbf{d},\boldsymbol{\lambda},\boldsymbol{\gamma},\boldsymbol{\xi}) &= \sum_{j=1}^{J} U_j^{\mathrm{bs}} + \frac{\omega}{\hat{S}}\left(\left(\frac{T}{\mathbf{C}_{\mathrm{sys}}^{\mathrm{sgw}}}\right)^2 + \left(\frac{hT}{\mathbf{C}_{\mathrm{sys}}^{\mathrm{mux}}}\right)^2\right) \\ &= \Psi(\mathbf{d},\boldsymbol{\lambda},\boldsymbol{\gamma},\boldsymbol{\xi}) + \frac{\omega}{\hat{S}}\left(\left(\frac{T}{\mathbf{C}_{\mathrm{sys}}^{\mathrm{sgw}}}\right)^2 + \left(\frac{hT}{\mathbf{C}_{\mathrm{sys}}^{\mathrm{mux}}}\right)^2\right)\end{aligned} \tag{4.19}$$

with $U_j^{\mathrm{bs}} = U_j(\mathbf{d}) + \mathcal{L}_j$ and

$$\mathcal{L}_j = \boldsymbol{\lambda}_j\left(\mathbf{d}_j^{\mathrm{in}} - \sum_{r=1}^{R}\mathbf{B}_{j,r}^{\mathrm{rt}}\mathbf{d}_r\right) + \sum_{n=1}^{N}\gamma_n\left(\sum_{r=1}^{R}\mathbf{A}_{n,r}\mathbf{B}_{j,r}^{\mathrm{rt}}\mathbf{d}_r - \mathbf{C}_n\right) - \sum_{r=1}^{R}\xi_r\mathbf{B}_{j,r}^{\mathrm{rt}}\mathbf{d}_r \tag{4.20}$$

4.5 Iterative Algorithms

The proposed distributed solution involves calculating the associated Lagrangian multipliers in (4.20), which is not tractable for any static implementation. Inspired by the iterative method solving network utility maximisation (NUM) problems in [24], we propose an iterative algorithm with gradient projection method to approximate the global solution asymptotically. Note the joint optimisation problem in (4.14) is equivalent to the sum of subproblems with fixed Lagrangian multipliers:

$$\min_{\mathbf{d}} \mathcal{L}(\mathbf{d},\boldsymbol{\lambda},\boldsymbol{\gamma},\boldsymbol{\xi}) = \sum_{j=1}^{J}\min_{\mathbf{d}} U_j^{\mathrm{bs}}. \tag{4.21}$$

By applying a closed-loop "pricing" feedback mechanism [24], a discrete-time and distributed dynamic gradient play method [177] can be used to derive the optimal $\mathbf{d}^*$.

Fig. 4.2 describes the concept of gradient method solving an optimisation problem $\min_d U(d)$, where $U(d)$ is continuous, differentiable and convex over the one dimensional argument d. The optimisation problem can be solved in an iterative manner as specified in [34]. An iteration index z is adopted to parameterise the argument d. Given a initial $d(0)$, the gradient method generates a sequence $d(1), d(2), \cdots$. In order to search

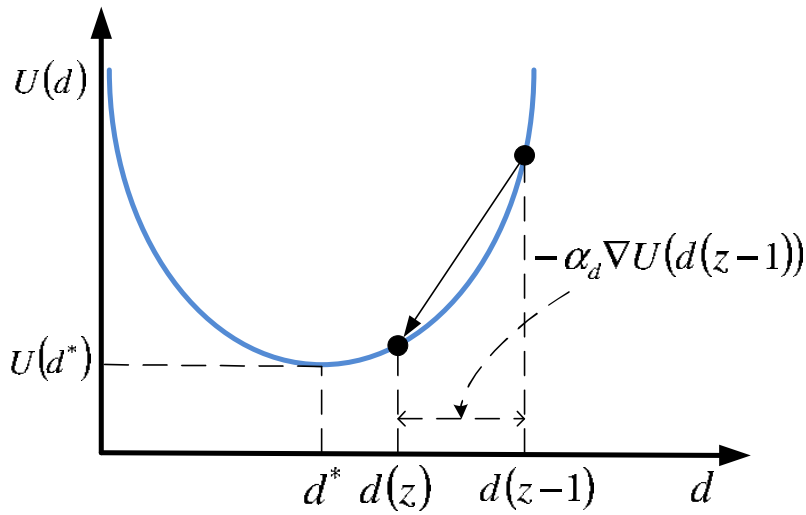

Figure 4.2: Example of gradient method solving $\min_d U(d)$ with a single dimension argument d

for d^* that minimise $U(d)$, the z-th entity $d(z)$, $z = 1, 2, \cdots$, is updated with the negative gradient $\nabla U(d(z-1))$ scaled by a step size α_d. With sufficient small step size α_d, the gradient method is guaranteed to converge but the convergence speed may be slow [34]. Note solving a concave optimisation problem with gradient method requires updates with the positive gradient scaled by a step size for each iteration.

To solve (4.21) we propose an iterative gradient method, which involves two operations within one iteration. Operation 1 is to update Lagrangian multipliers γ, $\boldsymbol{\lambda}$ and $\boldsymbol{\xi}$ given traffic distribution vector $\mathbf{d}$. The Lagrangian multipliers γ, $\boldsymbol{\lambda}$ and $\boldsymbol{\xi}$ are adjusted to the gradients $\nabla\Psi$ in (4.19) with *a prior* data traffic distribution vector $\mathbf{d}(z-1)$ such that

$$\gamma_n(z) = [\gamma_n(z-1) + \alpha_\gamma (\mathbf{A}_n \mathbf{d}(z-1) - \mathbf{C}_n)]^+ \tag{4.22}$$

$$\boldsymbol{\lambda}_j(z) = \boldsymbol{\lambda}_j(z-1) + \alpha_\lambda \left(\mathbf{d}_j^{\text{in}} - \mathbf{B}_j^{\text{rt}} \mathbf{d}(z-1)\right) \tag{4.23}$$

$$\boldsymbol{\xi}_r(z) = \left[\boldsymbol{\xi}_r(z-1) - \alpha_\xi \mathbf{d}_r(z-1)\right]^+ \tag{4.24}$$

where z denotes the index corresponding to the z-th iteration of the Lagrangian multipliers toward the solution. Term $\alpha_\lambda > 0$, $\alpha_\gamma > 0$ and $\alpha_\xi > 0$ denote the gradient step sizes for $\boldsymbol{\lambda}$, γ and $\boldsymbol{\xi}$ respectively. Operation $[x]^+ = \max(0, x)$. Note operation $[x]^+$ does not apply to (4.23) due to equality constraint in (4.6).

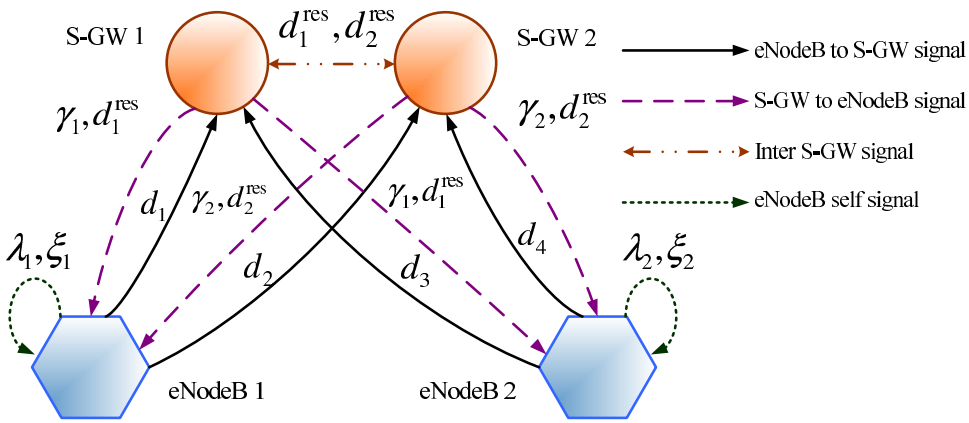

Figure 4.3: Signaling flow for the distributed interactive traffic control system with 2 eNodeB and 2 S-GW nodes.

In operation 2, given the updated Lagrangian multipliers $\boldsymbol{\lambda}$, $\boldsymbol{\gamma}$ and $\boldsymbol{\xi}$ from (4.23), (4.22) and (4.24), the subproblem for eNodeB j can be solved by adjusting $\mathbf{d}_r$ with $\mathbf{B}_{j,r}^{\text{rt}} = 1$ to the opposite direction of the gradient such that

$$\mathbf{d}_r(z) = \mathbf{d}_r(z-1) - \alpha_d \sum_{j=1}^{J} \frac{\partial U_j^{\text{bs}}}{\partial \mathbf{d}_r} \mathbf{B}_{j,r}^{\text{rt}} \tag{4.25}$$

where $\alpha_d > 0$ denotes the gradient step size with unit of $(\text{time})^{-2}$ chosen to align with the unit of $\mathbf{d}_r$. The gradient is given by

$$\begin{aligned} \frac{\partial U_j^{\text{bs}}}{\partial \mathbf{d}_r} &= (1-\omega) \sum_{n=1}^{N} \left((1-\beta_n) \frac{\mathbf{B}_{j,r}^{\text{rt}} \mathbf{A}_{n,r}}{\mathbf{C}_n P^{\max}} P_n^{\max} \right) + \sum_{i=1}^{I} \frac{2\omega \mathbf{B}_{j,r}^{\text{rt}} \mathbf{A}_{i,r}^{\text{sgw}}}{\hat{S} I \mathbf{C}_i^{\text{sgw}}} \left(\frac{\mathbf{d}_i^{\text{sgw}}}{\mathbf{C}_i^{\text{sgw}}} - \frac{T}{\mathbf{C}_{\text{sys}}^{\text{sgw}}} \right) \\ &+ \sum_{m=1}^{M} \frac{2\omega \mathbf{B}_{j,r}^{\text{rt}} \mathbf{A}_{m,r}^{\text{mux}}}{\hat{S} M \mathbf{C}_m^{\text{mux}}} \left(\frac{\mathbf{d}_m^{\text{mux}}}{\mathbf{C}_m^{\text{mux}}} - \frac{hT}{\mathbf{C}_{\text{sys}}^{\text{mux}}} \right) - \lambda_j \mathbf{B}_{j,r}^{\text{rt}} + \sum_{n=1}^{N} \gamma_n \mathbf{B}_{j,r}^{\text{rt}} \mathbf{A}_{n,r} - \xi_r \mathbf{B}_{j,r}^{\text{rt}} \end{aligned} \tag{4.26}$$

Figure 4.3 describes the information flow for the proposed iterative traffic schedule system with 2 eNodeBs and 2 S-GWs. At iteration $z = 1, 2, \cdots$, eNodeBs signal the connected S-GWs of the current traffic distribution decision $\mathbf{d}(z) = [\mathbf{d}_1(z), \cdots, \mathbf{d}_R(z)]^T$ as shown in Figure 4.3. Then *resource* $n = 1, \cdots, N$ gathers the information of intended traffic $\mathbf{d}_r$ from the associated eNodeBs based on the mapping matrix $\mathbf{A}$ defined in (3.1) to update the aggregated traffic load $\mathbf{d}_n^{\text{res}}(z)$. The Lagrangian multiplier $\gamma_n(z+1)$ is updated as specified in (4.22) and *resource* n sends a signal to the corresponding eNodeBs. This

signal indicates the *price* representing the Lagrangian multiplier that each *resource* wants to charge the associated eNodeB based on the expected load for the current iteration. Each eNodeB utilises local information to update Lagrangian multipliers $\boldsymbol{\lambda}_j(z+1)$ and $\boldsymbol{\xi}_j(z+1)$ specified in (4.23), (4.24) and (4.24) respectively. Upon receiving the Lagrangian multiplier updates, each eNodeB will re-evaluate its traffic distribution strategy based on (4.25). This iterative process will continue until the system reaches an equilibrium, in which every Lagrangian multiplier in (4.23), (4.24) and (4.24) converges to a steady state.

4.6 Stability Analysis

The gradient method shown in Section 4.5 is a discrete-time solution of the problem. Due to the complexity of dynamics in (4.22)∼(4.25), we impose a time-scale separation between dynamics in (4.22)∼(4.24) and (4.25) and conduct the stability analysis in continuous time as specified in [178]. We conduct the stability analysis in two steps since it is difficult to construct a single Lyapunov function for $\mathbf{d}$, $\boldsymbol{\lambda}$, $\boldsymbol{\gamma}$ and $\boldsymbol{\xi}$.

Step 1, of a two step process to prove stability, is the process of deriving the optimal traffic $\mathbf{d}^*$ given fixed Lagrangian multipliers $\boldsymbol{\lambda}$, $\boldsymbol{\gamma}$ and $\boldsymbol{\xi}$ from the previous iteration. For step 1, we consider the following Lyapunov function,

$$V(\mathbf{d}) = \mathcal{L}(\mathbf{d}, \boldsymbol{\lambda}, \boldsymbol{\gamma}, \boldsymbol{\xi}) + \Delta \tag{4.27}$$

where $\mathcal{L}(\mathbf{d}, \boldsymbol{\lambda}, \boldsymbol{\gamma}, \boldsymbol{\xi})$ is defined in (4.14) and Δ is a constant such that $U(\mathbf{d}^*) + \Delta = 0$ with $\mathbf{d}^*$ denotes the equilibrium point to achieve (4.5). Note $\boldsymbol{\lambda}^T \left(\mathbf{d}^{\text{in}} - \mathbf{B}^{\text{rt}}\mathbf{d}^*\right) = \mathbf{0}$, $\boldsymbol{\gamma}^T \left(\mathbf{A}\mathbf{d}^* - \mathbf{C}\right) = 0$ and $\boldsymbol{\xi}^T\mathbf{d}^* = 0$ due to the complementary slackness [176]. This indicates that $V(\mathbf{d}^*) = 0$. In addition, the joint cost function $U(\mathbf{d})$ is convex as proved in Theorem 4.1. We show that $V(\mathbf{d}) \geq \mathbf{0}$. Given fixed $\boldsymbol{\lambda}$, $\boldsymbol{\gamma}$ and $\boldsymbol{\xi}$ at each iteration, the derivative of $V(\mathbf{d})$ along the trajectories of $\mathbf{d}$ over t, denoted as $\dot{V}(\mathbf{d})$, is expressed as

$$\dot{V}(\mathbf{d}) = \sum_{r=1}^{R} \frac{\partial V(\mathbf{d}_r)}{\partial \mathbf{d}_r} \dot{\mathbf{d}}_r, \quad \dot{\mathbf{d}}_r = -\tilde{\alpha}_d \sum_{j=1}^{J} \frac{\partial U_j^{\text{bs}}}{\partial \mathbf{d}_r} \mathbf{B}_{j,r}^{\text{rt}} \tag{4.28}$$

where $\dot{\mathbf{d}}_r$ is the continuous version of (4.26) and step size $\tilde{\alpha_d}$ has different units $(\text{time})^{-3}$ compared to α_d. Note each route $r_{j\to i}$ from eNodeB j (source) to S-GW i (destination) is unique and loop-less. $\frac{\partial V(\mathbf{d}_r)}{\partial \mathbf{d}_r} = \frac{\partial U_j^{\text{bs}}}{\partial \mathbf{d}_r}$ where $\frac{\partial U_j^{\text{bs}}}{\partial \mathbf{d}_r}$ is the gradient specified in (4.26). We show Eq. (4.28) can be further expressed as

$$\dot{V}(\mathbf{d}_r) = -\tilde{\alpha_d}\left(\frac{\partial U_j^{\text{bs}}}{\partial \mathbf{d}_r}\right)^2 < 0,\ \forall \mathbf{d}_r \neq \mathbf{d}_r^* \tag{4.29}$$

This means $\dot{V}(\mathbf{d}) < 0, \forall \mathbf{d} \neq \mathbf{d}^*$ and $\dot{V}(\mathbf{d}^*) = 0$. We have shown that the multi-objective function is convex in Theorem 4.1. Therefore, given Lagrangian $\boldsymbol{\lambda}$, $\boldsymbol{\gamma}$ and $\boldsymbol{\xi}$, the unique equilibrium point $\mathbf{d}^*$ that minimise the multi-objective function is asymptotically stable by using Theorem 4.1 in [179].

Step 2, the updated traffic $\mathbf{d}$ in Step 1 is used to further refine the Lagrangian multipliers. We consider the following Lyapunov function

$$V(\boldsymbol{\gamma}, \boldsymbol{\lambda}, \boldsymbol{\xi}) = \mathcal{L}(\boldsymbol{\lambda}, \boldsymbol{\gamma}, \boldsymbol{\xi}) + \Delta' \tag{4.30}$$

Note that given traffic $\mathbf{d}$, $\mathcal{L}(\boldsymbol{\lambda}, \boldsymbol{\gamma}, \boldsymbol{\xi})$ is linear function, which is also concave for it's arguments. Δ' is a constant such that $\max_{\boldsymbol{\gamma},\boldsymbol{\lambda},\boldsymbol{\xi}} \mathcal{L}(\boldsymbol{\gamma}, \boldsymbol{\lambda}, \boldsymbol{\xi}) + \Delta' = 0$. Then we show $V(\boldsymbol{\gamma}, \boldsymbol{\lambda}, \boldsymbol{\xi}) \leq 0$. Given fixed $\mathbf{d}$ at each iteration, the derivative of $V(\boldsymbol{\gamma}, \boldsymbol{\lambda}, \boldsymbol{\xi})$ along the trajectories of $\boldsymbol{\gamma}, \boldsymbol{\lambda}, \boldsymbol{\xi}$ over time, denoted as $\dot{V}(\boldsymbol{\gamma}, \boldsymbol{\lambda}, \boldsymbol{\xi})$, is

$$\dot{V}(\boldsymbol{\gamma}, \boldsymbol{\lambda}, \boldsymbol{\xi}) = \sum_{j=1}^{J} \frac{\partial V}{\partial \boldsymbol{\lambda}_j}\dot{\boldsymbol{\lambda}}_j + \sum_{n=1}^{N} \frac{\partial V}{\partial \boldsymbol{\gamma}_n}\dot{\boldsymbol{\gamma}}_n + \sum_{r=1}^{R} \frac{\partial V}{\partial \boldsymbol{\xi}_r}\dot{\boldsymbol{\xi}} \tag{4.31}$$

From (4.14), it can be seen that

$$\frac{\partial V}{\partial \boldsymbol{\lambda}_j} = \mathbf{d}_j^{\text{in}} - \mathbf{B}_j^{\text{rt}}\mathbf{d} \quad \frac{\partial V}{\partial \boldsymbol{\gamma}_n} = \mathbf{A}_n\mathbf{d} - \mathbf{C}_n \quad \text{and} \quad \frac{\partial V}{\partial \boldsymbol{\xi}_r} = -\mathbf{d}_r.$$

Also the applied distributed dynamic gradient method for $\boldsymbol{\gamma}$, $\boldsymbol{\lambda}$ and $\boldsymbol{\xi}$ in (4.22), (4.23) and (4.24) indicates that

$$\dot{\boldsymbol{\lambda}}_j = \tilde{\alpha_\lambda}\left(\mathbf{d}_j^{\text{in}} - \mathbf{B}_j^{\text{rt}}\mathbf{d}\right), \quad \dot{\boldsymbol{\gamma}}_n = \tilde{\alpha_\gamma}\left(\mathbf{A}_n\mathbf{d} - \mathbf{C}_n\right), \quad \dot{\boldsymbol{\xi}}_r = -\tilde{\alpha_\xi}\mathbf{d}_r$$

where the unit for step sizes $\tilde{\alpha_\lambda}, \tilde{\alpha_\gamma}, \tilde{\alpha_\xi}$ is chosen to match the continuous version of $\dot{\lambda}_j, \dot{\gamma}_n, \dot{\xi}_r$ respectively. Therefore we show $\dot{V}(\gamma, \lambda, \xi) > 0$. Given the updated traffic distribution vector $\mathbf{d}$, the equilibrium point γ^*, λ^* and ξ^* that maximise $\mathcal{L}(\lambda, \gamma, \xi)$ with fixed $\mathbf{d}$ is stable. We do not have a stability result for the combined scheme consisting of step 1 and step 2. The convergence of the system is investigated numerically in the next section.

4.7 Simulations

4.7.1 Simulation Setup

We use Matlab to simulate the distributed solution for mobile backhaul traffic distribution. We consider a simple system as illustrated in Fig. 4.1 with 2 eNodeBs, 2 MUXs 3 S-GWs and 12 predefined routes. We use the input traffic over half a diurnal cycle specified in Table 4.2 to show how the 2 eNodeBs distribute traffic over the 12 predefined routes. The topologies of *resource*-route $\mathbf{A}$ matrix and eNodeB-route $\mathbf{B}^{\text{rt}}$ matrix are specified in Table 4.3 with notation explained in Table 4.4. The topology related matrices $\mathbf{A}$ and $\mathbf{B}^{\text{rt}}$ explained in Section 4.2 can be derived from Table 4.3. For simplicity, all link configurations are omitted in Table 4.3, which can be easily derived from the connected nodes in the table.

Table 4.2: Input Traffic (Gbps) for 2 eNodeBs (half diurnal cycle)

Name\test	$t1$	$t2$	$t3$	$t4$	$t5$	$t6$	$t7$	$t8$	$t9$
eNodeB 1	0.1	0.2	0.3	0.4	0.5	0.6	0.7	0.8	0.9
eNodeB 2	0.5	0.6	0.7	0.8	0.9	1.0	1.1	1.2	1.3
total	0.6	0.8	1.0	1.2	1.4	1.6	1.8	2.0	2.2

In order to show the impact of different backhaul links on the system performance, we propose three different test cases:

1. All fibre backhaul links ("All Fibre")

2. Mixture of optical and microwave backhaul links ("Hybrid")

3. All microwave backhaul links ("All Micro")

Table 4.3: Resource/eNodeB-route mapping $\mathbf{A}/\mathbf{B}^{\mathrm{rt}}$ for system with 2 eNodeBs, 2 MUXs, 3 S-GWs and 12 routes

Name\Route	1	2	3	4	5	6
S-GW 1	1	0	0	1	0	0
S-GW 2	0	1	0	0	1	0
S-GW 3	0	0	1	0	0	1
MUX 1	1	1	1	0	0	0
MUX 2	0	0	0	1	1	1
eNodeB 1	1	1	1	1	1	1
eNodeB 2	0	0	0	0	0	0
Name\Route	7	8	9	10	11	12
S-GW 1	1	0	0	1	0	0
S-GW 2	0	1	0	0	1	0
S-GW 3	0	0	1	0	0	1
MUX 1	1	1	1	0	0	0
MUX 2	0	0	0	1	1	1
eNodeB 1	0	0	0	0	0	0
eNodeB 2	1	1	1	1	1	1

We set the weighting factor $\omega = 0.5$ for those three test cases. The "All Fibre" system has all fibre backhaul links with the related parameters for S-GW nodes, MUX nodes and links specified in Table 4.4. Note for all fibre backhaul links in Table 4.4, Idle/max power ratio $\beta = 1.0$ which indicates the power consumption of a fibre link is independent of the carried traffic. The "Hybrid" system has both microwave and optical fibre backhaul links. The system topology remains the same and the system input traffic is unchanged. Most of the *resource* parameters other than Link2 and Link4 in Table 4.4 remain unchanged. Link2 and Link4 are microwave backhaul links with parameters shown in Table 4.5. The "All Micro" system has the microwave link parameters specified in Table 4.5. From Table 4.4, it indicates that of all S-GWs, S-GW 2 is the most energy efficient (with least incremental power consumption [166]) but not significantly better than S-GW 3. In addition MUX 1 and 2 have similar characteristics in terms of incremental energy per bit. For the "All Fibre" system, the backhaul links have zero incremental energy per bit since $\beta = 1$ for optical links.

As stated in [32, 33], using mixed integer programming methods for optimising this type of network does not scale to larger networks. In contrast, by adopting the power consumption model in Eq. (3.12), we prove the optimisation problem (4.5) is a convex

problem in Theorem 4.1. A major advantage of the approach described here is its ability to scale to larger networks due to the convexity of (4.5) [34]. However, one issue that may arise is the selection of the initial utilisation ratio ρ_n^{res} illustrated in Fig. 3.5 to start the optimisation. Inappropriate choice of ρ_n^{res} may result in the solution being a local, rather than global, optimum. However, as network equipment becomes more energy-proportional [135, 136], meaning β_n goes to zero, this problem goes away and the selection of an initial value for ρ_n^{res} can be increasingly arbitrary. Even in the case of non-energy-proportional equipment, with collected network historical information, appropriate initial values for ρ_n^{res} can be determined. The key point is that, with a reasonable choice of ρ_n^{res} based on system historical information and domain knowledge of network operation, the methodology described here can be applied to large networks to which MIP methods cannot scale.

Finally we introduce another four configurations to examine the effect of weighting factor ω. The system topology and the corresponding *resources* are the same as the "Hybrid" test case with $\omega = 0.5$. By choosing $\omega = 0.0$, the focus is on incremental power consumption only and not on load balancing. In contrast, the load balancing condition is the sole focus of the optimisation when $\omega = 1.0$. Test cases with $\omega = 0.25$ and $\omega = 0.75$ imply dual emphases on the total power consumption and load balance respectively.

4.7.2 Simulation Results

4.7.2.1 Impact of Backhaul Link Types

All Fibre: First we use the test case $t5$ in Table 4.2 to show the performance of the proposed distributed solution. In Fig. 4.4, "All Fibre" illustrates the simulation results for the traffic allocation over all predefined routes with all fibre optical backhaul links. Note only routes 2, 5, 8 and 11 receive data traffic in this case. Using the predefined *resource*-route mapping in Table 4.3 and the allocated route traffic in Fig. 4.4, we derived the normalised load over all *resources* shown in Fig. 4.5. Note backhaul links 5, 7, 8 and 10 receive no data traffic. As a consequence, S-GW 1 and 3 have no distributed data traffic based on the topology in Table 4.3.

Table 4.4: Parameters of *resources* for All Fibre

items n	Name	C_n (Gbps)	$P_n^{\max}$ (Watts)[1]	Power ratio β_n
1	S-GW1	0.6	1326	0.8
2	S-GW2	4.0	1336	0.8
3	S-GW3	4.0	1772	0.8
4	MUX1	10.0	130	0.8
5	MUX2	10.0	100	0.8
6	Link1: eNodeB1∼MUX1	1.0	10.5	1.0
7	Link2: eNodeB1∼MUX2	1.0	10.5	1.0
8	Link3: eNodeB2∼MUX1	1.0	10.5	1.0
9	Link4: eNodeB2∼MUX2	1.0	10.5	1.0
10	Link5: MUX1∼S-GW1	10.0	30.0	1.0
11	Link6: MUX1∼S-GW2	10.0	30.0	1.0
12	Link7: MUX1∼S-GW3	10.0	30.0	1.0
13	Link8: MUX2∼S-GW1	10.0	30.0	1.0
14	Link9: MUX2∼S-GW2	10.0	30.0	1.0
15	Link10: MUX2∼S-GW3	10.0	30.0	1.0

[1] Capacity and power are based on typical equipment values [180]

Table 4.5: Parameters for all microwave backhaul links

items n	Name	C_n (Gbps)[1]	$P_n^{\max}$ (Watts)[1]	power ratio β_n
6	Link1	0.57	147	0.25
7	Link2	0.57	147	0.25
8	Link3	0.812	294	0.25
9	Link4	0.57	147	0.25
⋮	⋮	⋮	⋮	⋮
15	Link10	0.57	147	0.25

[1] Parameters are based on typical equipment values [181]

Hybrid: Fig. 4.4 illustrates how the proposed algorithm responds to the changes of backhaul links Link2 and Link4 specified in Table 4.5. In the "Hybrid" case, only routes 2 and 8 carry data traffic. As a consequence, the selected backhaul links and MUX nodes leading to the corresponding S-GW nodes are different for the "Hybrid" case and the "All Fibre" case as shown in Fig. 4.5. Although the resulting aggregated data traffic for S-GW nodes in EPC remains the same for "Hybrid" and "All Fibre" cases, all traffic is routed through MUX1 with no traffic on MUX2 for the "Hybrid" case, where the input traffic of MUX1 is via microwave backhaul Link2 and Link4.

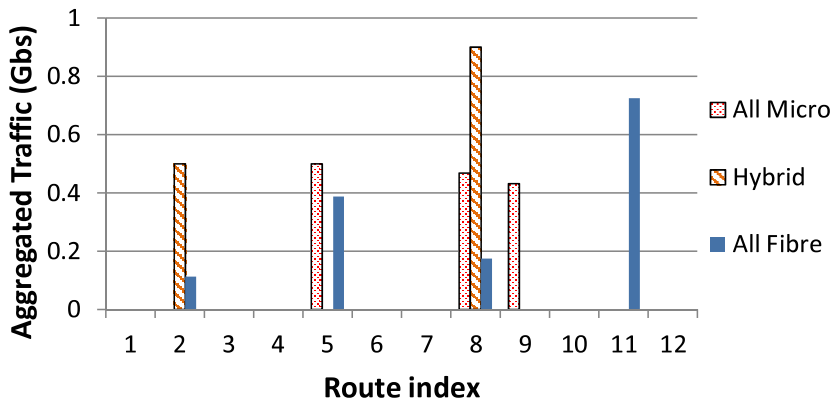

Figure 4.4: Comparison of traffic on each route with $\omega = 0.5$ for the distributed solution

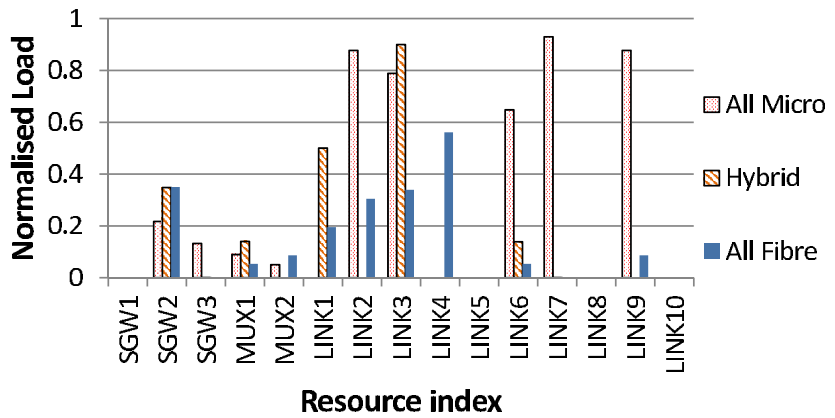

Figure 4.5: Resource normalised load comparison with $\omega = 0.5$ for the distributed solution

All Micro: Fig. 4.4 illustrates the traffic carried on each predefined route for the all microwave backhaul links case. Compared to the "Hybrid" case, data traffic is distributed over more routes. However, route 1, 4, 7 and 10 still bear no traffic, which in turn results in no traffic on S-GW1. This also explains why no traffic is allocated to Link 5 and 8, which are connected to the least energy efficient S-GW1. Compared to other 2 cases, the "All Micro" case has more highly loaded links since microwave backhaul links have much less bandwidth compared to optical fibre links.

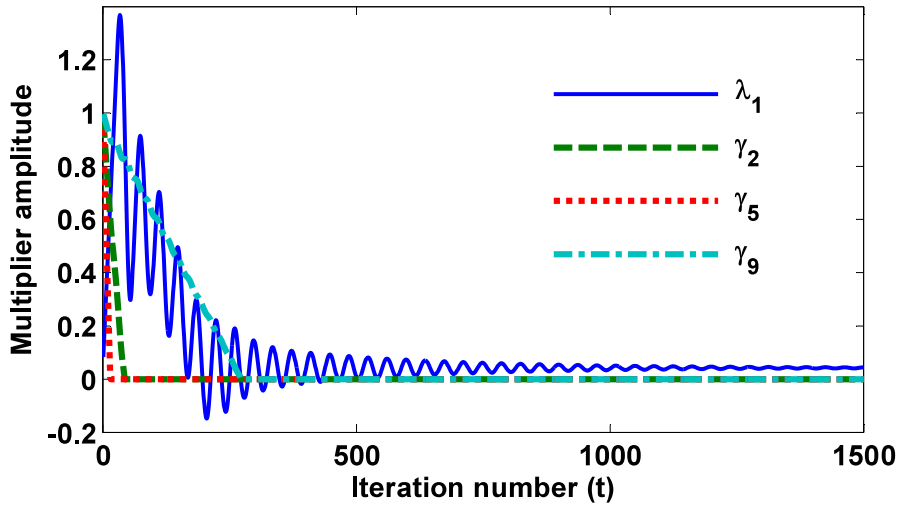

Figure 4.6: Convergence of selected Lagrangian multiplier with $\omega = 0.5$ for all fibre links

4.7.2.2 Convergence

To illustrate the convergence of the proposed algorithm, we have captured values of Lagrangian multipliers over iterations. Fig. 4.6 demonstrates trajectories for Lagrangian multipliers $\boldsymbol{\lambda}$ and γ in (4.14) for the 'All Fibre" case with $\omega = 0.5$. For illustrative purposes, only a few representative curves are chosen because other curves follow the similar trend. The value of $\boldsymbol{\lambda}_1$ associated with the equality constraint in (4.6) for eNodeB 1 varies significantly at the beginning and decreases quickly before 200 iterations. Then the value of $\boldsymbol{\lambda}_1$ oscillates around the x axis as it converges to a small positive value. For the inequality constraint in (4.7) for the traffic processing capacity of S-GW 2 and MUX 2, the "prices" of γ_2 and γ_5 converge to zero more quickly with less than 50 iterations. The Lagrangian multipliers for the other S-GW and MUX nodes follow the similar trend. On the other hand, the convergence of γ_9 for backhaul link 4 is slower than other illustrated Lagrangian multipliers.

For all three cases with different backhaul configuration and $\omega = 0.5$, the proposed algorithm shows similar behaviour in terms of system convergence. After some iterations, the Lagrangian multiplier γ for inequality constraint in (4.7) reaches zero and remains unchanged. On the other hand the Lagrangian multiplier $\boldsymbol{\lambda}$ for equality constraint in (4.6) converges to a small positive number. The convergence behaviour of Lagrangian

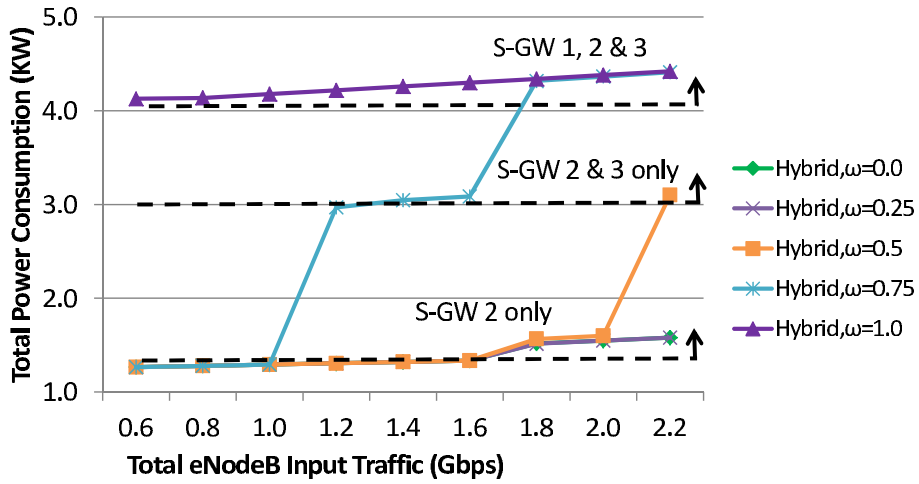

Figure 4.7: System power consumption with different weights for the distributed solution

multipliers for inequality and equality constrains reflects the complementary slackness of KKT theorem as specified in [176]. The figures for convergence of "Hybrid" and "All Micro" cases are omitted since they exhibit similar behaviour as "All Fibre".

4.7.2.3 Effect of Weighting Factor

Next we show how the system performs with different weighting factors ω and input traffic. Table 4.2 shows the eNodeB input traffic setup from test cases $t1$ to $t9$ with an increasing step of 0.1 Gbps for each eNodeB. Fig. 4.7 illustrates the total system power consumption for the system input traffic with different weighting factor $\omega = 0.0$, 0.25, 0.5, 0.75 and 1.0 for the "Hybrid" case. The dependence of total power consumption on input traffic scenarios t1 to t9 for the values of ω is shown Fig. 4.7. The three dashed lines in Fig. 4.7 represent where a S-GW is energised to handle the routed traffic.

With the optimisation weighted to consider energy consumption only, ($\omega = 0$), we get minimal power consumption with all the traffic directed toward the least energy consuming gateway (S-GW 2) via the most energy efficient links as shown in Fig. 4.7. However, this weight configuration does not distribute the traffic at all, resulting in a highly loaded S-GW. As the value of ω is increased, we start to see other gateways and routes carrying traffic with corresponding increases in power consumption. For example, with $\omega = 0.5$, S-GW 3 is activated at high load for the distributed solution. For $\omega = 0.75$, S-GW 3

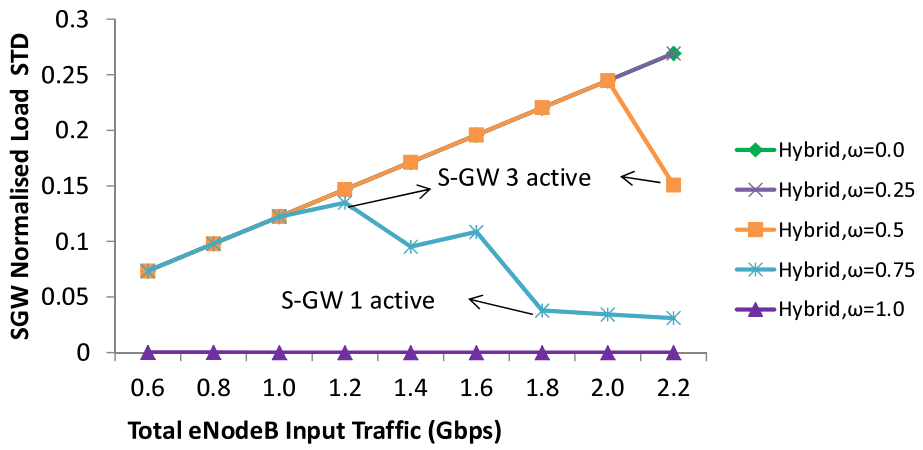

Figure 4.8: S-GW normalised load standard deviation σ^{sgw} with different weights for the distributed solution

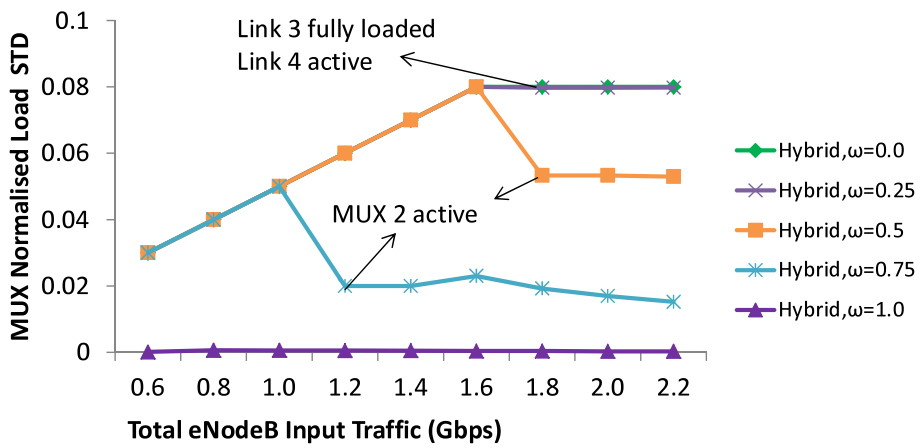

Figure 4.9: MUX normalised load standard deviation σ^{mux} with different weights for the distributed solution

and S-GW 1 are activated at medium load and high load respectively. The total power consumption displays significant jumps as each additional service gateway is energised. With $\omega = 1$, all S-GWs are already energised at low load and the gradual increase in the total system power consumption arises from the linear increase of the incremental power consumption of the active network elements.

Fig. 4.8 and Fig. 4.9 show the standard deviations of the resulting normalised load over S-GWs and MUXs respectively as shown in Eq. (4.4). It is easy to understand that $\sigma^{\text{sgw}} = 0$ for $\omega = 1.0$ and σ^{sgw} increases with the total input traffic for $\omega = 0.0$. For $\omega = 0.5, 0.75$, the slope of σ^{sgw} decreases sharply when an extra S-GW is activated due to

increasing traffic. This is because more S-GW capacity is available to balance the traffic. For σ^{mux} in Fig. 4.9, the curves with $\omega < 0.5$ (some degree of energy minimisation) are almost the same from low to medium load. With the total traffic more than 1.6 Gbps, σ^{mux} is flat with the increase of the total traffic. This is because for MUX 2, energy efficient link 3 (optic) is fully loaded. The extra traffic from eNodeB 2 can only be routed to less energy efficient link 4 (microwave) such that the resulting σ^{mux} is constant even with the increase of the total traffic. Simulation results show similar behaviour of σ^{mux} for $\omega = 0.5, 0.75$. With a new active MUX, the slope of σ^{mux} decreases due to more MUX capacity to balance the traffic. For $\omega = 1$ (pure load balance without energy minimisation), near zero STD for the normalised load on MUXs is expected.

4.7.3 Observations

Although the three cases considered in this paper are relatively simple, they represent three distinctly different situations that are relevant to wireless backhaul. The "All Fibre" case represents a situation in which the backhaul network is homogenous and makes a minimal contribution to network energy consumption. In this case we find that the power and load optimisation gives routes relatively independent of links between the nodes in the network. The traffic distribution solutions when compromising between load and power are dominated by the power consumption of S-GWs and load balancing across MUXs if the link capacity constraints are not violated. The "All Micro" case is also a homogeneous network. In this case the power consumption of the links is significant and fewer links are energised to minimise the total system power consumption. However due to link capacity constraints, not all traffic can be routed to the most energy efficient S-GW. For $\omega = 0.5$, the results show that the solution for "All Micro" require more energised S-GWs that for "All Fibre" as shown in Fig. 4.5. This because the capacity of microwave links connecting to a S-GW is unable to accommodate all input traffic. A portion of input traffic has to be distributed to another S-GW via other microwave links. This in turn leads to more energised network elements, which results in more power consumption than the "All Fibre" case. The "Hybrid" case is a heterogeneous network in which the power consumption of the different types of links (fibre and microwave) will make significantly

different contributions to network power. For $\omega = 0.5$, the power consumption of microwave links outweighs the load balance criteria for MUX nodes. Therefore, no traffic is routed over the microwave links, which leads to completely unbalanced traffic over MUX nodes compared to the "All Fibre" and "All Micro" cases.

The system power consumption will be significantly impacted by the choice of ω, the incoming traffic, the underlying network topology and the energy characteristics of network elements. The resulting route selection and traffic distribution will impact the behaviour of the network depending on which factor dominates. Viewing Fig. 4.7, we see that for $\omega = 0$ (i.e. power minimisation only) the slope of total network power consumption relative to total traffic is relatively flat. This is because the optimisation will only activate higher power consuming links as a "last resort". Similarly, the slope for the case $\omega = 1$ has small slope because most of the equipment is already active to balance the load across all the links. However, for the case $\omega = 0.5, 0.75$ in which the optimisation attempts to compromise between network power and load balancing, we get sudden, large increases in total power as the total traffic increases. This is because, at low load, the network can easily spread its load across the low energy consuming paths (i.e. optical paths). However, at certain values of network traffic, a high power consuming link will have to be energised to keep the load relatively balanced across paths. This will cause a significant increase in total network power. Note those sudden jumps do not occur in a fixed sequence as the incoming traffic increases. This is because different network configurations have different "bottlenecks" for a certain traffic pattern. Those "bottlenecks" may not be due to the capacities of S-GW/MUX nodes with high power consumption. Network topologies with inappropriate link types or capacities could cause significant system power consumption variations over a diurnal cycle, which could otherwise be avoided with proper network design.

The challenge for the network planner is to learn the dynamic range and the pattern of the traffic to be handled. Network planning needs to consider all network elements rather than elements with high power consumption only. Network topology design and links selection could well impact future network power management. The challenge for the operator, who must manage its network power consumption, is to know when these

sudden steps will occur and what factors cause them and how to mitigate their effect without significantly degrading service quality. In addition, network operators need to consider real network operations. The cost of network elements reconfiguration in terms of extra energy consumption and response time has to be taken into account so as to run the network in an energy efficient manner.

4.8 Conclusions

In this chapter, we have proposed a general framework for heterogeneous backhaul traffic allocation in mobile networks. We formulated a multi-objective optimisation problem with respect to conflicting targets of minimising total system power consumption and achieving load balancing across network elements. We applied a distributed approach to solve the optimisation problem with each eNodeB minimising their own cost functions relating to energy consumption of transporting their traffic to S-GWs and system load balancing conditions. We proved the stability of the proposed distributed algorithm by applying Lyapunov stability analysis. To evaluate the performance of the framework, we presented a backhaul traffic distribution example with different backhaul technology configurations to demonstrate the distributed method of solving a global optimisation problem. The simulation results showed how the system responded to the change of backhaul links by choosing different predefined routes. In addition, system convergence was verified by simulation results for the related Lagrangian multipliers.

The diurnal characteristic of traffic provides opportunities to improve the energy efficiency of mobile networks by changing the effective routing topology of the network. With the proposed algorithm, choosing ω close to 1.0 can handle the peak time traffic according to the system capacity with high network availability. For off-peak period, choosing ω close to 0.0 can save network energy consumption by shutting down redundant equipment. Note using $\omega = 0.0$ could degrade network availability in a traffic flash-crowd scenario. However, by setting an appropriate $\omega \in [0, 1]$, the proposed algorithm provides a mechanism of dynamic traffic routing, which can improve system energy efficiency while maintaining a certain level of network availability.

Chapter 5

A Game-theoretic Analysis of Energy Efficiency and Performance for Cloud Computing in Communication Networks

5.1 Introduction

In the previous chapter we have developed a distributed optimisation framework for improving energy efficiency of mobile backhaul networks. This framework is based on the assumption that the network is own by a single party and there is no direct mutual influence among individual network users. This assumption does not address the multi-ownership of the network resources in a more general network such as the Internet. Moreover, end users in a shared network may compete to use network resources such as long-haul bandwidth and cloud computing resources. The non-cooperative behaviour of end users would deteriorate the overall network performance as discussed in [61]. To illustrate such networking scenarios, we consider a cloud-based metro/core network shared by multiple end users. Problems $4 \sim 7$ specified in 1.1 are addressed in this chapter. The proposed non-cooperative game approach is different from the distribution optimisation method specified in chapter 4 by considering interactions and rational of individual network users. We first start with the motivation of improving energy efficiency and performance for cloud computing in communication networks.

The exponential growth of Internet traffic continues with diversified and increasingly mobile applications requiring a large amount of network bandwidth [3]. The inherent

"best effort" nature of traditional IP protocols does not guarantee end-to-end bandwidth for all data traffic. Data traffic imbalances result in poor network performance and service availability [182]. Furthermore, the concern for energy consumption is now drawing both academic and industrial attention to the sustainable growth of the future telecommunications and data networks [3]. Cloud computing is gaining importance for providing cloud services to both business and individual customers. Previous works for energy efficient cloud computing focus mainly on data centre (DC) servers and storage facilities [112]. Recently, the study [113] highlights the impact of energy consumption of transport networks, indicating that both academia and industry may have underestimated the energy consumption of cloud computing by ignoring the transport aspect. By taking the energy consumption of transport networks into account, the proclaimed "green" cloud could in fact be "dirty" under certain circumstances [113].

This chapter proposes a general framework for distributing data traffic to data centres through transport networks in an energy efficient manner. The energy consumption of data centres and transport networks carrying the traffic is taken into account explicitly. Instead of focusing on a segment of the cloud system such as data centres, we endeavor to provide end-to-end solutions to energy efficient traffic distribution for the whole system. For transport networks, queueing theoretic principles are applied to model the overall network performance. Then, we introduce load balancing across servers in order to account for service availability. The proposed solution manages the traffic in the system, (i.e. in transport networks and data centres,) in an energy-aware manner. Furthermore, in contrast to the classic elastic data traffic routing such as in [24], this chapter introduces bandwidth guarantees for users' traffic as discussed in Section 5.4.2.

Previous works, such as [21], assume that a single centralised entity controls the whole network. While this may be valid for some of the existing systems, future networks will potentially be owned by multiple stakeholders with different objectives. Using game theory [57], we develop a distributed algorithm for network data traffic distribution for such service providers. Then, we use Lyapunov theory to analyze the convergence of the proposed algorithm. System performance for several optimisation scenarios are examined and compared using numerical simulations. The simulation results provide insights

for improving energy efficiency while minimising system traffic delay and maintaining the service availability for network applications.

Existing literature on traffic routing using game theory are mainly focused on the total system performance often based on queuing theory such as in [100]. Growing importance of energy consumption in networks makes it an important factor when designing and managing networks. However, *little work has been done to jointly consider energy efficiency in combination with network parameters used by operators to design and manage networks, such as load balancing and transport network performance.* Moreover, simple or specific network topologies have usually been assumed to facilitate theoretical analysis of game theory approaches to network traffic distribution in the literatures, e.g. [183].

The rest of the chapter is structured as follows. The next section describes the general system model for traffic distribution from end users to server farms via transport networks. The multiple objectives to optimise the system are specified in Section 5.3 followed by a strategic game design in Section 5.4. An iterative algorithm is specified in Section 5.5 with Nash Equilibrium and stability analysis. In Section 5.6, the performance efficiency loss is investigated by comparing the performance of the global optimal solution and the strategic game solution. Section 5.7 illustrates the simulation results and Section 5.8 concludes the chapter.

5.2 System Model

We consider a general system model, which consists of J edge routers, M intermediate multiplexing/aggregation (MUX/router) nodes and I virtualised server nodes as shown in Fig. 5.1. Edge routers, MUXs and the links compose the transport network while the server farm includes the server nodes connected to the transport network. The network has L links connecting edge routers and servers via MUX nodes. Then the system has in sum $N = I + M + L$ *resources*. Each *resource* is characterised by the maximum data traffic processing capacity $\mathbf{C}_n$ with $n = 1, \cdots, N$. Assume at time t edge router $j = 1, \cdots, J$, generates an aggregated data traffic with a data rate $\mathbf{d}_j^{\text{in}}(t)$ (bit/sec). Then all traffic generated by edge routers can be expressed as a vector $\mathbf{d}^{\text{in}}(t) = [\mathbf{d}_1^{\text{in}}(t), \cdots, \mathbf{d}_J^{\text{in}}(t)]^T$. We

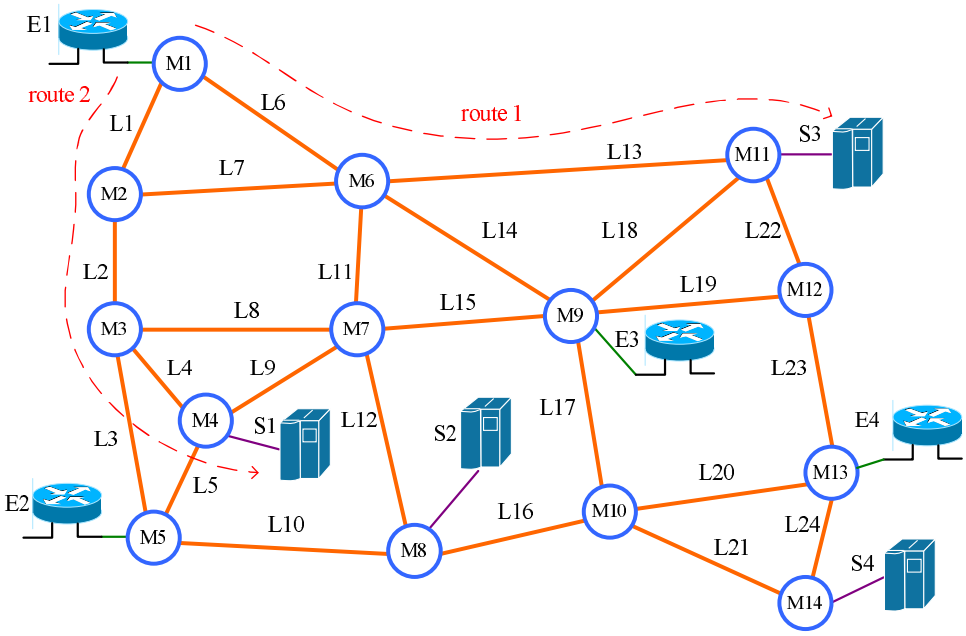

Figure 5.1: System model for content cloud with 4 edge nodes, 14 MUX and 4 server nodes.

assume $\mathbf{d}^{\text{in}}(t)$ is approximately constant during a short period. For simplicity we omit t for the rest of the chapter. Let Ω_R be a set of all possible routes from edge routers to servers with cardinality R and route $r = \{1, \cdots, R\}$ be a predefined route carrying an averaged traffic $\mathbf{d}_r$ from an ingress edge router to a server such that the traffic on all routes can be expressed as a vector $\mathbf{d} = [\mathbf{d}_1, \cdots, \mathbf{d}_R]^T$. Fig. 5.1 illustrates the route $1 \in \Omega_R$ from edge router 1 to server 1 via MUX 1. Each edge router then distributes its traffic $\mathbf{d}_j^{\text{in}}$ over a subset of Ω_R to the designated servers. We use the $J \times R$ routing matrix $\mathbf{B}^{\text{rt}}$ defined in Eq. (3.2) of Section 3.3.1 to represent the mapping between edge routers and routes such that $\mathbf{B}_{j,r}^{\text{rt}} = 1$ indicates edge router j can dispatch traffic via route r while $\mathbf{B}_{j,r}^{\text{rt}} = 0$ indicates not. This in turn indicates $\mathbf{d}^{\text{in}} = \mathbf{B}^{\text{rt}}\mathbf{d}$. In addition, the topology of the system in Fig. 5.1 can be represented by the $N \times R$ matrix $\mathbf{A}$ defined in Eq. (3.1) of Section 3.3.1. Let $\mathbf{d}_n^{\text{res}}$ be the aggregated traffic at *resource* n such that all aggregated traffic on server nodes, MUX nodes and links can be expressed as a vector $\mathbf{d}^{\text{res}} = [\mathbf{d}_1^{\text{res}}, \cdots, \mathbf{d}_N^{\text{res}}]^T$. The relationship between the aggregated traffic on each *resource* and the traffic on each route can be expressed as $\mathbf{d}^{\text{res}} = \mathbf{A}\mathbf{d}$. Using Eq. (3.3) in Section 3.3.1, we can derive a 1-0 edge router-*resource* mapping matrix $\mathbf{B}^{\text{res}}$ where $\mathbf{B}_{j,n}^{\text{res}} = 1$ indicates there is a available route

Table 5.1: Term Notation

Term	Explanation
J	Number of edge router nodes
M	Number of MUX nodes
I	Number of server nodes
L	Number of links connecting nodes
N	Number of resources including virtual server nodes, MUX nodes and links with $N = I + M + L$
R	Number of routes from edge routers to virtual servers
$\mathbf{C}$	Vector of network *resource* capacity $\mathbf{C}_n$ for all virtual servers, MUX nodes and links
Ω_R	Set of routes with route $r = \{1, \cdots, R\}$ carrying an averaged traffic $\mathbf{d}_r$
$\mathbf{B}^{\text{rt}}$	0-1 matrix with J-by-R dimension mapping R predefined routes to J edge routers
$\mathbf{B}^{\text{srv}}$	0-1 matrix with J-by-I dimension mapping I virtual servers to J edge routers
$\mathbf{B}^{\text{mux}}$	0-1 matrix with J-by-M dimension mapping M MUXs to J edge routers
$\mathbf{A}$	0-1 matrix with N-by-R dimension mapping R predefined routes to N *resources* with sub-matrices $\mathbf{A}^{\text{srv}}$ and $\mathbf{A}^{\text{mux}}$ for servers and MUXs respectively
$\mathbf{d}^{\text{in}}$	Vector of input traffic with the entity $\mathbf{d}_j^{\text{in}}$ denoting the traffic generated by edge router j
$\mathbf{d}$	Vector of traffic $\mathbf{d}_r$ carried by route $r = \{1, \cdots, R\}$
$\mathbf{d}^{\text{res}}$	Vector of aggregated traffic $\mathbf{d}_n^{\text{res}}$ on *resource* $n = 1, \cdots, N$ with sub-vectors $\mathbf{d}^{\text{srv}}$ and $\mathbf{d}^{\text{mux}}$ for servers and MUXs respectively. $\mathbf{d}_n^{\text{res}}$ is calculated and signaled by *resource* n.

linking edge router j and network element n. Further, we can obtain the $J \times I$ edge-server mapping matrix $\mathbf{B}^{\text{srv}} \subset \mathbf{B}^{\text{res}}$ and the $J \times M$ edge-MUX mapping matrix $\mathbf{B}^{\text{mux}} \subset \mathbf{B}^{\text{res}}$ such that $\mathbf{B}_{j,i}^{\text{srv}} = 1$ and $\mathbf{B}_{j,m}^{\text{mux}} = 1$ indicate edge router j having at least 1 route connected to server i and MUX m respectively. Table 5.1 summarises the main terms and variables used in this chapter.

5.3 Problem Formulation

We formulate a traffic distribution problem in order to find the optimal traffic for each ingress edge router to dispatch over the predefined routes through transport networks to

the server farm such that the associated cost function is minimised. We propose a joint cost function with 3 potentially conflicting objectives:

- normalised power consumption of resources in the transport network and the server farm,
- data traffic load balancing for the server farm,
- total traffic delay for the transport network.

5.3.1 Objective 1: Power Consumption

The normalised total power consumption for traffic routing and processing includes the power consumption of all *resources* shown in Fig. 5.1 such as links, edge routers and servers. We approximate the power consumption of a network element $n = 1, \cdots, N$ as shown in Eq. (3.10). Note that Eq. (3.10) is an approximation of the actual power consumption of network element n as a function of the aggregated traffic $\mathbf{d}_n^{\text{res}}$. This approximation is only accurate when $\rho_n^{\text{res}}\mathbf{C}_n = \mathbf{d}_n^{\text{res}}$. Because the actual idle power $\beta_n P_n^{\max}$ is independent of $\mathbf{d}_n^{\text{res}}$, the optimisation of the total power consumption with respect to $\mathbf{d}_n^{\text{res}}$ is a nonlinear Mixed Integer Programming (MIP) problem, which is NP-hard. In this chapter we incorporate the idle power into the linear function Eq. (3.10). For scaling purpose, we define the normalised total incremental power consumption for the whole system as

$$P_{\text{sys}}(\mathbf{d}) = \frac{\sum_{n=1}^{N} P_n}{P^{\max}} \tag{5.1}$$

where $P^{\max}$ denotes the sum of the maximal power over all *resources* shown in Fig. 5.1. With the adoption of resource consolidation and service aggregation, modern data centres are more scalable than before. The resulting resource pool can be dynamically configured by turning on/off virtual and physical machines based on processing requests. The power consumption of individual element in the pool can be approximated by using Eq. (3.10). As a consequence, the power consumption of data centres is likely to grow linearly with the increase of the traffic load. By treating data centres as virtualised entities, we approximate the data centre power consumption by Eq. (3.10).

5.3.2 Objective 2: Load Balancing

New Internet applications and services are more likely to be provisioned over multiple geographically distributed data centres. The limited capacity of a single server/data centre may not be able to handle arbitrarily high volumes of incoming IP traffic. Inter-data centre load balancing is becoming increasingly important for rich media applications and services [184]. The adoption of virtualisation allows transforming isolated server nodes in data centres into shared resource pools. Server clustering with load balancing has become a technology of choice to improve the performance of IP applications for availability, scalability and reliability. By orchestrating server farms with geographic diversity, balanced traffic dissemination facilitates optimising resource use, avoiding traffic overload and minimising service response time [182]. Various of load balancing technologies are summarised in works such as [185].

We set the second objective to be load balancing over the server farms shown in Fig. 5.1. Due to asymmetrical allocations of servers, edge node only considers load balancing over the allocated servers, which is a subset of all servers. Define the load balanced condition for edge node j as,

$$\eta_{i,j}^{\text{srv}} = \frac{T_j}{\mathbf{C}_{\text{sys},j}^{\text{srv}}}, \forall \quad \mathbf{B}_{j,i}^{\text{srv}} = 1 \tag{5.2}$$

where $T_j = \sum_{i=1}^{I} \mathbf{B}_{j,i}^{\text{srv}} \mathbf{d}_i^{\text{srv}}$ denotes the aggregated traffic on servers allocated to edge node j, $\mathbf{C}_{\text{sys},j}^{\text{srv}} = \sum_{i=1}^{I} \mathbf{B}_{j,i}^{\text{srv}} \mathbf{C}_i^{\text{srv}}$ denotes the total capacity of those servers, and $\eta_{i,j}^{\text{srv}} = \frac{\mathbf{A}_i^{\text{srv}} \mathbf{d}}{\mathbf{C}_i^{\text{srv}}}$ denotes the normalised load for server i from edge node j perspective. Note that $\mathbf{d}_i^{\text{srv}}$ denotes the aggregated load over server i which can be split over user j and the rest users other than j as

$$\mathbf{d}_i^{\text{srv}} = \mathbf{A}_i^{\text{srv}} \mathbf{d} = \sum_{r=1}^{R} \mathbf{B}_{j,r}^{\text{rt}} \mathbf{A}_{i,r}^{\text{srv}} \mathbf{d}_r + \sum_{h \neq j}^{J} \sum_{r=1}^{R} \mathbf{B}_{h,r}^{\text{rt}} \mathbf{A}_{i,r}^{\text{srv}} \mathbf{d}_r.$$

However, representing the global load balanced condition illustrated in (5.2) in the model is difficult. In order to address this problem, we propose an alternative implementation of load balancing by introducing a normalised load balancing variance for edge

node j as,

$$\bar{S}_j(\mathbf{d}) = \frac{1}{\hat{S}^{\text{srv}}\bar{I}} \sum_{i=1}^{I} \mathbf{B}_{j,i}^{\text{srv}} \left(\frac{\mathbf{d}_i^{\text{srv}}}{\mathbf{C}_i^{\text{srv}}} - \frac{T_j}{\mathbf{C}_{\text{sys},j}^{\text{srv}}} \right)^2 \tag{5.3}$$

where $\hat{S}^{\text{srv}} = \left(\frac{\sum_{j=1}^{J} \mathbf{d}_j^{\text{in}}}{\sum_{i=1}^{I} \mathbf{C}_i^{\text{srv}}} \right)^2$ denotes the upper bound (The extreme case that all packets directed to any servers are dropped) of the load balancing variance for all servers and $\bar{I} \leq I$ is a normalisation factor as the averaged number of servers used by each edge node.

Theorem 5.1. *Minimising the load balancing variance in* (5.3) *leads to the balanced load condition* (5.2).

Proof: Note $\hat{S}^{\text{srv}}$ and $\bar{I}$ are constants. $\mathbf{d}_i^{\text{srv}} = \mathbf{A}_i^{\text{srv}}\mathbf{d}$ and $\eta_{i,j}^{\text{srv}}(\mathbf{d}) = \frac{\mathbf{A}_i^{\text{srv}}\mathbf{d}}{\mathbf{C}_i^{\text{srv}}}$ lead to

$$\min_{\mathbf{d}} \bar{S}_j(\mathbf{d}) = \min_{\mathbf{d}} \sum_{i=1}^{I} \frac{\mathbf{B}_{j,i}^{\text{srv}}}{\hat{S}^{\text{srv}}\bar{I}} \left(\eta_{i,j}^{\text{srv}}(\mathbf{d}) - \frac{T_j}{\mathbf{C}_{\text{sys},j}^{\text{srv}}} \right)^2 \tag{5.4}$$

Note $\mathbf{B}_{j,i}^{\text{srv}} = 1$ if edge node j route traffic to server i and 0 otherwise. It is clear that (5.4) is a convex problem with the minimium of 0. Then,

$$\bar{S}_j(\mathbf{d}) = 0 \Rightarrow \mathbf{B}_{j,i}^{\text{srv}} \left(\eta_{i,j}^{\text{srv}}(\mathbf{d}) - \frac{T_j}{\mathbf{C}_{\text{sys},j}^{\text{srv}}} \right)^2 = 0, i = 1, \cdots, I$$

such that $\eta_{i,j}^{\text{srv}}(\mathbf{d}) - \frac{T_j}{\mathbf{C}_{\text{sys},j}^{\text{srv}}} = 0$ when $\mathbf{B}_{j,i}^{\text{srv}} = 1$. ■

5.3.3 Objective 3: Transport Network Performance

Transport network performance is of paramount importance for network applications and services. In this chapter, we apply the fluid flow concept [24] to model the data traffic. Inspired by the queuing theory [186], we also use the M/M/1 model to analyse the transport network performance. Although the M/M/1 model is simple, it captures the main cause of queuing delay due to the packet processing capacity of network elements and the carried traffic load. This makes it a very useful model to evaluate the performance of network elements [186].

The third objective is to minimise the traffic delay over the transport network. Assume the data traffic arrives at MUX nodes according to a Poisson process and the service time is exponentially distributed. Inspired by the M/M/1 queue theory [186], we model the average traffic delay of MUX m as

$$D_m(\mathbf{d}) = \frac{1}{\hat{S}_m^{\text{mux}}\left(\mathbf{C}_m^{\text{mux}} - \mathbf{d}_m^{\text{mux}}\right)} \tag{5.5}$$

where $\mathbf{d}_m^{\text{mux}} = \mathbf{A}_m^{\text{mux}}\mathbf{d}$ denotes the aggregated traffic arriving at MUX m and $\hat{S}_m^{\text{mux}} = \frac{1}{\mathbf{C}_m^{\text{mux}}(1-\rho_m^{\text{mux}})}$ is the normalisation factor with the pre-defined capacity utilisation ratio ρ_m^{mux}.

5.4 Strategic Game Design

Most of the existing literature, such as in [21], assume centralised control and single ownership of the transport networks and data centre infrastructure. Therefore, centralised optimisation algorithms can be applied to improve energy consumption and system performance such as traffic load balancing and IP application service response time. This assumption is not appropriate in many scenarios where transport networks, server farms or segments of them could belong to different stakeholders who share the same transport networks or infrastructure to provide their services. Driven by individual and potentially very different interests, different stakeholders often adopt selfish operation strategies, which means a global objective is unlikely to be achieved.

Game theory is suitable for modeling interaction between multiple stakeholders or decision makers [44]. For many telecommunication and cloud services, the stakeholders involved choose strategies to share common resources under one or multiple constrains following their own self interests. This situation leads to a strategic game formulation, in which a number of rational decision makers with potentially conflicting interests try to maximise their own payoff or alternatively minimise the corresponding costs.

5.4.1 Strategic Game Model

To account for the rational behaviour of individual users and the multi-ownership of network resources, we propose a strategic game Γ model. In this strategic game, the j-th end node is modelled as a game player acting as a "selfish" individual associated with a cost function $f_j(\vec{\mathbf{x}})$, where $\vec{\mathbf{x}}$ denotes the strategy profile over all players. A strategy profile is defined as $\vec{\mathbf{x}} = \{\mathbf{x}_1, \mathbf{x}_2, \cdots, \mathbf{x}_J\}$ where $\mathbf{x}_j$ denotes a possible strategy of player j. Assume individual cost function $f_j(\vec{\mathbf{x}})$ is strictly convex, continuous and twice differentiable. Let $\tilde{j}$ denote the fact that this term dose not include any term with index j. Given a strategy profile $\vec{\mathbf{x}}_{\tilde{j}} = \{\mathbf{x}_1, \cdots, \mathbf{x}_{j-1}, \mathbf{x}_{j+1}, \cdots, \mathbf{x}_J\}$ for all other players such that $\vec{\mathbf{x}} = \mathbf{x}_j \cup \vec{\mathbf{x}}_{\tilde{j}}$, a rational game player j will adjust its own strategy $\mathbf{x}_j$ to minimise the corresponding cost function $f_j\left(\mathbf{x}_j, \vec{\mathbf{x}}_{\tilde{j}}\right)$.

The Nash Equilibrium (NE) of the strategic game Γ defined above is the strategy profile $\vec{\mathbf{x}}^*$ such that for each player j, the optimal strategy satisfies,

$$\mathbf{x}_j^* = \arg\min_{\mathbf{x}_j} f_j\left(\mathbf{x}_j, \vec{\mathbf{x}}_{\tilde{j}}^*\right) \tag{5.6}$$

The NE for the proposed strategic game is the strategy profile by which no player can further decrease its cost function given other player's NE strategies. In other words, in NE, no player can obtain better "payoff" by unilaterally deviating from its equilibrium strategy to another feasible strategy [44].

5.4.2 User Objectives

We apply the weighted sum method to construct a multi-objective cost function $U_j(\mathbf{d})$ for a player with a-priori user-specific preference [43] at edge router j:

$$U_j(\mathbf{d}) = \boldsymbol{\omega}_j^{\text{pow}} \bar{P}_j(\mathbf{d}) + \boldsymbol{\omega}_j^{\text{srv}} \bar{S}_j(\mathbf{d}) + \boldsymbol{\omega}_j^{\text{mux}} \bar{D}_j(\mathbf{d}) \tag{5.7}$$

where $\boldsymbol{\omega}_j^{\text{pow}}$, $\boldsymbol{\omega}_j^{\text{srv}}$ and $\boldsymbol{\omega}_j^{\text{mux}}$ denote the weighting factor of user j for normalised incremental power consumption $\bar{P}_j(\mathbf{d})$, server load balancing variance $\bar{S}_j(\mathbf{d})$ and transport network delay $\bar{D}_j(\mathbf{d})$ respectively. The rational user j only considers the power con-

sumption of its own traffic expressed as

$$\bar{P}_j(\mathbf{d}) = \sum_{n=1}^{N} \frac{\tilde{\mathcal{E}}_n}{P^{\max}} \sum_{r=1}^{R} \mathbf{B}^{\mathrm{rt}}_{j,r} \mathbf{A}_{n,r} \mathbf{d}_r \tag{5.8}$$

where $\mathbf{B}^{\mathrm{rt}}_{j,r}\mathbf{A}_{n,r}\mathbf{d}_r$ represent the traffic routed to network element n via route r from user j. User j also intends to minimise the normalised load balancing variance shown in (5.3) over only those servers which deal with traffic from user j. Finally each user tries to minimise the normalised averaged delay of its own traffic expressed as

$$\bar{D}_j(\mathbf{d}) = \sum_{m=1}^{M} \frac{\mathbf{B}^{\mathrm{mux}}_{j,m}}{\hat{S}^{\mathrm{mux}}_m \bar{M}} \sum_{h=1}^{R} \frac{\mathbf{B}^{\mathrm{rt}}_{j,h}\mathbf{A}^{\mathrm{mux}}_{m,h}}{\mathbf{C}^{\mathrm{mux}}_m - \sum_{r=1}^{R} \mathbf{A}^{\mathrm{mux}}_{m,r}\mathbf{d}_r} \tag{5.9}$$

where the delay of a given MUX used in different routes from the same user will be duplicated and $\bar{M} \leq M$ is a normalisation factor. Then user j's goal is to choose a traffic distribution strategy $\mathbf{d}$ such that

$$\min_{\mathbf{d}} U_j(\mathbf{d}) \tag{5.10}$$

$$\text{subject to } \mathbf{B}^{\mathrm{rt}}_j \mathbf{d} = \mathbf{d}^{\mathrm{in}}_j \tag{5.11}$$

$$0 \leq \mathbf{A}\mathbf{d} \leq \mathbf{C} \tag{5.12}$$

- The first constraint (5.11) indicates the input traffic flow conservation for user $j = 1, \cdots, J$. This bandwidth guarantee for each user is not implemented in [24].

- The second constraint (5.12) indicates the aggregated traffic on each *resource* is limited by the corresponding processing capacity or bandwidth.

We define a strategic traffic routing game for the weighted multi-objective optimisation problem in (5.7) as

Definition 5.1. *The strategic traffic routing game* $\Gamma = \langle J, \{\mathbf{x}_j\}, \{U_j : \vec{\mathbf{x}} \longrightarrow \Re\}\rangle$ *consists of* J *edge routers*

- Players*: Each edge router* $j = 1, \cdots, J$ *is a rational game player.*

- Strategies*: Each edge router is associated with a set of feasible traffic distribution strategies* $\mathbf{x}_j = [\mathbf{d}_1\mathbf{B}^{rt}_{j,1}, \cdots, \mathbf{d}_R\mathbf{B}^{rt}_{j,R}]^T \subset \Re^R$.

- Preferences*: Each edge router's preference is represented by individual cost function* $U_j(\mathbf{d})$ *defined in* (5.7) *such that strategy* $\mathbf{x}^*_j$ *is preferred to strategy* $\mathbf{x}'_j$ *if and only if* $U_j\left(\mathbf{x}^*_j\right) < U_j\left(\mathbf{x}'_j\right)$ *with the constraints in* (5.11) *and* (5.12).

5.5 Game Analysis and Solution

In this chapter, we only concentrate on pure strategy game where each *player* chooses a pure strategy from its strategy set given other *players'* strategies. In addition each *player* analyses the signallings of other *players'* actions and proactively anticipates the effect of his own strategy.

5.5.1 Nash Equilibrium Analysis

Lemma 5.1. *The cost function* $U_j(\mathbf{d})$ *of user i is strictly convex for the related individual argument of* $\mathbf{d}$*, i.e.,* $\frac{\partial^2 U_j(\mathbf{d})}{\partial \mathbf{d}_r^2} > 0$ *if* $\mathbf{B}^{rt}_{j,r} = 1$.

Proof: The cost function for edge router $j = 1, \cdots, J$ is continuous, twice differentiable. For $\mathbf{B}^{\text{rt}}_{j,r} = 1$,

$$\frac{\partial^2 U_j(\mathbf{d})}{\partial \mathbf{d}_r^2} = \frac{2\omega^{\text{srv}}_j \left(\mathbf{B}^{\text{rt}}_{j,r}\right)^2}{\hat{S}^{\text{srv}}\bar{I}} \sum_{i=1}^{I} \mathbf{B}^{\text{srv}}_{j,i} \left(\frac{\mathbf{A}^{\text{srv}}_{i,r}}{\mathbf{C}^{\text{srv}}_i} - \frac{\mathbf{A}^{\text{srv}}_{i,r}}{\mathbf{C}^{\text{srv}}_{\text{sys},j}}\right)^2 + \frac{2\omega^{\text{mux}}_j}{\bar{M}} \sum_{m=1}^{M} \frac{\mathbf{B}^{\text{mux}}_{j,m}}{\hat{S}^{\text{mux}}_m} \sum_{h=1}^{R} \frac{\mathbf{B}^{\text{rt}}_{j,h}\mathbf{A}^{\text{mux}}_{m,h}(\mathbf{A}^{\text{mux}}_{m,r})^2}{\left(\mathbf{C}^{\text{mux}}_m - \sum_{r=1}^{R}\mathbf{A}^{\text{mux}}_{m,r}\mathbf{d}_r\right)^3}.$$

Note edge router j connects to at lest one server, which indicates $\sum_{i=1}^{I} \mathbf{B}^{\text{srv}}_{j,i} \left(\frac{\mathbf{A}^{\text{srv}}_{i,r_j}}{\mathbf{C}^{\text{srv}}_i} - \frac{\mathbf{A}^{\text{srv}}_{i,r}}{\mathbf{C}^{\text{srv}}_{\text{sys},j}}\right)^2 > 0$. Also edge router j will use at least one network resource. This in turn indicates that

$$\sum_{m=1}^{M} \frac{\mathbf{B}^{\text{mux}}_{j,m}}{\hat{S}^{\text{mux}}_m} \sum_{h=1}^{R} \frac{\mathbf{B}^{\text{rt}}_{j,h}\mathbf{A}^{\text{mux}}_{m,h}(\mathbf{A}^{\text{mux}}_{m,r})^2}{\left(\mathbf{C}^{\text{mux}}_m - \sum_{r=1}^{R}\mathbf{A}^{\text{mux}}_{m,r}\mathbf{d}_r\right)^3} > 0.$$

Then for edge router j, $\frac{\partial^2 U_j(\mathbf{d})}{\partial \mathbf{d}_r^2} > 0$ if $\mathbf{B}^{\text{rt}}_{j,r} = 1$. ■

Lemma 5.2. *Given other user's decision on* $\mathbf{d}$*, the optimisation problem for user* j *in* (5.10) *with the associated constrains in* (5.11) *and* (5.12) *is a convex optimisation problem.*

Proof: Let $\tilde{\mathbf{e}} = \left[\frac{\tilde{\mathcal{E}}_1}{P^{\max}}, \cdots, \frac{\tilde{\mathcal{E}}_N}{P^{\max}}\right]$ be the normalised slope (approximated incremental energy per bit) vector for all *resources* in the system. Note we assume there is no loop in the network topology and 1 route can only be occupied by one user. But one user can have multiple routes defined by the $J \times R$ routing matrix $\mathbf{B}^{\text{rt}}$. Then the normalised total incremental power consumption of the system can be expressed as

$$\bar{P}_j(\mathbf{d}) = \sum_{n=1}^{N} \sum_{r=1}^{R} \frac{\tilde{\mathcal{E}}_n \mathbf{B}^{\text{rt}}_{j,r} \mathbf{A}_{n,r} \mathbf{d}_r}{P^{\max}} = \tilde{\mathbf{e}} \mathbf{A} \left(\mathbf{B}^{\text{rt}}_j\right)_{\text{diag}} \mathbf{d} \tag{5.13}$$

where $(\mathbf{a})_{\text{diag}}$ denotes the diagonal matrix from vector $\mathbf{a}$. Let $\mathbf{A}(I) \subseteq \mathbf{A}$ be the I-by-R matrix representing routes allocation for all servers. Note there is no route r shared by more than one server and the corresponding route graph is cycle-free such that $\mathbf{A}(I)$ has full row rank. Therefore the aggregated traffic vector $\mathbf{d}^{\text{srv}} = [\mathbf{d}^{\text{srv}}_1, \cdots, \mathbf{d}^{\text{srv}}_I]^T$ over all servers can be expressed as

$$\mathbf{d}^{\text{srv}} = \mathbf{A}(I)\mathbf{d} \tag{5.14}$$

Given the mapping matrix $\mathbf{B}^{\text{srv}}$, the load balancing variance for user j can be further expressed as

$$\bar{S}_j(\mathbf{d}) = \frac{1}{\hat{S}^{\text{srv}} \bar{I}} (\mathbf{d}^{\text{srv}})^T (\mathbf{Q}^j)^T \mathbf{Q}^j \mathbf{d}^{\text{srv}} = (\mathbf{d})^T \tilde{\mathbf{Q}}^j \mathbf{d} \tag{5.15}$$

where

$$\mathbf{Q}^j = \left(\mathbf{B}^{\text{srv}}_j\right)_{\text{diag}} \mathbf{Q}^{\text{srv},j} \left(\mathbf{B}^{\text{srv}}_j\right)_{\text{diag}}$$

$$\tilde{\mathbf{Q}}^j = \frac{1}{\hat{S}^{\text{srv}} \bar{I}} \mathbf{A}(I)^T (\mathbf{Q}^j)^T \mathbf{Q}^j \mathbf{A}(I)$$

We define $\left(\mathbf{B}_j^{\text{srv}}\right)_{\text{diag}} = \text{diag}\left(\mathbf{B}_j^{\text{srv}}\right)$. The I-by-I matrix $\mathbf{Q}^{\text{srv},j}$ can be expressed as

$$\mathbf{Q}^{\text{srv},j} = \begin{bmatrix} \frac{1}{\mathbf{C}_1^{\text{srv}}} - \frac{1}{\mathbf{C}_{\text{sys},j}^{\text{srv}}} & \cdots & \frac{-1}{\mathbf{C}_{\text{sys},j}^{\text{srv}}} \\ \vdots & \ddots & \vdots \\ \frac{-1}{\mathbf{C}_{\text{sys},j}^{\text{srv}}} & \cdots & \frac{1}{\mathbf{C}_I^{\text{srv}}} - \frac{1}{\mathbf{C}_{\text{sys},j}^{\text{srv}}} \end{bmatrix} \tag{5.16}$$

Because $\frac{1}{\hat{S}^{\text{srv}}\bar{I}} > 0$ and $\mathbf{A}(I)^T(\mathbf{Q}^j)^T\mathbf{Q}^j\mathbf{A}(I) \succeq 0$, it is clear that the second order derivative

$$\nabla^2\left(\bar{S}_j\left(\mathbf{d}\right)\right) = 2\tilde{\mathbf{Q}}^j \succeq 0. \tag{5.17}$$

Also note $\bar{D}_j\left(\mathbf{d}\right)$ can be decomposed over all MUXs such that

$$\bar{D}_j\left(\mathbf{d}\right) = \sum_{m=1}^{M} \frac{\mathbf{B}_{j,m}^{\text{mux}}}{\hat{S}_m^{\text{mux}}\bar{M}} D_{m,j}\left(\mathbf{d}\right) \tag{5.18}$$

where $D_{m,j}\left(\mathbf{d}\right) = \sum_{h=1}^{R} \frac{\mathbf{B}_{j,h}^{\text{rt}}\mathbf{A}_{m,h}^{\text{mux}}}{\mathbf{C}_m^{\text{mux}} - \mathbf{d}_m^{\text{mux}}}$ denotes the total averaged delay on network resource m for user j regarding traffic allocation vector $\mathbf{d}$ and the route-to-MUX mapping vector $\mathbf{A}_m^{\text{mux}} \subset \mathbf{A}^{\text{mux}}$. Note $\mathbf{d}_m^{\text{mux}} = \sum_{r=1}^{R} \mathbf{A}_{m,r}^{\text{mux}}\mathbf{d}_r$ and $D_{m,j}\left(\mathbf{d}\right)$ is twice differentiable. Then the Hessian of $D_{m,j}\left(\mathbf{d}\right)$ can be expressed as

$$\nabla^2\left(D_{m,j}\left(\mathbf{d}\right)\right) = \begin{bmatrix} \frac{\partial^2 D_{m,j}(\mathbf{d})}{\partial \mathbf{d}_1^2} & \cdots & \frac{\partial^2 D_{m,j}(\mathbf{d})}{\partial \mathbf{d}_1 \partial \mathbf{d}_R} \\ \vdots & \ddots & \vdots \\ \frac{\partial^2 D_{m,j}(\mathbf{d})}{\partial \mathbf{d}_R \partial \mathbf{d}_1} & \cdots & \frac{\partial^2 D_{m,j}(\mathbf{d})}{\partial \mathbf{d}_R^2} \end{bmatrix}$$

where the entity $\nabla^2\left(D_{m,j}\left(\mathbf{d}\right)\right)_{r',r''}$ can be expressed as,

$$\frac{\partial^2 D_{m,j}\left(\mathbf{d}\right)}{\partial \mathbf{d}_{r'}\partial \mathbf{d}_{r''}} = \sum_{h=1}^{R} \frac{2\mathbf{B}_{j,h}^{\text{rt}}\mathbf{A}_{m,h}^{\text{mux}}\mathbf{A}_{m,r'}^{\text{mux}}\mathbf{A}_{m,r''}^{\text{mux}}}{\left(\mathbf{C}_m^{\text{mux}} - \mathbf{d}_m^{\text{mux}}\right)^3} = \begin{cases} \frac{2K_m}{\left(\mathbf{C}_m^{\text{mux}} - \mathbf{d}_m^{\text{mux}}\right)^3} & \text{if } \mathbf{B}_{j,h}^{\text{rt}} = \mathbf{A}_{m,h}^{\text{mux}} = \mathbf{A}_{m,r'}^{\text{mux}} = \mathbf{A}_{m,r''}^{\text{mux}} = 1 \\ 0 & \text{otherwise} \end{cases}$$

with $r', r'' = 1, \cdots, R$. Term K_m is the number of routes aggregated at MUX m where both route r' and r' present. Then it is easy to show that $\nabla^2\left(D_{m,j}\left(\mathbf{d}\right)\right) \succeq 0$, which in turn

leads to

$$\nabla^2 \left(\bar{D}_j \left(\mathbf{d}\right)\right) \succeq 0. \tag{5.19}$$

From (5.13), (5.17) and (5.19), it shows that $\nabla^2 \left(U_j \left(\mathbf{d}\right)\right) \succeq 0$ with non-negative weights $\boldsymbol{\omega}_j^{\text{pow}}$, $\boldsymbol{\omega}_j^{\text{srv}}$ and $\boldsymbol{\omega}_j^{\text{mux}}$. In addition, the constraints in (5.11) and (5.12) are linear. Therefore the optimisation problem in (5.10) with constraints (5.11) and (5.12) is a convex problem. This in turn indicates the first order KKT condition [176] is sufficient and necessary for optimisation. ■

Solving (5.10) requires consideration of the boundary conditions with respect to (5.11) and (5.12). To simplify dealing with this we relax the constraints in (5.11) and (5.12) by introducing penalty functions. First we define a continuous and twice differentiable penalty function for the equality constraint in (5.11) of user j as

$$\mathbf{f}_j^{\text{ert}} \left(\mathbf{d}\right) = \lambda \left(\mathbf{d}_j^{\text{in}} - \mathbf{B}_j^{\text{rt}} \mathbf{d}\right)^2 \tag{5.20}$$

where $\lambda > 0$ is the weight for the penalty function. Second we define a continuous and twice differentiable penalty function for the inequality constraint in (5.12) for network element n as

$$\mathbf{f}_n^{\text{res}} \left(\mathbf{d}\right) = \begin{cases} 0 & \text{if } \mathbf{A}_n \mathbf{d} - \mathbf{C}_n \leq 0 \\ \gamma(\mathbf{A}_n \mathbf{d} - \mathbf{C}_n)^2 & \text{if } \mathbf{A}_n \mathbf{d} - \mathbf{C}_n > 0 \end{cases} \tag{5.21}$$

where $\gamma > 0$ is the weight for the penalty function. Define vector $\mathbf{f}^{\text{res}} \left(\mathbf{d}\right) = [\mathbf{f}_1^{\text{res}} \left(\mathbf{d}\right) = , \cdots , \mathbf{f}_N^{\text{res}} \left(\mathbf{d}\right)]^T$. Then we can formulate the relaxed problem as finding $\mathbf{d}$ to minimise

$$\mathcal{U}_j(\mathbf{d}) = U_j \left(\mathbf{d}\right) + \mathbf{f}_j^{\text{ert}} \left(\mathbf{d}\right) + \mathbf{B}_j^{\text{res}} \mathbf{f}^{\text{res}} \left(\mathbf{d}\right) \tag{5.22}$$

where $\mathbf{B}_j^{\text{res}} \mathbf{f}^{\text{res}} \left(\mathbf{d}\right) = \sum_{n=1}^{N} \mathbf{B}_{j,n}^{\text{res}} \mathbf{f}_n^{\text{res}} \left(\mathbf{d}\right)$.

Proposition 5.1. *The proposed game* Γ *in Definition 5.1 with the relaxed cost function in* (5.22) *admits a Nash Equilibrium.*

Proof: The strategy space for game Γ is convex, compact and has nonempty interior. Lemma 5.2 holds such that the cost function for each edge router j is continuous, twice differentiable and convex with $\nabla^2 \left(U_j \left(\mathbf{d}\right)\right) \succeq 0$ Similarly, it is easy to show that

$\nabla^2\left(\mathbf{f}_j^{\text{ert}}(\mathbf{d})\right) \succeq 0$ and $\nabla^2\left(\sum_{n=1}^{N}\mathbf{B}_{j,n}^{\text{res}}\mathbf{f}_n^{\text{res}}(\mathbf{d})\right) \succeq 0$. Then the proof of the existence of Nash Equilibrium immediately follows the theorem of the existence of NE in [44]. ■

Theorem 5.2. *Introduce a small arbitrary variable $\tau > 0$ in the normalised load balancing variance* (5.3) *for each user such that*

$$\bar{S}_j(\mathbf{d}) = \sum_{i=1}^{I}\frac{\mathbf{B}_{j,i}^{srv}}{\hat{S}^{srv}\bar{I}}\left(\left(\frac{1}{\mathbf{C}_i^{srv}}+\tau\right)\mathbf{d}_i^{srv} - \frac{T_j}{\mathbf{C}_{sys,j}^{srv}}\right)^2. \tag{5.23}$$

Then there exists a unique pure strategy Nash Equilibrium in the proposed strategic game Γ with the relaxed cost function in (5.22).

Proof: Let $\mathbf{U} = [U_1(\mathbf{d}), \cdots, U_J(\mathbf{d})]^T$ as a vector of cost function for all users. Note there is no loop in the network topology and each route only maps to a single user. However, each user can have multiple routes as determined by the $J \times R$ mapping matrix $\mathbf{B}^{\text{rt}}$. Define the pseudo-gradient operator $\overline{\nabla}$ with respect to $\mathbf{d}$ on the cost vector $\mathbf{U}$ as

$$\overline{\nabla}\mathbf{U} := \left[\frac{\partial U_1^{\Gamma}(\mathbf{d})}{\partial \mathbf{d}_1}, \cdots, \frac{\partial U_R^{\Gamma}(\mathbf{d})}{\partial \mathbf{d}_R}\right]^T := g(\mathbf{d}).$$

such that $U_r^{\Gamma}(\mathbf{d}) = U_j(\mathbf{d})$ if $\mathbf{B}_{j,r}^{\text{rt}} = 1$ with $r = 1, \cdots, R$ and $j = 1, \cdots, J$. Note any entity $\frac{\partial U_j(\mathbf{d})}{\partial \mathbf{d}_r}$ with $\mathbf{B}_{j,r}^{\text{rt}} = 0$ is excluded from $\overline{\nabla}\mathbf{U}$ because the route is not valid for the corresponding user. This in turn indicates that the length of the pseudo-gradient is R. Let $G(\mathbf{d})$ be the Jacobian of $g(\mathbf{d})$ with respect to $\mathbf{d}$:

$$G(\mathbf{d}) = \begin{bmatrix} \frac{\partial^2 U_1^{\Gamma}(\mathbf{d})}{\partial \mathbf{d}_1^2} & \cdots & \frac{\partial^2 U_1^{\Gamma}(\mathbf{d})}{\partial \mathbf{d}_1 \partial \mathbf{d}_R} \\ \vdots & \ddots & \vdots \\ \frac{\partial^2 U_1^{\Gamma}(\mathbf{d})}{\partial \mathbf{d}_R \partial \mathbf{d}_1} & \cdots & \frac{\partial^2 U_R^{\Gamma}(\mathbf{d})}{\partial \mathbf{d}_R^2} \end{bmatrix}$$

From (5.7), it is not difficult to show that

$$G(\mathbf{d}) = \sum_{j=1}^{J}\left(\nabla^2\left(\boldsymbol{\omega}_j^{\text{srv}}\bar{S}_j(\mathbf{d})\right) + \nabla^2\left(\boldsymbol{\omega}_j^{\text{mux}}\bar{D}_j(\mathbf{d})\right)\right).$$

If any two servers have the same capacity, it indicates $\mathbf{Q}^{\text{srv},j}$ is singular. By introducing

the small dummy value τ, matrix $\mathbf{Q}^{\text{srv},j}$ in (5.16) can be modified as

$$\mathbf{Q}^{\text{srv},j} = \begin{bmatrix} \frac{1}{\mathbf{C}_1^{\text{srv}}} - \frac{1}{\mathbf{C}_{\text{sys},j}^{\text{srv}}} + \tau & \frac{-1}{\mathbf{C}_{\text{sys},j}^{\text{srv}}} & \cdots & \frac{-1}{\mathbf{C}_{\text{sys},j}^{\text{srv}}} \\ \frac{-1}{\mathbf{C}_{\text{sys},j}^{\text{srv}}} & \frac{1}{\mathbf{C}_2^{\text{srv}}} - \frac{1}{\mathbf{C}_{\text{sys},j}^{\text{srv}}} + \tau & \cdots & \vdots \\ \vdots & \vdots & \ddots & \frac{-1}{\mathbf{C}_{\text{sys},j}^{\text{srv}}} \\ \frac{-1}{\mathbf{C}_{\text{sys},j}^{\text{srv}}} & \cdots & \frac{-1}{\mathbf{C}_{\text{sys},j}^{\text{srv}}} & \frac{1}{\mathbf{C}_I^{\text{srv}}} - \frac{1}{\mathbf{C}_{\text{sys},j}^{\text{srv}}} + \tau \end{bmatrix}$$

Therefore symmetric matrix $\mathbf{Q}^{\text{srv},j}$ in non-singular and $(\mathbf{Q}^{\text{srv},j})^T \mathbf{Q}^{\text{srv},j} \succ 0$. Note

$$\sum_{j=1}^{J} \omega_j^{\text{srv}} \bar{S}_j(\mathbf{d}) = \mathbf{d}^T \left(\sum_{j=1}^{J} \omega_j^{\text{srv}} \tilde{\mathbf{Q}}^j \right) \mathbf{d}$$

where

$$\sum_{j=1}^{J} \omega_j^{\text{srv}} \tilde{\mathbf{Q}}^j = \frac{1}{\hat{S}I} \mathbf{A}(I)^T \left(\sum_{j=1}^{J} \omega_j^{\text{srv}} \left(\mathbf{Q}^j \right)^T \mathbf{Q}^j \right) \mathbf{A}(I)$$

with term $\mathbf{Q}^j = \left(\mathbf{B}_j^{\text{srv}} \right)_{\text{diag}} \mathbf{Q}^{\text{srv},j} \left(\mathbf{B}_j^{\text{srv}} \right)_{\text{diag}}$. Because each server node has at least a valid route, we show $\sum_{j=1}^{J} \omega_j^{\text{srv}} \left(\mathbf{B}_j^{\text{srv}} \right)_{\text{diag}}$ is a diagonal matrix with full rank. With simple proof, this indicates $\sum_{j=1}^{J} \nabla^2 \left(\bar{S}_j(\mathbf{d}) \right) \succ 0$. Note from (5.18) and (5.22), we can show $\sum_{j=1}^{J} \nabla^2 \left(\bar{D}_j(\mathbf{d}) \right) \succeq 0$, $\sum_{j=1}^{J} \nabla^2 \left(\mathbf{f}_j^{\text{ert}}(\mathbf{d}) \right) \succeq 0$, and $\sum_{j=1}^{J} \nabla^2 \left(\sum_{n=1}^{N} \mathbf{B}_{j,n}^{\text{res}} \mathbf{f}_n^{\text{res}}(\mathbf{d}) \right) \succeq 0$. Therefore, $G(\mathbf{d})$ is positive definite such that $G(\mathbf{d}) \succ 0$. In addition it is easy to show $G(\mathbf{d})$ is symmetric. By applying Theorem 2.1 in [187], we show there is a unique pure strategy Nash Equilibrium in the proposed game. ■

Remark: In (5.3), we introduce a dummy variable $\tau > 0$ such that $\tau \mathbf{d}_i^{\text{srv}}$ is a perturbation for the load balancing variance. We choose a small value for τ such that the aggregated load $\mathbf{d}_i^{\text{srv}}$ minimising (5.3) is close to the optimal load for ideal load balancing condition. Although the dummy variable τ has a negligible impact on minimising the load balance variance, it can provide uniqueness property for the Nash Equilibrium of the system by introducing non-singularity in $\mathbf{Q}^{\text{srv},j}$ such that $\nabla^2 \left(U_j(\mathbf{d}) \right) \succ 0$.

5.5.2 Dynamic Gradient Play Method

By applying a closed-loop "pricing" feedback mechanism, a discrete-time dynamic gradient play method [177, 188] can be used to derived the Nash Equilibrium $\mathbf{d}^*$ with guaranteed convergence. The subproblem for edge router j can be solved by adjusting $\mathbf{d}_r$ with $\mathbf{B}^{\text{rt}}_{j,r} = 1$ to the opposite direction of the gradient such that

$$\mathbf{d}_r(z) = \left[\mathbf{d}_r(z-1) - \alpha_d \frac{\partial \mathcal{U}_j(\mathbf{d})}{\partial \mathbf{d}_r}\right]^+ \tag{5.24}$$

where operation $[x]^+ = \max(0, x)$ and α_d denotes the gradient step size with unit of $(\text{time})^{-2}$ and the gradient is given by

$$\begin{aligned}\frac{\partial \mathcal{U}_j(\mathbf{d})}{\partial \mathbf{d}_r} &= \omega_j^{\text{pow}} \sum_{n=1}^{N} \left(\frac{\tilde{\mathcal{E}}_n \mathbf{B}^{\text{rt}}_{j,r} \mathbf{A}_{n,r}}{P^{\max}}\right) + \sum_{i=1}^{I} \frac{2\omega_j^{\text{srv}} \mathbf{B}^{\text{rt}}_{j,r} \mathbf{B}^{\text{srv}}_{j,i} \mathbf{A}^{\text{srv}}_{i,r}}{\hat{S}^{\text{srv}} \bar{I}} \left(\frac{1}{\mathbf{C}^{\text{srv}}_i} - \frac{1}{\mathbf{C}^{\text{srv}}_{\text{sys},j}}\right)\left(\frac{\mathbf{d}^{\text{srv}}_i}{\mathbf{C}^{\text{srv}}_i} - \frac{T_j}{\mathbf{C}^{\text{srv}}_{\text{sys},j}}\right) \\ &+ \sum_{m=1}^{M} \frac{\omega_j^{\text{mux}} \mathbf{B}^{\text{mux}}_{j,m}}{\hat{S}^{\text{mux}}_m \bar{M}} \sum_{h=1}^{R} \frac{\mathbf{B}^{\text{rt}}_{j,h} \mathbf{A}^{\text{mux}}_{m,h} \mathbf{A}^{\text{mux}}_{m,r}}{(\mathbf{C}^{\text{mux}}_m - \mathbf{d}^{\text{mux}}_m)^2} + \frac{\partial \mathbf{f}^{\text{ert}}_j(\mathbf{d})}{\partial \mathbf{d}_r} + \frac{\partial\left(\mathbf{B}^{\text{res}}_j \mathbf{f}^{\text{res}}(\mathbf{d})\right)}{\partial \mathbf{d}_r}\end{aligned} \tag{5.25}$$

Theorem 5.3. *The Nash Equilibrium $\mathbf{d}^*$ of the proposed game matches the solution of the dynamic gradient method with respect to* (5.24).

Proof: Note $\frac{\partial \mathbf{f}^{\text{ert}}_j(\mathbf{d})}{\partial \mathbf{d}_r} = -\frac{\mathbf{B}^{\text{rt}}_{j,r}\lambda}{\mathbf{d}^{\text{in}}_j}\left(\mathbf{d}^{\text{in}}_j - \mathbf{B}^{\text{rt}}_j \mathbf{d}\right)$. In addition the Nash Equilibrium $\mathbf{d}^*$ needs to meet the equality constraint such that $\mathbf{d}^{\text{in}}_j - \mathbf{B}^{\text{rt}}_j \mathbf{d}^* = 0$ for $j = 1, \cdots, J$. Therefore, we can show $\frac{\partial \mathbf{f}^{\text{ert}}_j(\mathbf{d}^*)}{\partial \mathbf{d}^*_r} = 0$. Also the capacity constraint in (5.12) indicates $\mathbf{A}_n \mathbf{d}^* - \mathbf{C}_n \leq 0$. Note $\frac{\partial \mathbf{f}^{\text{res}}_n(\mathbf{d})}{\partial \mathbf{d}_r} = 0$ if $\mathbf{A}_n \mathbf{d} - \mathbf{C}_n \leq 0$ as shown in (5.21). This in turn indicates $\frac{\partial\left(\mathbf{B}^{\text{res}}_j \mathbf{f}^{\text{res}}(\mathbf{d}^*)\right)}{\partial \mathbf{d}^*_r} = 0$. Then the gradient in (5.25) leads to

$$\frac{\partial \mathcal{U}_j(\mathbf{d}^*)}{\partial \mathbf{d}^*_r} = \frac{\partial U_j(\mathbf{d}^*)}{\partial \mathbf{d}^*_r}$$

From the game definition in (5.6), the first order condition directly leads to $\frac{\partial U_j(\mathbf{d}^*)}{\partial \mathbf{d}^*_r} = 0$. Therefore, the iterative gradient method converges such that $\mathbf{d}_r(z) = \mathbf{d}_r(z-1)$ if $\mathbf{d}_r(z-1) = \mathbf{d}^*$. ■

5.5.3 Stability Analysis

The gradient method shown in (5.24) is a discrete-time solution of the problem. We impose a time-scale separation between dynamics in (5.24) and adopt the widely used method [178], which treats discrete-time gradient updates as continuous stochastic approximation iterations, we apply the continuous-time Lyapunov stability analysis [179] to the algorithm such that the continuous-time gradient can be approximated by

$$\dot{\mathbf{d}}_r = -\alpha_d \frac{\partial \mathcal{U}_j(\mathbf{d})}{\partial \mathbf{d}_r}, \tag{5.26}$$

where $\alpha_d > 0$ denotes the gradient step size with unit of $(\text{time})^{-2}$. Note the positive projection in (5.24) is applied to assure non-negative traffic on each route. For analytical purpose, we ignore this positive projection in (5.26). The simulation results in Fig. 5.3 show the convergence of the gradient method.

Theorem 5.4. *For all users $j = 1, \cdots, J$, assume the same weight $\boldsymbol{\omega}_j^{srv} = \omega^{srv}$ for servers load balancing, the same weight $\boldsymbol{\omega}_j^{mux} = \omega^{mux}$ for MUXs average time delay and each user is allocated the same set of I servers. Then the gradient play dynamics with the continuous gradient* (5.26) *asymptotically converges to a unique solution, which is the Nash Equilibrium of the game defined in Definition 5.1 with the relaxed cost function in* (5.22).

Proof: Note if all users share the same I servers, the load balancing variance show in (5.3) can be expressed as,

$$\bar{S}_j(\mathbf{d}) = \frac{1}{\hat{S}^{\text{srv}} \bar{I}} \sum_{i=1}^{I} \mathbf{B}_{j,i}^{\text{srv}} \left(\frac{\mathbf{d}_i^{\text{srv}}}{\mathbf{C}_i^{\text{srv}}} - \eta^{\text{srv}} \right)^2 \tag{5.27}$$

where $\eta^{\text{srv}} = \frac{\sum_{j=1}^{J} \mathbf{d}_j^{\text{in}}}{\sum_{i=1}^{I} \mathbf{C}_i^{\text{srv}}}$ is a constant. We consider the following Lyapunov function over all edge routers,

$$\begin{aligned} V(\mathbf{d}) = & \sum_{j=1}^{J} \left(\boldsymbol{\omega}_j^{\text{pow}} \sum_{n=1}^{N} \sum_{r=1}^{R} \frac{\tilde{\mathcal{E}}_n \mathbf{B}_{j,r}^{\text{rt}} \mathbf{A}_{n,r} \mathbf{d}_r}{P^{\max}} \right) + \frac{\omega^{\text{srv}}}{\hat{S}^{\text{srv}} \bar{I}} \sum_{i=1}^{I} \left(\frac{\mathbf{d}_i^{\text{srv}}}{\mathbf{C}_i^{\text{srv}}} - \eta^{\text{srv}} \right)^2 \\ & + \sum_{m=1}^{M} \frac{\omega^{\text{mux}}}{\hat{S}_m^{\text{mux}} \bar{M}} \sum_{r=1}^{R} \frac{\mathbf{A}_{m,r}^{\text{mux}}}{\mathbf{C}_m^{\text{mux}} - \mathbf{d}_m^{\text{mux}}} + \sum_{j=1}^{J} \mathbf{f}_j^{\text{ert}}(\mathbf{d}) + \sum_{n=1}^{N} \mathbf{f}_n^{\text{res}}(\mathbf{d}) + \Delta \end{aligned} \tag{5.28}$$

where $\mathbf{d}_i^{\text{srv}} = \mathbf{A}_i^{\text{srv}}\mathbf{d}$, $\mathbf{d}_m^{\text{mux}} = \mathbf{A}_m^{\text{mux}}\mathbf{d}$ and Δ is a constant such that $V(\mathbf{d}^*) = 0$with $\mathbf{d}^*$ denotes the equilibrium point. It is easy to show that $V(\mathbf{d}) \geq \mathbf{0}$ since the Lyapunov function $V(\mathbf{d})$ is convex. At each iteration, the derivative of $V(\mathbf{d})$ along the trajectories of $\mathbf{d}$ over time, denoted as $\dot{V}(\mathbf{d})$, is expressed as

$$\dot{V}(\mathbf{d}) = \sum_{r=1}^{R} \frac{\partial V(\mathbf{d}_r)}{\partial \mathbf{d}_r} \dot{\mathbf{d}}_r \tag{5.29}$$

Note each route $r_{j\to i}$ from edge router j (source) to server i (destination) is unique and loop-less. This in turn means that if $r_{j'\to i'} = r_{j''\to i''}$, then $j' = j''$ and $i' = i''$. From (5.28) and (5.7), if $\mathbf{B}_{j,r}^{\text{rt}} = 1$, it can be seen that

$$\frac{\partial V(\mathbf{d}_r)}{\partial \mathbf{d}_r} = \frac{\partial \mathcal{U}_j(\mathbf{d})}{\partial \mathbf{d}_r}$$

where $\frac{\partial \mathcal{U}_j(\mathbf{d})}{\partial \mathbf{d}_r}$ is the gradient with $\boldsymbol{\omega}_j^{\text{srv}} = \omega^{\text{srv}}$, $\boldsymbol{\omega}_j^{\text{mux}} = \omega^{\text{mux}}$ and load balancing variance in (5.27) having a constant η^{srv}. Note for $\mathbf{B}_{j,r}^{\text{rt}} = 1$, $\dot{\mathbf{d}}_r = -\alpha_d \frac{\partial \mathcal{U}_j(\mathbf{d})}{\partial \mathbf{d}_r}$. Since $\mathcal{U}_j(\mathbf{d})$ is convex, (5.29) can be further expressed as

$$\dot{V}(\mathbf{d}_r) = -\alpha_d \left(\frac{\partial \mathcal{U}_j(\mathbf{d})}{\partial \mathbf{d}_r} \right)^2 < 0, \ \forall \mathbf{d}_r \neq \mathbf{d}_r^* \tag{5.30}$$

This in turn leads to $\dot{V}(\mathbf{d}) < 0, \forall \mathbf{d} \neq \mathbf{d}^*$ and $\dot{V}(\mathbf{d}^*) = 0$. Therefore the unique equilibrium point $\mathbf{d}^*$ that minimise the weighted sum multi-objective function is stable. ■

Although Theorem 5.4 only proves the convergence of cases with $\boldsymbol{\omega}_j^{\text{srv}} = \omega^{\text{srv}}$ and $\boldsymbol{\omega}_j^{\text{mux}} = \omega^{\text{mux}}$, the simulation results shown in Fig. 5.3 indicate the proposed gradient method converges with more general weight configurations.

5.6 Efficiency Loss

5.6.1 Benchmark System Solution

Define the global system cost function as the sum over all edge node object functions in (5.7) such that

$$U_{\text{sys}}(\mathbf{d}) = \sum_{j=1}^{J} U_j(\mathbf{d}) = P_{\text{sys}}(\mathbf{d}) + S(\mathbf{d}) + D(\mathbf{d}) \tag{5.31}$$

where $P_{\text{sys}}(\mathbf{d})$ denotes the normalised system power consumption, $S(\mathbf{d})$ denotes the normalised system load balancing variance with perturbation τ in (5.23) and $D(\mathbf{d})$ denotes the normalised total average delay of the system. Minimising the system cost function $U_{\text{sys}}(\mathbf{d})$ leads to the solution of the joint optimisation problem

$$\min_{\mathbf{d}} U_{\text{sys}}(\mathbf{d}) \tag{5.32}$$

$$\text{subject to } \mathbf{B}_j^{\text{rt}}\mathbf{d} = \mathbf{d}_j^{\text{in}} \tag{5.33}$$

$$0 \leq \mathbf{A}\mathbf{d} \leq \mathbf{C} \tag{5.34}$$

Lemma 5.3. *The joint optimisation problem* (5.32) *with the associated constraints is a convex optimisation problem.*

Proof: From Lemma 5.2, it indicates that $\nabla^2\left(U_j(\mathbf{d})\right) \succeq 0$. Then it is clear $\nabla^2\left(U_{\text{sys}}(\mathbf{d})\right) \succeq 0$. In addition, all constrains in (5.32) are linear. This in turn indicates the optimisation problem (5.32) is a convex problem such that the first order KKT condition [176] is sufficient and necessary for optimisation. ■

We apply the penalty functions in (5.20) and (5.21) to relax the constraints in (5.32). Then the solution of the global optimisation problem can be expressed as

$$\min_{\mathbf{d}} \mathcal{U}_{\text{sys}}(\mathbf{d}) \tag{5.35}$$

where

$$\mathcal{U}_{\text{sys}}(\mathbf{d}) = U_{\text{sys}}(\mathbf{d}) + \sum_{j=1}^{J} \mathbf{f}_j^{\text{ert}}(\mathbf{d}) + \sum_{j=1}^{J} \mathbf{B}_j^{\text{res}}\mathbf{f}^{\text{res}}(\mathbf{d}).$$

5.6.2 Nash Equilibrium Vs. Global Optimal

The strategic game defined in in Definition 5.1 is in fact a non-cooperative game. The Nash equilibrium of a non-cooperative game is usually inefficient relative to the global optimum [61]. One metric to capture the inefficiency in selfish network traffic routing

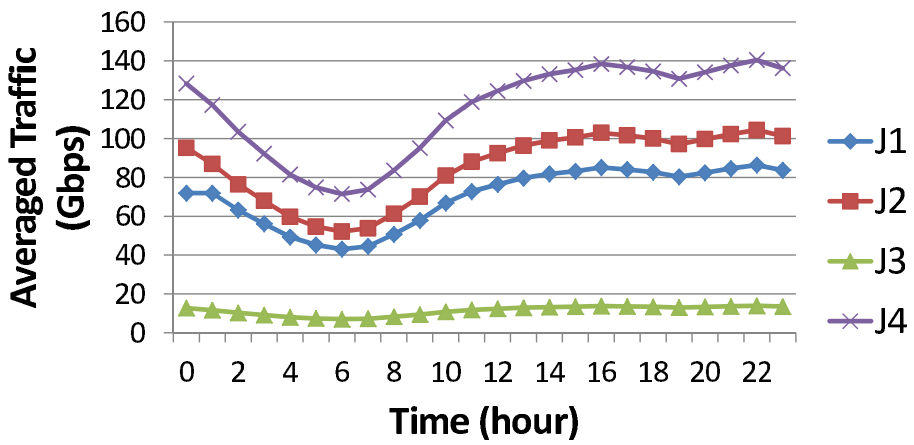

Figure 5.2: Input Traffic over 24 hours

games is the ratio between the value of the global object function using the Nash Equilibrium solution $\mathbf{d}^*$ and the value of the optimal solution of the global problem. This ratio is closely related to the well-known Price of Anarchy concept [61], which quantifies the suboptimality of non-cooperative game outcomes. In this chapter, the game has a unique Nash Equilibrium as shown in Proposition 5.2. Therefore we define the Game/Global ratio as,

$$\pi = \frac{\mathcal{U}_{\text{sys}}(\mathbf{d}^*)}{\mathcal{U}_{\text{sys}}(\mathbf{d}^g)} \tag{5.36}$$

where $\vec{\mathbf{x}}$ denotes the set of all possible strategies. $\mathbf{d}^*$ and $\mathbf{d}^g$ denote the strategies in Nash Equilibrium and global optimal separately. The numerical results in Section 5.7 show that the multi-objective cost function in (5.7) for individual users has a great impact on the performance efficiency loss between the game and the global solution.

5.7 Simulations

5.7.1 Simulation Setup

We use Matlab to calculate the strategic game solution in Section 5.5.2 and the benchmark system solution in Section 5.6.1. A part of USA backbone IP network (USNET) [21] is used as shown in Fig. 5.1 where nodes $M1 \sim M14$ are treated as MUXs connected by

Table 5.2: Parameters of network *resources*

resources n	Capacity C_n(Gbps)[1]	Max power $P_n^{\max}$ (Watts)[1]	Power ratio β_n	Utilisation ratio ρ_n^{res}
$S1$	347	6.54×10^6	0.8 or 0.3	0.3
$S2$	354	8.61×10^6	0.8 or 0.3	0.3
$S3$	786	1.99×10^7	0.8 or 0.3	0.3
$S4$	300	3.00×10^7	0.8 or 0.3	0.3
$M1$	180	1.43×10^4	0.8	0.3
$M2$	140	1.14×10^4	0.8	0.3
$M3$	140	1.14×10^4	0.8	0.3
$M4$	180	1.28×10^4	0.8	0.3
$M5$	220	1.71×10^4	0.8	0.3
$M6$	140	1.14×10^4	0.8	0.3
$M7$	140	1.14×10^4	0.8	0.3
$M8$	180	1.28×10^4	0.8	0.3
$M9$	160	1.14×10^4	0.8	0.3
$M10$	140	1.14×10^4	0.8	0.3
$M11$	400	1.63×10^4	0.8	0.3
$M12$	140	1.14×10^4	0.8	0.3
$M13$	280	1.99×10^4	0.8	0.3
$M14$	160	1.14×10^4	0.8	0.3
$L1 \sim L24$	200	344	1.0	0.9

[1] Parameters for data centres are based on data centre sizes and assumptions of power consumption per square meters. MUX and link parameters are derived from typical equipment values [180]

Table 5.3: Data Centre allocation

Users	$E1$	$E2$	$E3$	$E4$
Data centres	$S1, S2, S3, S4$	$S1, S2, S4$	$S1, S2, S3, S4$	$S2, S3, S4$

links $L1$ to $L24$. We consider 4 data centres, $S1$ to $S4$, which are attached to the nearest MUXs such that the power consumption and the delay between the those MUXs and data centres can be ignored. The parameters for data centres, MUXs and Links are summarized in Table 5.2. In Fig. 5.1, 4 edge routers $E1$ to $E4$ are introduced as users to distribute their traffic to the allocated data centres via pre-defined routes. The detailed route configuration is described in Table 8.1 of Appendix. Table 5.3 shows the allocated data centres for each user. The diurnal cycle of the input traffic for $E1 \sim E4$ is shown in Fig. 5.2. We also define test cases "Power", "Load Balance" and "Delay" with weights configured in Table 5.4. Fig. 5.3 illustrates the convergence of the traffic $\mathbf{d}$ over designated routes. The

Table 5.4: Weights configuration for $j = 1, 2, 3, 4$

Test cases	ω_j^{pow}	ω_j^{srv}	ω_j^{mux}
"Power"	0.8	0.1	0.1
"Load Balance"	0.1	0.8	0.1
"Delay"	0.1	0.1	0.8

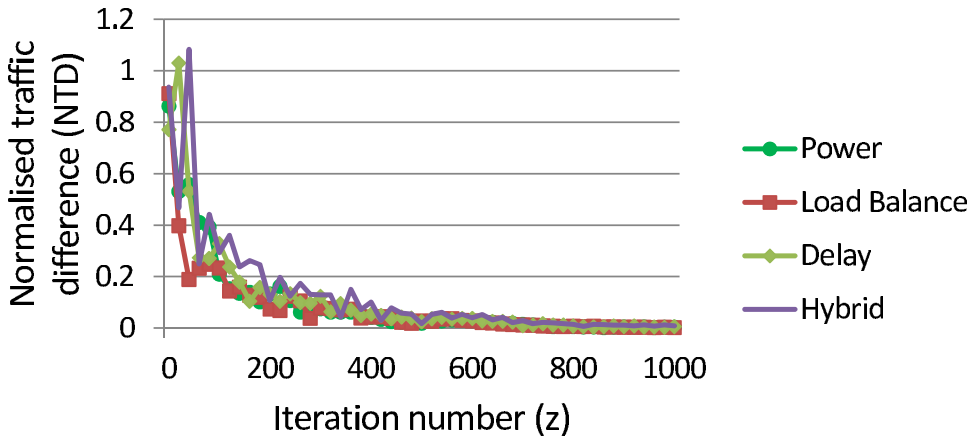

Figure 5.3: System convergence with different weights

vertical axis indicates the normalised routing traffic difference at iteration z expressed as

$$NTD(z) = \frac{\sum_{r=1}^{R} |\mathbf{d}_r(z) - \mathbf{d}_r(z - z_T)|}{\sum_{r=r}^{R} \mathbf{d}_r(z)} \tag{5.37}$$

where z_T denotes a fixed number of iterations. The weights for test cases "Power", "Load Balance" and "Delay" are defined in Table. 5.4. For the "Hybrid" case, the weights are randomly generated. As shown in Fig. 5.3, all test cases converge to stable status. In the simulation setup, we choose fixed step size $\alpha_d = 0.01$.

5.7.2 Simulation Results

Fig. 5.4 and Fig. 5.5 show the system performance with equal weights and different idle/max power ratios ($\beta = 0.8, 0.3$ for $S1 \sim S4$) for Game/Global ratio defined in (5.36) and power consumption for all users such that $\omega_j^{\text{pow}} = \omega_j^{\text{srv}} = \omega_j^{\text{mux}} = \frac{1}{3}, j \in \{1, 2, 3, 4\}$. Fig. 5.4 shows the numerical results for the Game/Global in (5.36), which indicates the overall performance gap between the game solution and the global solution with differ-

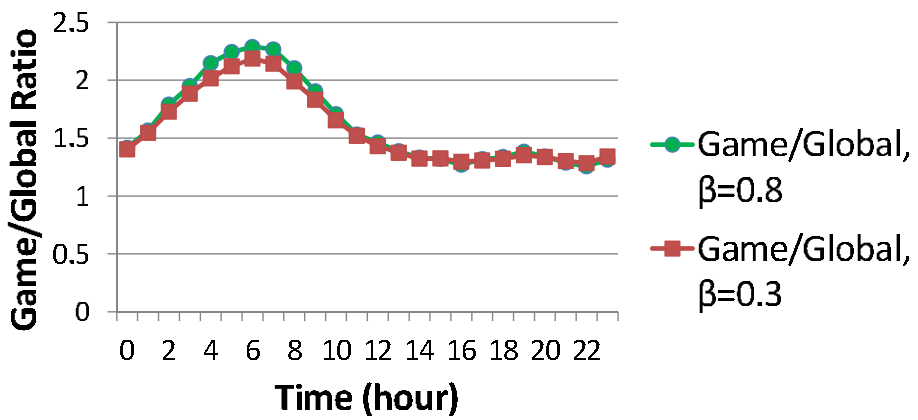

Figure 5.4: Game/Global ratio defined in (5.36) over 24-hour diurnal cycle with equal weights and $\beta = 0.8, 0.3$

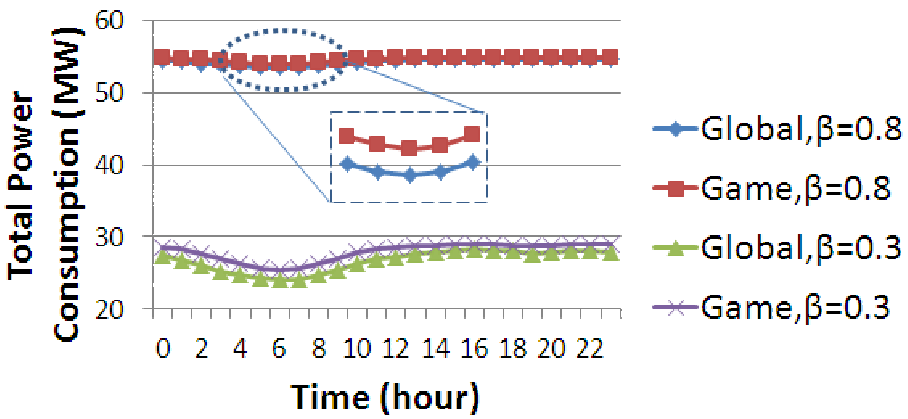

Figure 5.5: Total system power consumption over 24-hour diurnal cycle with equal weights and $\beta = 0.8, 0.3$

ent data centre idle power configurations. We can see $\pi > 1$ during the 24-hour diurnal cycle with maximal value at 6am, which is the time with the lowest total traffic in a day. The total power consumption for the game and global solutions is shown in Fig. 5.5. The global solution outperforms the game solution for the load balance variance in (5.3), but slightly underperforms the game solution for the transport network performance metrics in (5.5). Simulation results are omitted due to page constraint.

Fig. 5.6 illustrates the effects of different weights on the Game/Global ratio with the same traffic diurnal cycle shown in Fig. 5.2. The simulation results indicate that test cases "Load Balance" with a dominant weight on load balance and "Delay" with a dominant

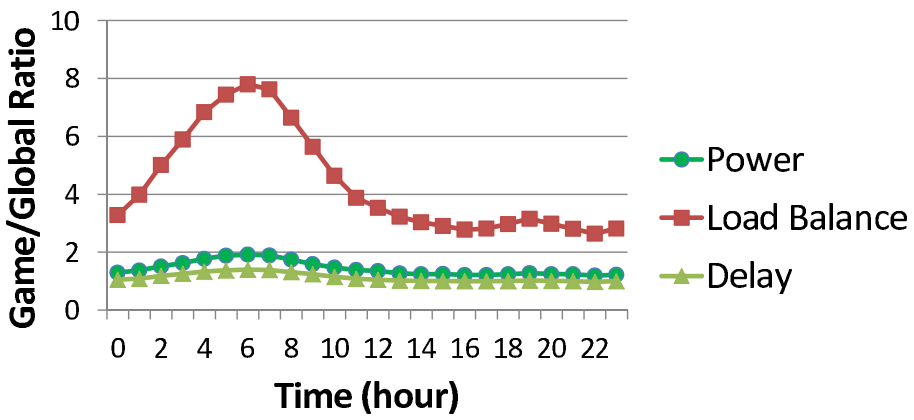

Figure 5.6: Impact of weights for power consumption, load balance and delay on system Game/Global ratio π in (5.36) with $\beta = 0.8$ for DCs

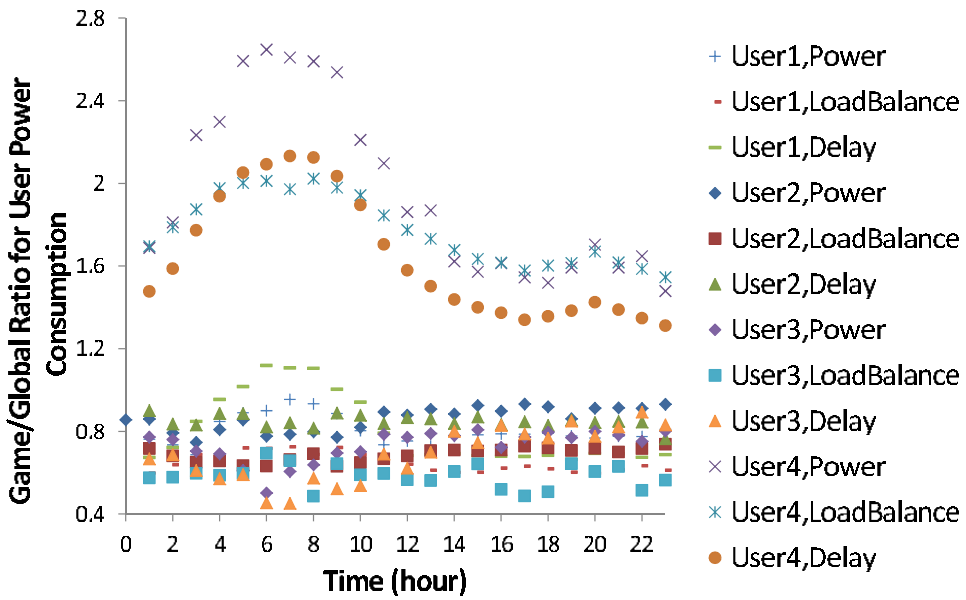

Figure 5.7: Impact of weights for power consumption, load balance and delay on Game/Global ratio for user power consumption in (5.8) with $\beta = 0.8$ for DCs

weight on transport network performance have the highest Game/Global and the lowest Game/Global respectively. Fig. 5.7 shows the Game/Global ratio $\frac{\bar{P}(j,\mathbf{d}^*)}{\bar{P}(j,\mathbf{d}^g)}$ for user normalised power consumption. The simulation results indicate that the normalised power consumption Game/Global ratios are not consistent for different users. For user4, the normalised power consumption Game/Global ratio is larger than 1 for all weights configurations. However, with the same weights configuration, the corresponding ratio is

less than 1 for user2. Fig. 5.7 shows the Game/Global power consumption ratio for each user with different weight configurations. Note the ratios for User4 are higher than 1.0 under different weights configurations, and larger than the ratios for other users. This is because the global solution can coordinate all users' actions to achieve optimal power consumption. For the game solution, the selfish action taken by each user usually results in suboptimal solution from a system view point. Compared to other users, User4 is close to the energy inefficient data centre $S4$ but far from other relatively energy efficient data centres. The "selfish" behavior let other users route traffic energy-efficiently without considering the global optimum. For User4 the cost such as the averaged delay in (5.9) is relatively high to route traffic to energy efficient data centres. Considering the individual load balance objective (5.3) and relatively high load utilisation of energy-efficient data-centres due to "selfish" traffic routed from other users, User4 needs to route more traffic to the energy inefficient data centre $S4$ in the game solution than in the global solution. This leads to system power efficiency loss and significant worse off for User4.

Fig. 5.8 illustrates the total system power consumption for both Global and Game solutions under the "Power" configuration in Table 5.4 with more emphasis on system power saving. The simulation results show a large power consumption gap between the Global solution and the Game solution. In this case, the energy inefficient data centre $S4$ is turned off for the Global solution such that the idle power of $S4$ is saved. In contrast, data centre $S4$ is energised for the Game solution, which results in higher system power consumption than the Global solution. By simply doubling the capacity of network elements on paths M13-L20-M10-L16-M8 and M13-L23-M12-L22, the system power consumption for the game solution ("Game,Power,Cap+" in Fig. 5.8) is greatly reduced to match the global solution. This is because User4 has less delay cost to route traffic to other energy efficient data centres such that energy inefficient $S4$ can be turned off to save energy.

Fig. 5.9 illustrates the effects on the normalised load of data centres due to link capacity changes with "sub" denoting the data centre allocation in Table 5.3. In this test case, the link capacity of $L2$ (link between $M2$ and $M3$) and $L11$ (link between $M6$ and $M7$) is reduced from 100G to 10G. This effectively reduces the total traffic user $J1$ can distribute to data centre $S1$. The game solution in Fig. 5.9 shows that the normalised load

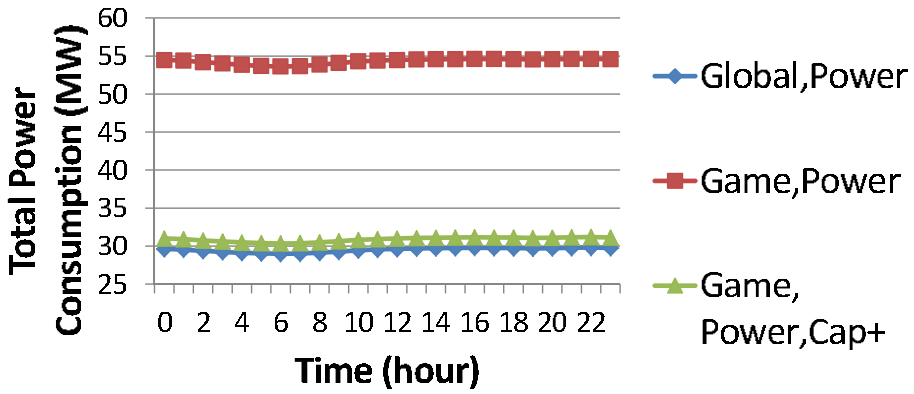

Figure 5.8: Power consumption with "Power" weights and high DC idle power $\beta = 0.8$

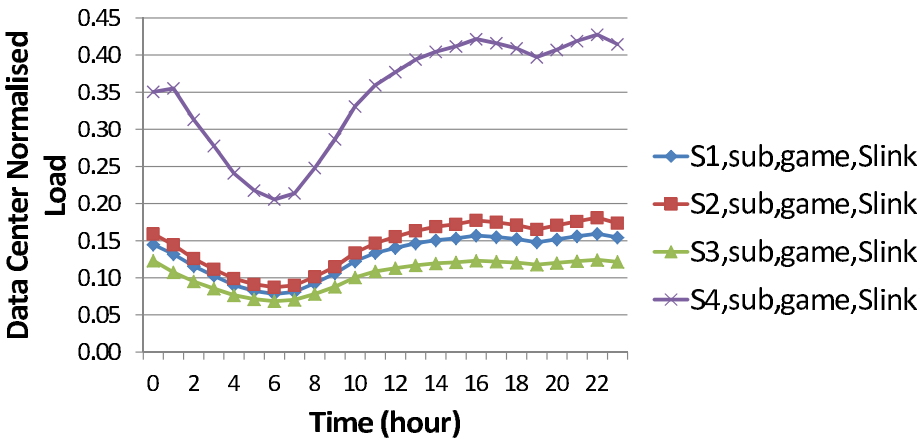

Figure 5.9: Impact of link capacity on the normalised load of data centres

for data centre $S4$ is higher than other data centres even $S4$ is the least energy efficient one as specified in Table 5.2. Fig. 5.10 compares the normalised load of data centre $S4$ for game and global solutions with different link capacities and data centre allocation ("full" denotes all 4 data centres are share by all users with route configuration specified in Table 8.1 and Table 8.2 of Appendix). Terms for "game" and "global" stand for the game solution and the global solution respectively. "Slink" means capacities for $L2$ and $L11$ are set to 10G while "Llink" indicates 100G for $L2$ and $L11$. With same link capacities and "sub" data centre allocation, the normalised load of data centre $S4$ for the game solution is larger than that of data centre $S4$ for the global solution. By reducing capacities for $L2$ and $L11$, the normalised load gap between the game solution and the global solution is

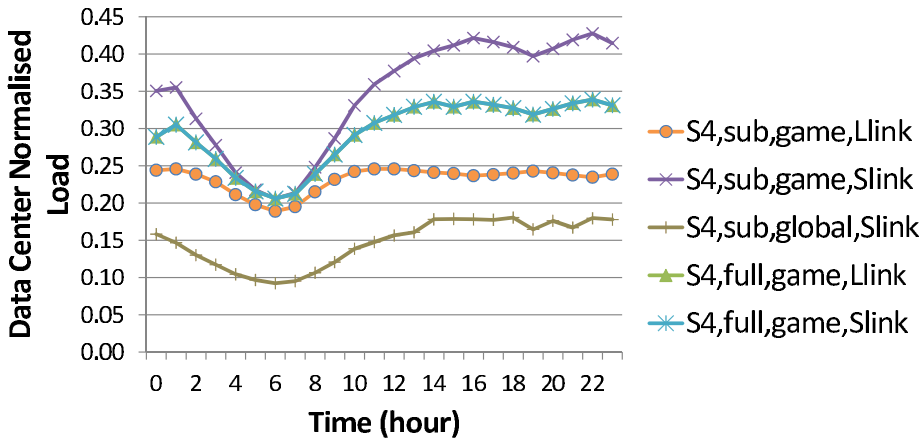

Figure 5.10: Impact of link capacity on the normalised load of data centre $S4$ for game and global solutions with different link capacities and data centre allocation

even bigger. However for "full" data centre allocation, the normalised load of data centre $S4$ is identical for both "Slink" and "Llink" conditions.

5.7.3 Observations

- *The power consumption of the proposed game solution is close to the global solution with equal weights*. In Fig. 5.5, the power consumption for the game solution only increases by less than 1%. This in turn indicates the centralised approach adopted by GreenTouch™[3] to address energy efficiency of communications networks is a valid option under certain conditions. With sufficient network provisioning and moderate objectives, individual ISP may just need to optimise her/his own performance metrics. The resulting power consumption of the whole networks may not be far worse than that of the solution with the centralised control as shown in Fig. 5.5.

- The curves for the total power consumption are flat for both game and global solutions as shown in Fig. 5.5. This is because the idle power of data centres dominates the total power consumption of the system. *Reducing idle power of data centres such that data centres are more energy-proportional [189] for traffic processing will significantly improve the energy efficiency of the system*.

- *The user-specific cost functions* (5.7) *are nonlinear and represent multi-objectives. Therefore the NE solutions will display a rich diversity of outcomes depending upon their local behaviour for different weights configurations and network conditions.*

- *Misalignment of objectives and asymmetrical allocation of limited resources for game players lead to inefficient resources usage in terms of energy and traffic load for the game solution compared to the global optimal solution.* If the individual objective deviates far from the global objective, game players will not act to favour the global optimisation causing the system performance to degrade. This in turn leads to high Game/Global ratio defined in (5.36) for the whole system as illustrated by the "Load Balance" curve in Fig. 5.6. For the load balancing objective, game players are more focused on load balancing over their own data centre sets. Due to the selfish nature, game players opt to adopt rational traffic routing decisions. This could result in high utilisation of energy inefficient resources as shown in Fig. 5.9.

- *Network topology and transport network capacity play important roles in system optimisation.* From an end-to-end viewpoint, improving energy efficiency of the system requires not only enhancing energy efficiency of data centres but also appropriate planning and provisioning of transport network. This is explained by the simulation results in Fig. 5.9 and Fig. 5.10. Note links $L2$ and $L11$ are physically far away from data centre $S4$. For the game solution, reducing capacity of $L2$ and $L11$ results in more traffic flowing to $S4$ even though $S4$ is the least energy efficient data centre.

5.8 Conclusion

In this chapter, we have proposed a general framework for energy efficient cloud computing with transport networks. We formulated a multi-objective optimisation problem for conflicting goals of minimising total system power consumption considering transport network performance and load balancing across data centres. A strategic game approach is proposed to address the multi-ownership of the network resources and services where each game player adopts rational strategies. Nash Equilibrium of the game and stability of the algorithm is analysed. Simulation results show challenges of improving network

energy efficiency in combination with other performance requirements such as server load balance and transport network delay.

Chapter 6

An Energy-Efficiency Framework in Optical Core Networks Using Software Defined Networking

6.1 Introduction

In Chapter 5, we developed a game theoretical framework to address the energy efficiency of cloud-based metro/core networks. We form the optimisation problem from end users' perspective because it is difficult to implement a global controller by using traditional networking technologies. We show there is potential system performance loss for the non-cooperative game theory solution if individual users are focusing on self-interests and taking rational decisions. In this chapter, we consider applying software defined networking (SDN) to optical core networks and focus on addressing challenges $8 \sim 9$ in Section 1.1. The emerging SDN technology is capable of implementing a logically centralised controller as described in Section 1.2.3. By leveraging the centralised SDN controller, core network operators can energy-efficiently distribute traffic from a system viewpoint rather than from individual network users' perspective shown in Chapter 5. To better answer the corresponding challenges in Section 1.1, we start with motivation of improving energy efficiency of optical core networks by using the SDN technology.

With the unprecedented growth of global IP traffic, the concern of the corresponding energy consumption is now drawing great attention to the sustainable growth of communication and data networks [3]. Further the corresponding economic and environmental impacts are highlighted in [14] such that the Information and Communication

Technology (ICT) industrial alone accounts for 3% of global electricity consumption and 2% global carbon footprint. Optical technologies are generally regarded as cost and energy efficient approaches to next-generation networks [190]. As shown in [191], energy efficiency of current optical communication systems and networks is yet to be improved to handle future data traffic.

Software Defined Networking is a emerging paradigm to accommodate the performance and heterogeneity requirements of next-generation networks [192]. By decoupling the control plane and the data plane of the underlying physical network infrastructure [192], SDN facilitates programmability of network control functionality. This separation provides unique solutions to complex network control problems, which are usually difficult to handle with traditional network architectures [63].

In this chapter, we propose an optimisation framework for distributing real-time traffic across a optical communication network in an energy efficient manner. A multi-objective optimisation scheme [43] is developed to explore independent, and possibly conflicting, system requirements on system power consumption, server load balance to improve service availability and network latency to enhance QoS. We design a generic weighted-sum scheme to provide flexible controls using weights for different optimisation objectives. Inspired by previous work such as in [72, 128], we implement a SDN-based network platform in Mininet [193] along with a customised POX controller [194] to demonstrate the optimisation problem. In contrast with the recent work [72], we propose a generic SDN framework considering multiple optimisation objectives. Unlike the work in [128], our framework is not restricted to a specific network architecture.

In contrast with the game theoretical framework specified in Chapter 5, we adopt centralised optimisation solution such as the mixed integer programming specified in Section 1.2.1. Because the centralised SDN controller has global information of the network. We think the non-cooperative solution in Chapter 5 is not suitable for SDN based networks. It is rather reasonable to implement global optimal solution with the full system knowledge such as network topology and user traffic. In this chapter, we show that the centralised controller facilitates implementation of global optimal solutions, which is otherwise difficult to achieve using non-cooperative game approach as explained in

Chapter 5.

The proposed Mininet simulation framework is able to support customised network topologies and real network protocols such as ARP, ICMP and UDP. By leveraging the SDN technology, we adopted a configurable VLAN-switching mechanism resulting a simple and flat transport network for statistical multi-path traffic distribution. This L2-switching mechanism can be easily replaced by the GMPLS-based (Generalized Multi-Protocol Label Switching) method with the support of OpenFlow protocol. The main contributions of this chapter are:

- We develop a general system model for next generation communication networks that allows core networks performance such as power consumption, load balance and network latency to be evaluated and compared.
- The system model encompasses an multi-objective optimisation framework to optimise both network power consumption and balancing of load over generic network elements with defined QoS requirements.
- We implement a SDN-based platform in Mininet, which enables demonstration of customised network functions such as statistical switching, multi-path routing and QoS-energy-aware traffic distribution in a systematic manner.
- The Mininet simulation results show that unintended individual stringent QoS requirements could introduce unfair network resource allocation and result in system power consumption and server load balance performance degradation.
- Network operators need to balance the tradeoff of providing customised traffic control and managing system performance such as system power consumption and server load balance. It is necessary for network operators to choose judicious QoS rules for end users such that potential impacts on system performance is foreseeable and controllable.

The rest of the chapter is structured as follows. The next section describes the general system model for traffic distribution in a communication network. The multiple objectives to optimise the system are specified in Section 6.3. A Mininet-based framework is

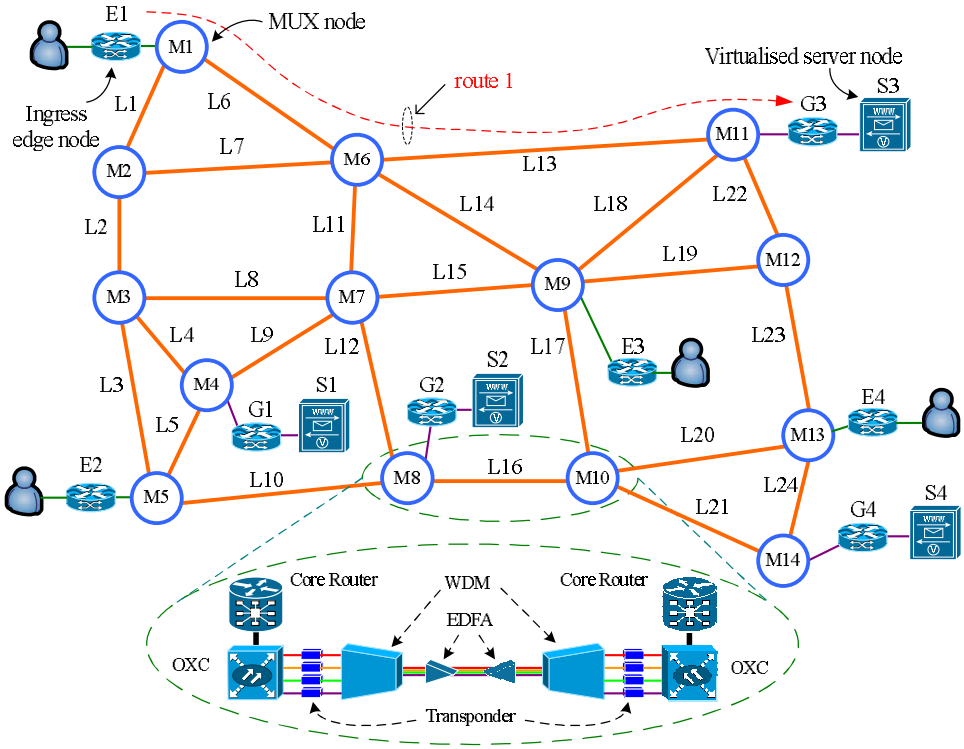

Figure 6.1: System model with 4 ingress edge nodes, 4 server nodes, 14 MUXs and 24 links.

specified in Section 6.4 with description on statistical packet distribution. Section 6.5 illustrates the simulation results with observation specified in Section 6.6 and Section 6.7 concludes this chapter.

6.2 System Model

Referring to Fig. 6.1, we consider a general system model for core networks, which consists of J ingress edge nodes, M intermediate multiplexing/aggregation (MUX) nodes and I virtualised server nodes. The network has L links connecting edge nodes and servers via MUX nodes. Table 5.1 summarises the main notations used in this chapter. Fig. 6.1 shows a typical IP-over-WDM network, which comprises core routes, Optical Cross-Connectors (OXC), transponders and Erbium-Doped Fiber Amplifiers (EDFA). By abstracting the physical network elements, the system has in sum $N = I + M + L$ *resources* for ingress edge nodes to share. Each element is characterised by the maximum

data traffic processing capacity $\mathbf{C}_n$ with $n = 1, \cdots, N$. Assume at time t edge node $j = 1, \cdots, J$, generates a aggregated data traffic with a data rate $\mathbf{d}_j^{\text{in}}(t)$ (bit/sec). Then all traffic generated by edge nodes can be expressed as a vector $\mathbf{d}^{\text{in}}(t) = [\mathbf{d}_1^{\text{in}}(t), \cdots, \mathbf{d}_J^{\text{in}}(t)]^T$. Note the aggregated data traffic from each edge node is slowly varying over a diurnal cycle as shown in [195]. For simplicity we omit the time index notation t for the rest of the chapter.

Define Ω_R as a set of all possible routes from edge nodes to servers with cardinality R. Let route $r = \{1, \cdots, R\}$ be a predefined route carrying an averaged (in order of minutes) traffic $\mathbf{d}_r$ from an ingress edge node to a server such that the traffic on all routes can be expressed as a vector $\mathbf{d} = [\mathbf{d}_1, \cdots, \mathbf{d}_R]^T$. Fig. 6.1 illustrates the route $1 \in \Omega_R$ from edge node 1 to server 3. Each edge node then distributes its traffic $\mathbf{d}_j^{\text{in}}$ over a subset of Ω_R to the designated servers. We use the $J \times R$ routing matrix $\mathbf{B}^{\text{rt}}$ defined in Eq. (3.2) of Section 3.3.1 to represent the mapping between edge nodes and routes. This in turn indicates $\mathbf{d}^{\text{in}} = \mathbf{B}^{\text{rt}}\mathbf{d}$. In addition, the topology of the system in Fig. 6.1 can be represented by the $N \times R$ matrix $\mathbf{A}$ defined in Eq. (3.1) of Section 3.3.1, which maps each device to the associated route. Let $\mathbf{d}_n^{\text{res}}$ be the aggregated traffic at device n such that all aggregated traffic on server nodes, MUX nodes and links can be expressed as a vector $\mathbf{d}^{\text{res}} = [\mathbf{d}_1^{\text{res}}, \cdots, \mathbf{d}_N^{\text{res}}]^T$. The relationship between the aggregated traffic on each device and the traffic on each route can be expressed as $\mathbf{d}^{\text{res}} = \mathbf{A}\mathbf{d}$. Using Eq. (3.3) in Section 3.3.1, we derive a 1-0 edge router-*resource* mapping matrix $\mathbf{B}^{\text{res}}$ where $\mathbf{B}_{j,n}^{\text{res}} = 1$ indicates there is a available route linking edge router j and network element n. Further, we can obtain the $J \times I$ edge-server mapping matrix $\mathbf{B}^{\text{srv}} \subset \mathbf{B}^{\text{res}}$ and the $J \times M$ edge-MUX mapping matrix $\mathbf{B}^{\text{mux}} \subset \mathbf{B}^{\text{res}}$.

6.3 Problem Formulation

We formulate a traffic distribution problem in order to find the optimal traffic for each edge node to dispatch over the predefined routes such that the associated cost function is minimised. In this chapter, we propose a joint cost function where potentially conflicting objectives are considered:

1. total system power consumption minimisation

2. system traffic load balancing

3. latency QoS enforcement

We assume a fixed number of network elements including servers, MUXs and links are provisioned. The number of network elements will be energised depends on the traffic load, the latency requirements and the energy-saving/load-balance criteria.

6.3.1 Power Consumption Objective

The normalised total power consumption for data traffic routing and processing includes the power consumption of links connecting the edge, the MUX and the server nodes shown in Fig. 6.1. We model the power consumption of a network element $n = 1, \cdots, N$ with a general affine function defined in Eq. (3.6) of Section. 3.3.3

Note the idle power consumption $\beta_n P_n^{\max}$ in Eq. (3.6) is independent of the carried traffic $\mathbf{d}_n^{\text{res}}$. Currently, network equipments are always turned on, even the carried traffic is nearly zero [173]. By adopting the sleep or the switch-off mode [196], the network equipment power consumption in Eq. (3.6) can be expressed as,

$$P_n^* = \begin{cases} P_n^0 & \text{if } \mathbf{A}_n \mathbf{d} = 0 \\ P_n & \text{if } \mathbf{A}_n \mathbf{d} > 0 \end{cases} \tag{6.1}$$

where $P_n^0 = 0$ for the switch-off mode and $0 < P_n^0 < \beta_n P_n^{\max}$ denotes the power consumption for the sleep mode. Then the normalised total power consumption of the whole system including servers, MUXs and links can be expressed as,

$$P_{\text{sys}}^* (\mathbf{d}) = \frac{\sum_{n=1}^{N} P_n^*}{P^{\max}} \tag{6.2}$$

where $P^{\max} = \sum_{n=1}^{N} P_n^{\max}$ denotes the sum of the maximal power over all network elements.

6.3.2 Load Balance Objective

Load balancing is a technology that assures reliable and scalable deployment of large web applications. As explained in [197] load balancing can produce highly available, scalable, and predictable application services. Unbalanced traffic load can cause throughput degradation and result in suboptimal utilisation of network resources.

The load balancing objective addresses the traffic throughput of the virtualised server nodes shown in Fig. 6.1. Let $T = \sum_{j=1}^{J} \mathbf{d}_j^{\text{in}}$ be the total traffic generated by all edge nodes. Assume all traffic shall be forwarded in the transport network and processed in the server nodes, which leads to a system throughput $\sum_{i=1}^{I} \mathbf{d}_i^{\text{srv}} = T$. Let $\mathbf{C}_{\text{sys}}^{\text{srv}} = \sum_{i=1}^{I} \mathbf{C}_i^{\text{srv}}$ denotes the total processing capability of the server nodes. Define the load balanced condition over all server nodes as,

$$\eta_1^{\text{srv}} = \eta_2^{\text{srv}} = \cdots = \eta_I^{\text{srv}} = \frac{T}{\mathbf{C}_{\text{sys}}^{\text{srv}}} \tag{6.3}$$

where $\eta_i^{\text{srv}} = \frac{\mathbf{A}_i^{\text{srv}}\mathbf{d}}{\mathbf{C}_i^{\text{srv}}}$ denotes the normalised load for server node i.

However, implementing the load balanced condition illustrated in (6.3) is not easy from a mathematical perspective when solving for the optimal operation point. In order to handle this challenge, we propose an alternative implementation of load balancing by introducing a normalised load balancing variance over server nodes as,

$$S(\mathbf{d}) = \frac{1}{\hat{S}I}\sum_{i=1}^{I}\left(\frac{\mathbf{A}_i^{\text{srv}}\mathbf{d}}{\mathbf{C}_i^{\text{srv}}} - \frac{T}{\mathbf{C}_{\text{sys}}^{\text{srv}}}\right)^2 + \frac{1}{\hat{S}M}\sum_{m=1}^{M}\left(\frac{\mathbf{A}_m^{\text{mux}}\mathbf{d}}{\mathbf{C}_m^{\text{mux}}} - \frac{T}{\mathbf{C}_{\text{sys}}^{\text{mux}}}\right)^2 \tag{6.4}$$

where

$$\hat{S} = \frac{1}{I}\left(\left(1 - \frac{T}{\mathbf{C}_{\text{sys}}^{\text{srv}}}\right)^2 + (I-1)\left(\frac{T}{\mathbf{C}_{\text{sys}}^{\text{srv}}}\right)^2\right) + \frac{1}{M}\left(\left(1 - \frac{T}{\mathbf{C}_{\text{sys}}^{\text{mux}}}\right)^2 + (M-1)\left(\frac{T}{\mathbf{C}_{\text{sys}}^{\text{mux}}}\right)^2\right)$$

denotes the upper bound of the load balancing variance for server nodes. The upper bound denotes the extreme case that all traffic directed to only one server node which has a capacity the same as the total traffic. Minimising the load balancing variance leads to the balanced load condition (6.3).

6.3.3 Traffic Delay Constraints

Network latency is becoming a performance bottleneck of the Internet and has a significant impact on the deployment of new services and applications [198]. Latency is one of the key factors of network performance and Quality of Experience (QoE) for end customers. In [198], the authors summarised the related techniques aiming to tackle the network latency problem.

In this chapter, we introduce network delay constraints as a requirement of QoS for the proposed system. First, we model the network latency for route r as a accumulated delay over the traversed network elements expressed as

$$z(r) = \sum_{n=1}^{N} \mathbf{A}_{n,r} \mathbf{z}_n \tag{6.5}$$

where $\mathbf{z}_n$ denotes the delay for network element n. Note a network element can be a link, MUX node or a server node. For an optical long haul link $l \in \Omega_L$(set of link elements), the corresponding latency can be modeled as,

$$z = \mathbb{L} \times \tau_g \times (1 + \rho_{dc}) \tag{6.6}$$

where $\mathbb{L}$ is the length (km) of the link. τ_g is the group delay of the fiber (around 5μs/km) and ρ_{dc} (up to 15%) accounts for the extra delay due to dispersion compensation [199]. For MUX and server nodes, the associated delay is related to switching, routing or other traffic processing undertaken. We use the following model to approximate the delay for MUX and server node as $z = z_{SF} + z_{FB} + z_Q$,where z_{SF} denotes the store and forward delay, z_{FB} indicates the device fabric latency and z_Q is the processing delay. The detail description of those parameters can be found in [200]. In order to meet the latency requirement for the data traffic, each user applies a latency policy to the routes it uses such that $z(r) \leq \boldsymbol{\tau}_r$, where $\boldsymbol{\tau}_r$ denotes a upper bound of the network latency for route r.

6.3.4 Multi-objective Optimisation

The first objective of minimising the system power consumption tends to direct data traffic to the more energy efficient server nodes via energy efficient links while the second objective of minimising the load balancing variance tends to distribute data traffic over all server nodes. In order to compromise between the two objectives in (6.2) and (6.4), we apply the weighted sum method to construct the joint problem

$$\min_{\mathbf{d}} U(\mathbf{d}) = \min_{\mathbf{d}} \Big((1-\omega) P^{*}_{\text{sys}}(\mathbf{d}) + \omega S(\mathbf{d}) \Big) \tag{6.7}$$

$$\text{subject to } \mathbf{B}^{\text{rt}}\mathbf{d} = \mathbf{d}^{\text{in}} \tag{6.8}$$

$$\mathbf{A}\mathbf{d} \leq \mathbf{C} \tag{6.9}$$

$$0 \leq \mathbf{d}_r, r = 1, \cdots, R \tag{6.10}$$

$$(\mathbf{A}\mathbf{z} - \boldsymbol{\tau})_{\text{diag}} \mathbf{d} \leq \mathbf{0} \tag{6.11}$$

where $0 \leq \omega \leq 1$ denotes the weighting factor between power consumption and load balancing. $\mathbf{z} = [\mathbf{z}_1, \cdots, \mathbf{z}_N]^T$ denotes the delay for all network elements and $\boldsymbol{\tau} = [\boldsymbol{\tau}_1, \cdots, \boldsymbol{\tau}_R]^T$ represents the delay threshold for each route.

- The first constraint (6.8) indicates the input traffic flow conservation.
- The second constraint (6.9) indicates the aggregated traffic on each device shall not exceed its corresponding processing capacity or bandwidth.
- Constraint (6.9) also states that all traffic generated by each edge node needs to be processed in the server nodes. If no feasible solution exists, a portion of data traffic shall be dropped at edge nodes until a feasible solution can handle.
- The third constraint (6.10) gurantees non-negtive traffic carried on each route.
- The fourth constraint (6.11) indicates the latency requirement for the traffic distributed to a route.

As soon as the aggregated traffic $\mathbf{d}_n^{\text{res}}$ for equipment n is positive, the idle power $\beta_n P_n^{\max}$ which is a fixed cost is incurred. As a consequence, the power consumption of

individual network equipment in (6.1) is not continuous and twice differentiable. In order to circumvent the discontinuity of the individual power consumption, we introduce variable

$$\mathbf{y}_n = \begin{cases} 0 & \text{if } \mathbf{A}_n\mathbf{d} = 0 \\ 1 & \text{if } \mathbf{A}_n\mathbf{d} > 0 \end{cases}$$

such that the system power consumption can be modified as,

$$P^*_{\text{sys}}(\mathbf{d}) = \frac{1}{P^{\max}} \sum_{n=1}^{N} \left(\mathbf{y}_n \bar{P}_n + (1-\mathbf{y}_n)P^0_n + \hat{P}_n\right) \tag{6.12}$$

Then the discontinuous multi-objective function (6.7) is transformed as a Mixed Integer Non-linear Programming (MINLP) problem:

$$\min_{\mathbf{d}} U(\mathbf{d}) = \min_{\mathbf{d}} \Big((1-\omega)P^*_{\text{sys}}(\mathbf{d}) + \omega S(\mathbf{d})\Big) \tag{6.13}$$

$$\text{subject to} \quad \mathbf{A}_n\mathbf{d} \leq u\mathbf{y}_n, \quad \forall n \in \{1, \cdots, N\} \tag{6.14}$$

$$\mathbf{y}_n \in \{0,1\}, \quad \forall n \in \{1, \cdots, N\} \tag{6.15}$$

where constant u is a sufficiently large number and constraint (6.14) is introduced to exclude the case when $\mathbf{A}_n\mathbf{d} > 0$ and $\mathbf{y}_n = 0$.

6.4 Mininet Platform Setup

6.4.1 Software Defined Networking

SDN has potential to change network design, deployment and operation by introducing flexibility and programmability. With SDN, the control and manage functions can be implemented in a (*logically*) centralised controller [77]. Compared to the traditional control plane integrated in vendor-specific devices, SDN control plane can be implemented and hosted on a standard off-the-shelf hardware platform. Therefore, implementing customised network policies to address different user requirements is becoming possible [63]. In addition, with global knowledge of network states such as topology and traffic,

it is possible to implement sophisticated network functions and applications.

6.4.2 OpenFlow Protocol

OpenFlow is one realisation of SDN protocols to facilitate the communication between the Controller and the data plane abstraction. It is now widely regarded as a key technology enabler of SDN by the network community [192]. OpenFlow is designed to support remote controllers on determining forwarding pathe for network packets through networked devices [77]. Initially OpenFlow was developed for Ethernet switches in IP packet domain. A new generic and extended optical OpenFlow specification was proposed in [78] to support emerging optical transport technologies.

6.4.3 Mininet

The Mininet open-source network emulator is designed to support research, development, prototyping, testing SDN systems on a standard PC platform [81]. It can run unmodified code interactively on virtual hardware, providing prototyping convenience and realism at low cost. A virtual software-defined network can be created in Mininet on-the-fly, which consists of an OpenFlow controller, multiple OpenFlow-enabled Ethernet switches, multiple host and ethernet links connecting those elements. The authors of [82] demonstrated that Mininet can be used to reproduce published results by running networks on a single PC, using lightweight OS visualisation.

In this chapter, we use Mininet to model the generic system in Section6.2 with optimisation objectives defined in Section6.3.4. The platform is implemented in a Ubuntu virtual machine (Mininet 2.0.0 VM - Ubuntu 12.10 server 64-bit - OVF - 11.30.12). The VM is mounted on a Dell desktop (OptiPlex 990 DT) using VirtualBox. Fig. 6.2 illustrates the system architecture for the proposed framework including 3 main blocks:

- Customised network topology
- SDN controller module implemented with POX [194]
- Traffic monitor: Bandwidth Monitor NG [201]

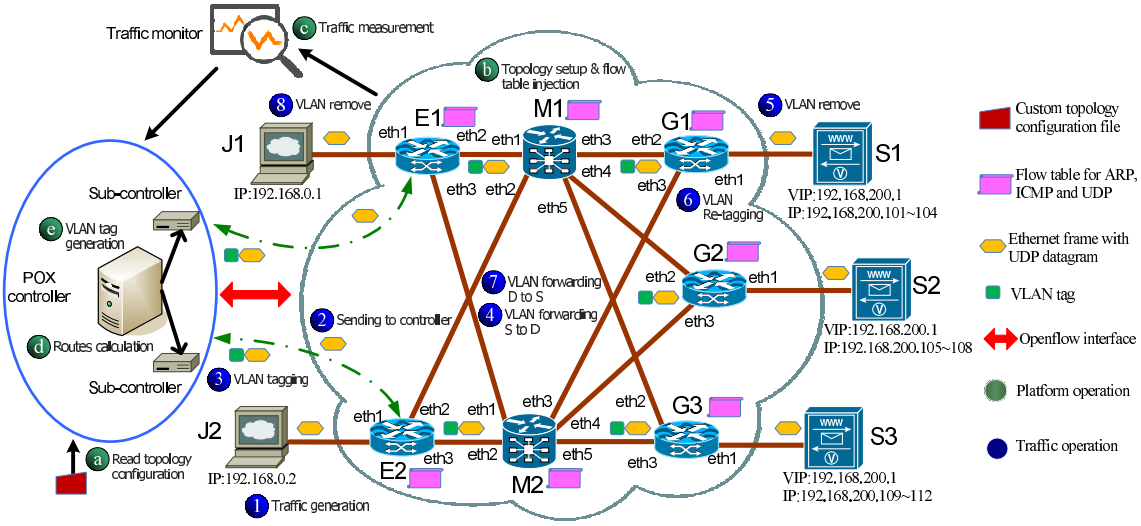

Figure 6.2: Mininet platform setup and traffic distribution.

In Fig. 6.2 we show the emulated topology comprising 3 server nodes, 2 MUX nodes, 2 host nodes and 5 edge nodes. E1 and E2 represent the ingress edge nodes connected to the host nodes h1 and h2. The nodes G1∼G3 denote the egress nodes linked to the server nodes S1∼S3 respectively. Each host has multiple routes leading to a server nodes such that the whole topology can be represented by matrix **A** specified in Table 5.1. Table 6.1 shows the predefined routes for the topology in Fig. 6.2.

In the proposed Mininet framework, each packet will have an attached VLAN ID (VID), which is mapped to a defined route shown in Table 6.1. The external controller will decide which VID will be attached to each packet before it leaves the edge node. A switch may have multiple flow entries depending on how many routes are mapped to this switch, which is determined by the predefined routes in Table 6.1. Based in the matched VID, a switch will forward the received packet to the port associated with that VID.

In order to generate a customised topology, we implemented a Python model, which can read a topology file in the "CSV" format. Each line of the topology file specifies 2 nodes (host, switch or server) connected by a link. Detail information such as VLAN ID, link bandwidth, link delay, source/destination ID, source/destination port number, source/destination IP (only for host and sever nodes) and node power consumption related parameters will be specified in each line. By reading this topology file (ⓐ), Mininet

Table 6.1: Route definition

ID	path	ID	path
1	$h_1E_1M_1G_1S_1$	7	$h_2E_1M_1G_1S_1$
2	$h_1E_1M_1G_2S_2$	8	$h_2E_1M_1G_2S_2$
3	$h_1E_1M_1G_3S_3$	9	$h_2E_1M_1G_3S_3$
4	$h_1E_1M_2G_1S_1$	10	$h_2E_1M_2G_1S_1$
5	$h_1E_1M_2G_2S_2$	11	$h_2E_1M_2G_2S_2$
6	$h_1E_1M_2G_3S_3$	12	$h_2E_1M_2G_3S_3$

can generate a customised virtual network with the required Ethernet port connections (ⓑ).

The Traffic Monitor in Fig. 6.2 is built upon a console-based live network monitoring tool: BWM-NG [201]. The traffic information of all Ethernet ports for OpenFlow switches is updated in the linux operation system. BWM-NG can access the data traffic statistics and derive the averaged value over a defined period. We design a module to periodically query these results and extract the traffic statistics for all switches and links (ⓒ). Based on the traffic information, we can further derive the traffic statistics for host and server nodes. In addition, by using the model in Eq. (3.6), the Traffic Monitor will calculate the power consumption of each network device followed by the system power consumption. The resulting traffic measurement will be forwarded to the POX controller. By using this information, the POX controller can make traffic distribution decision such that the joint cost in (6.13) is minimised (ⓓ).

The POX controller in Fig. 6.2 is in charge of logic network mapping, flow table injection, traffic routes calculation and VLAN tagging. For proof-of-concept purpose, we only implement a single controller in the Mininet platform, which can be extended to multiple distributed controllers with better performance for load management [202]. We build a module to extract each host's topology information as demonstrated in Fig. 6.1 for the POX controller. With the parsed information, this module will build a database to describe:

- For each host, what are the routes (by VLAN ID) reserved for it, which specifies a row of $\mathbf{B}^{\text{rt}}$ specified in Table 5.1
- For each route, what are the network elements (host, switch,link,server) allocated

to this route, which specifies a column of **A** specified in Table 5.1

- For each network element, which VLAN ID it will carry and how this ID is mapped to Ethernet ports (ingress and egress), which specifies a row of **A**.

By accessing this database, the POX controller can create flow tables for each OpenFlow switches in the system with VLAN tags in the match field. Those flow tables are preliminarily injected in the OpenFlow switches (ⓑ). For real practice, flow tables can be dynamically injected in OpenFlow switches on demand.

After receiving traffic measurement from the Traffic Monitor, the controller starts calculating routing decision for each host. Note only ingress nodes' input traffic is measured initially. To solve the problem in (6.13), we use a CPLEX solver and build a Python wrapper to run it in Linux. Once the traffic distribution calculation is finished, the POX controller will send traffic ratio vectors to sub-controllers shown in Fig. 6.2. A traffic ratio vector is associated with a host and specifies the ratio of traffic on each reserved route for that host. Upon receiving the vector, each sub-controller will generate a sequence of VLAN tags (ⓔ). Those VLAN tags will be attached to packets from hosts in a first-in-first-out fashion as demonstrated in Fig. 6.3. If the end of the sequence is reached, a new sequence can be generated or the current sequence can be recycled at its beginning. We design an weighted random algorithm to create the random sequence, which reflects the statistics of the traffic ratio vector. Fig. 6.3 illustrates an example for the VID sequence generation and the cyclical tagging for input packet frames.

Fig. 6.2 also demonstrates the life cycle of packets from hosts to servers and back to hosts. The whole operation includes ARP, ICMP and UDP processing. In this example, we define a virtual IP (VIP) address 192.168.200.1 for all server nodes. Each host will continuously send UPD packets with constant bit-rate to this VIP by using the *iperf* tool in Mininet (①). Without pre-knowledge of this VIP, each host will first send an ARP request to the ingress edge node (ingress OpenFlow switch) asking for MAC address of that VIP. Instead of flooding the ARP request, the edge node will forward this request to POX controller via OpenFlow protocol. The POX controller will respond with a dummy MAC address back to the host. Then the host will start sending UDP packets to that VIP with this dummy destination MAC address. Receiving the Ethernet frame with the UDP

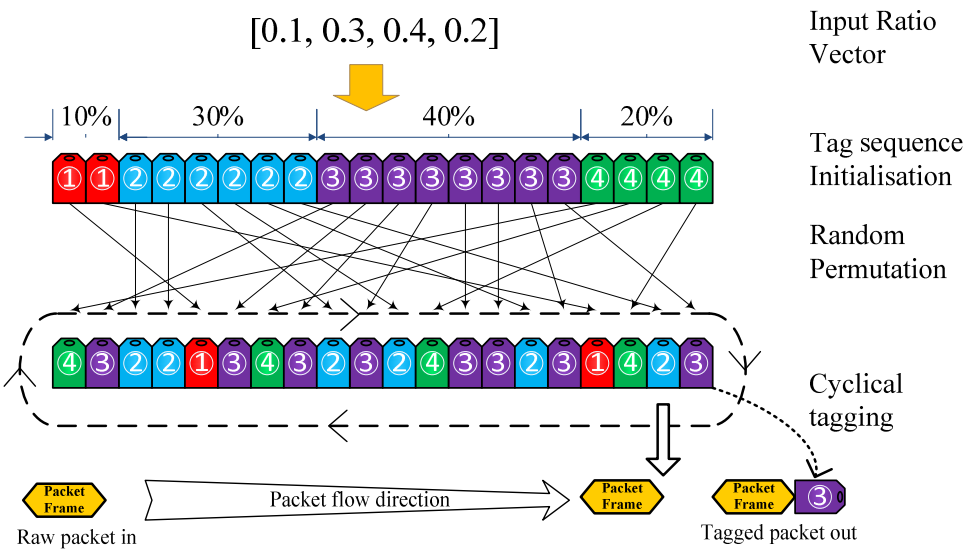

Figure 6.3: VLAN sequence generation and packet tagging.

payload from the host, the ingress edge node will again forward the frame to the controller (②). This time the corresponding sub-controller will take over. The dummy MAC address is replaced by a valid one belonging to a server node, and the VIP is replaced by the IP of that server. Note the new MAC address and IP are associated with the first available VID (③). Next Ethernet frame will possibly use a different destination MAC-IP pair related to the next available VID. Then the corresponding VID is inserted in the frame, which is sent back to the edge node. By matching the VID in a defined flow table, the edge node will forward this packet to a designated port. The following OpenFlow switches will do the same such that only L2 switching is required to forward packets (④). At egress edge node, the VID of a Ethernet frame is removed before forwarded to the port linked with a server (⑤). In the reverse path, the packet processing is similar to the aforementioned procedure (⑥,⑦,⑧).

6.5 Simulation Results

The proposed framework is run in Mininet hosted in a single system. Therefore, the simulated network is subject to the limitation of CPU or bandwidth of the host system.

Table 6.2: Parameters of network devices

Devices n	Capacity C_n(Gbps)[1]	Max power $P_n^{\max}$ (Watts)[1]	power ratio β_n
$S1$	347	6.54×10^6	0.8
$S2$	354	8.61×10^6	0.8
$S3$	786	1.99×10^7	0.8
$S4$	300	3.00×10^7	0.8
$M1$	180	1.43×10^4	0.8
$M2$	140	1.14×10^4	0.8
$M3$	140	1.14×10^4	0.8
$M4$	180	1.28×10^4	0.8
$M5$	220	1.71×10^4	0.8
$M6$	140	1.14×10^4	0.8
$M7$	140	1.14×10^4	0.8
$M8$	180	1.28×10^4	0.8
$M9$	160	1.14×10^4	0.8
$M10$	140	1.14×10^4	0.8
$M11$	400	1.63×10^4	0.8
$M12$	140	1.14×10^4	0.8
$M13$	280	1.99×10^4	0.8
$M14$	160	1.14×10^4	0.8
$L1 \sim L24$	200	344	1.0

[1] Parameters for data centers are based on data center sizes and assumptions of power consumption per squre meters. MUX and link parameters are derived from typical equipment values [180]

In order to show test cases with high throughput, we scale down the input traffic rate to the extent that Mininet can handle. The following sections demonstrate the system performance of the proposed multi-objective optimisation framework implemented in Mininet.

Fig. 6.1 illustrates a partial USA backbone IP network (USNET) topology, which consists of 4 data centers (sever nodes $S1 \sim S4$ each has a egress edge node), 14 MUX nodes and 4 ingress edge nodes. Edge nodes $E_1 \sim E_4$ are introduced to distribute input traffic to the data centers via pre-defined 56 routes. The detailed route configuration is described in Table 8.1 of Appendix. Table 6.2 specifies the parameters for the network devices considered in the topology. Note we deliberately set S_4 the least energy efficient data center for demonstration purpose. We also use Fig. 5.9 to illustrate the input traffic diurnal cycle for edge nodes $E_1 \sim E_4$. The route latency for each user is obtained by using (6.5).

The delay for each link is approximated using (6.6) and fixed delays are applied to MUX and server nodes. For this topology, we apply different delay constraints to show system performance in terms of system power consumption and network latency. First we setup an infinite delay threshold for each user such that traffic distributing is not subject to the delay constraints in (6.11). Second we apply delay threshold 25ms and 20ms for user 3 and user 4 respectively.

Fig. 6.4∼Fig. 6.7 show the system total power consumption, the server load balance and the network latency. Term "No delay QoS" indicates no delay constraint for all users ($1 \sim 4$). "Partial delay QoS" denotes no delay constraint for user 1 and 2, but user 3 and 4 have delay constraint 25ms and 20ms respectively. With no delay constraints, the diurnal cycle of the system power consumption is deep as shown in Fig. 6.4. This is because the energy inefficient server node S_4 is turned off during off-peak time while all server nodes are energised during peak hour. On the other hand, with tight delay constraints for users 3 and 4, the system power consumption demonstrates shallow diurnal cycle following the trend of the input traffic shown in Fig. 6.4. Energy inefficient server node S_4 perpetually remains active to meet the latency requirement of some local traffic. This confirms the results in [196] that the system needs to consume more energy to handle traffic with high QoS requirements.

The latency requirement also affects the load balance performance of server nodes as illustrated in Fig. 6.5. Without delay constraints, the proposed system manages the server load balance well with low load balance variance during peak time. Increased load balance variance is observed during off-peak period, which is due to zero traffic on inactive server node S_4. By setting the aforementioned delay constraints for user 3 and 4, we observe a notable increase of the server load balance variance in Fig. 6.5. This indicates that ideal server load balance is difficult to achieve with stringent latency requirements. Delay sensitive traffic could render unbalance traffic over server nodes, which may cause degraded service availability for the whole system.

Network delay performance for individual users is sensitive to stringent latency requirements. In the proposed Mininet platform, we measure the network delay from hosts to server nodes by issuing ICMP request (*ping*) at each host. Along with the UDP traf-

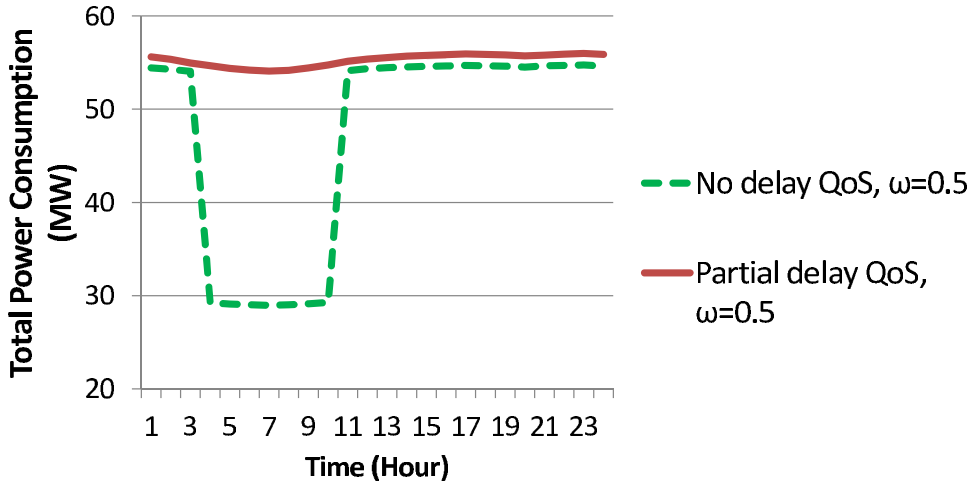

Figure 6.4: System power consumption for $\omega = 0.5$

fic, each host will send ICMP echo packets to the VIP shared by all server nodes such that ICMP packets will be routed the same way as UDP packets. Each host issues 1000 echo requests and the corresponding echo reply will be captured to derive the network latency statistics. Fig. 6.6 and Fig. 6.7 demonstrates the Cumulative Density Functions (CDF) of delay for each user without and with delay constraints respectively. Setting no delay constraints on all users' traffic, traffic of user 1 and 2 spends no more than 30ms and 15ms respectively to reach a server node. Around 95% of user 3's IP traffic arrives to a server node within 25ms. Only a small portion of traffic needs more travelling time. User 4 has the worst delay performance that more than 30% of the traffic needs at least 30ms to finish a one-way trip. Note the step of user 4's curve indicates that the traffic of this user is distributed over multiple routes, each has a different delay. Fig. 6.7 shows the traffic latency for each user with tight delay constraint applied to user 3 and 4. We observe that the traffic latency for user 3 and 4 is less than 20ms, which meets the required delay constraints. However, the delay performance for user 1 and 2 is much worse off. Compared to the no delay constraints case in Fig. 6.6, it costs user 1 and 2 even more time to send traffic to a server node.

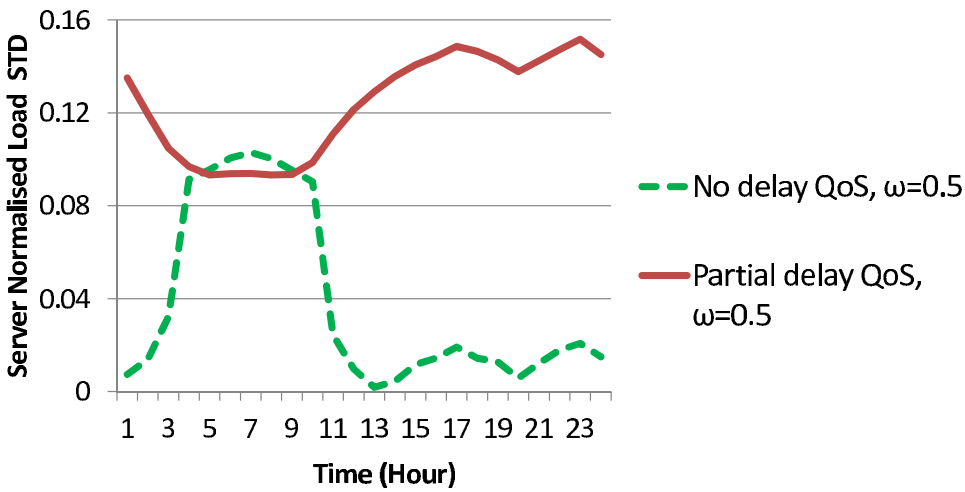

Figure 6.5: Data center normalised load STD for $\omega = 0.5$

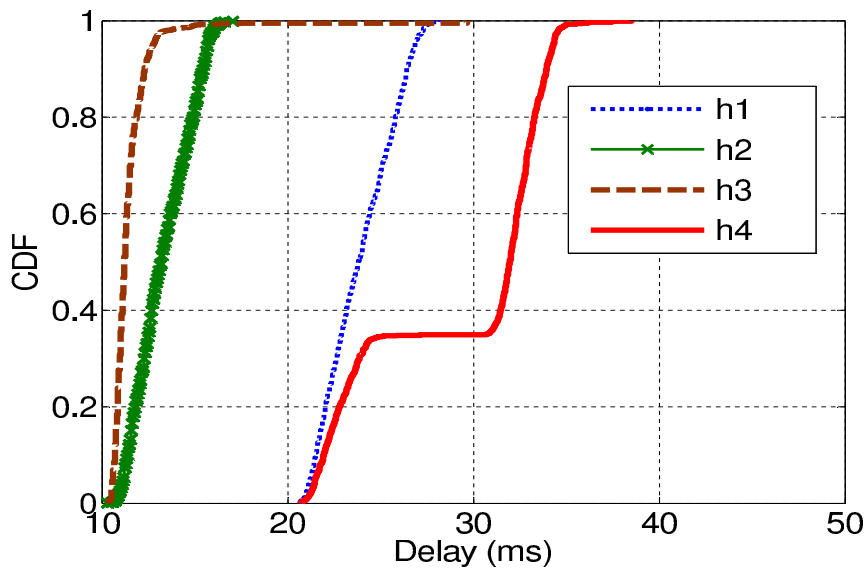

Figure 6.6: Network latency with no delay constraint and $\omega = 0.5$

6.6 Discussion

The Mininet simulation results show opportunities and challenges for energy efficient network plan, design and operation. The proposed framework provides an alternative option to implement network functions such as statistical switching, multi-path routing and QoS-energy-aware traffic distribution in a systematic manner, which is difficult to realise with traditional network architectures. The challenge for the network operator

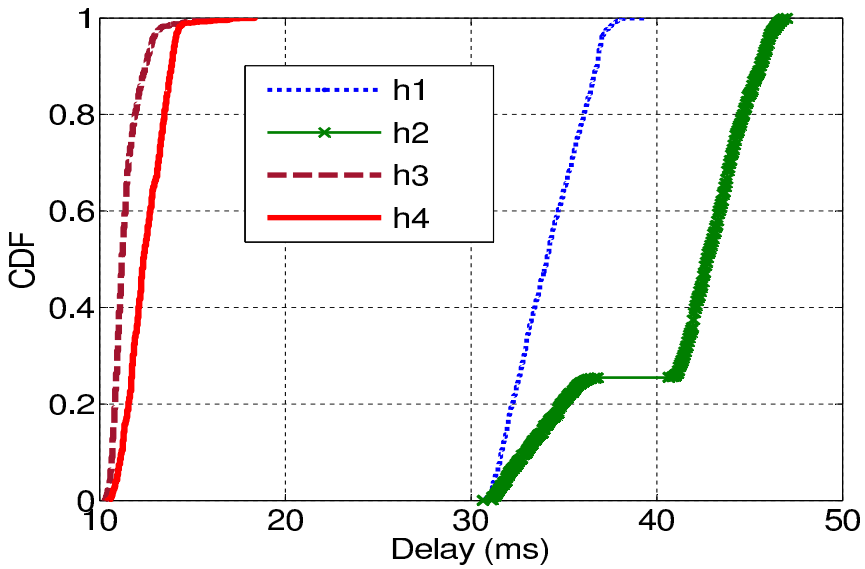

Figure 6.7: Network latency with delay constraint and $\omega = 0.5$

is to learn not only the dynamic range and the pattern of the traffic to be handled in an energy efficient manner but also the associated user specific QoS requirements to be accommodated. In summary, we show

- The proposed SDN-based framework enables individual traffic QoS manipulation in an end-to-end manner, which entitles end customers more control on their data traffic over core networks.
- The negative "externality" caused by the individual stringent QoS requirements could introduce unfair network resource allocation and result in system power consumption performance degradation.
- Network operators need to balance the tradeoff of providing customised traffic control and managing system performance such as system power consumption and server load balance.
- It is necessary for network operators to choose judicious QoS rules for end users such that potential impacts on system performance is foreseeable and controllable. Unintended customer service level agreement (SLA) could cost the network operator great efforts to comply.

6.7 Conclusions

In this chapter, we have proposed a general framework for real-time traffic distribution over heterogeneous communication networks including transport networks and virtual server nodes. A multi-objective optimisation problem is formulated to minimise the system power consumption and achieving load balance over IT infrastructure with customised QoS constraints. In order to demonstrate the proposed joint optimisation frame work, we have implemented a SDN based network system controlled by a logically centralised POX controller in the Mininet platform. By off-loading the control intelligence to the logically centralised controller, higher layer applications and services can utilise the unified control abstraction to implement customised network functionalities without detail knowledge of the underlying physical networks. Also, the resulting L2-switching data plane structure is simple but efficient in data traffic operation.

This chapter demonstrates a new direction of optimising energy efficiency and performance of next-generation optical core networks by leveraging SDN technologies. The proposed proof-of-concept framework provides insights of implementing complex network optimisation functions in SDN-based networks. Traditional network architecture in contrast finds it difficult to provide the flexibility and extendability that SDN offers. We show new algorithms and protocols can be evaluated in a fast and cost-effective way by leveraging the Mininet platform. Future work will be implementing distributed controllers for edge nodes to improve the statistical traffic distribution capability.

Chapter 7
Conclusion

7.1 Summary of Contributions

Reducing energy consumption of communication network is of paramount importance because of the economic benefits and environmental impacts. In addition, energy consumption is likely to be the "bottleneck" of the future communication networks considering the future global data traffic growth and the current network energy efficiency improvement. This dissertation is motivated by the consensuses among the ICT industry and the academic community that further technology advances for energy efficiency of communication networks are required to sustain the growth of Next Generation Networks [83]. The contributions of this dissertation are summarised into three areas:

- Multi-objective optimisation for energy efficiency and load balance of heterogeneous backhaul networks

- Cloud-based network energy efficiency optimisation with non-cooperative game theory

- Power consumption minimisation for optical core networks by using software defined networking (SDN)

In the following sections, we outline key findings of this dissertation for each of the areas described above.

7.1.1 Multi-objective Optimisation in Heterogeneous Backhual networks

Radio access networks were studied in previous literature to identify available solutions to improve the corresponding energy efficiency. This is due to the fact that current macro base stations account for major energy consumption of the mobile communication networks. With the growing mobile data traffic and the massive deployment of small cells with high-capacity low-power small base stations, a backhaul network is likely to consume more energy. However, there has been little discussion in the literature on the energy efficiency of backhaul networks. Furthermore, not much research has focused on jointly optimising energy efficiency and load balancing in heterogeneous backhaul networks. This in turn stimulated the first research problem in this dissertation: Multi-objective optimisation for energy efficiency and load balancing of heterogeneous backhaul networks.

To study this problem, we developed a general system model for next generation heterogeneous backhaul networks in Chapter 3. A binary network element/route matrix and a binary source/route matrix was adopted to describe the network topology. In Chapter 4 we formed an multi-objective traffic distribution problem in order to find the optimal traffic for each eNodeB to distribute over heterogeneous backhaul networks to serving gateways (S-GWs) such that the proposed joint cost is minimised. The joint cost encompasses conflicting objectives: system power consumption minimisation and system traffic load balancing. Each objective is multiplied by a weighting factor which represents the relative preference between confliction objectives. By decomposing the joint optimisation problem, we derived a distributed algorithm capable of scaling to large systems, which is difficult to scale up for centralised solutions such as mixed integer programming.

The simulation results show that the diurnal characteristic of data traffic can be utilised to reduce energy consumption of wireless backhaul networks. With the proposed distributed algorithm, the effective network routing topology can be changed to accommodate different traffic patterns. We also demonstrated that given a certain system throughput, reducing network energy consumption generally leads to unbalanced traffic load. In contrast balance traffic load results in system power consumption increase. Network

operators can choose proper weighting factors to provide high network availability for traffic peak, reduce network energy consumption during off-peak period or achieve a certain level of compromising between those two conflicting objectives.

We observed that the backhaul network system power consumption is significantly impacted by multiple factors such as the input traffic, the underlying network topology and the energy characteristics of network elements. Given enough link capacity, the system power consumption is more dominated by the power consumption of S-GWs. System power consumption performance can be compromised merely by inadequate provisioning of link capacities. Load balancing over heterogeneous backhaul networks is difficult to achieve when system power reduction is also considered to a certain extent.

It is important for network operators to understand the traffic dynamics and patterns so as to reduce the power consumption of backhaul networks. Deploying energy efficient network equipment is not sufficient to improve the energy efficiency of heterogeneous backhaul networks. Network topology optimisation and proper link capacity provisioning are critical for the power management of backhaul networks. Network operators need to understand causes for sudden energy consumption changes to mitigate the impact on other system performance such as traffic load balance.

7.1.2 Non-cooperative Game Theoretical Analysis of Energy Efficiency for Cloud-based Communication Networks

The significant growth of multimedia IP traffic results in the current telecommunications and data networks suffering from extensive load congestion and severe service request rejection. The ever increasing multimedia traffic does not adapt to changes of throughput, delay and packet loss for communication networks. In addition, large communication networks such as the Internet are usually highly distributed and complex. It is rather difficult for each network operator and service provider to obtain the global information about the whole network such as resources provisioning and traffic patterns for all end users. In reality, network users are generally self-interest driven to minimise individual costs such as energy consumption regardless of the global optimum. However, the impact of end users' rational on energy efficiency of communication networks encompass-

ing cloud infrastructure is largely unknown. This in turn motivate the second research problem in this dissertation: Analysing energy efficiency of cloud-based communication networks by using non-cooperative game theory.

We also used the general system model in Chapter 3 to investigate the performance tradeoff over energy consumption, server load balance and transport network delay for a cloud-based communication network in Chapter 5. In stead of optimising a global objective function as specified in Chapter 4, we introduced end user cost functions including multiple optimisation objectives, i.e. energy consumption, server load balance and transport network delay. The network resource allocation is asymmetric such that some network devices are shared by end users but some are exclusively occupied by a single end user. This also reduces the incentive for end users to cooperate in a way to achieve the global optimum.

Compared to the optimisation frame work with conflicting objectives described in Chapter 4, we also considered rational behaviour of individual network users, who are competing over limited network resources to minimise individual cost. Traditional optimisation techniques such as those specified in Section 1.2.1 are generally incapable of handling this scenario. In this dissertation, we provided a distributed solution to this optimisation problem by applying the non-cooperative game theory discussed in Section 1.2.2, which is more suitable to tackle large network optimisation in the real world from our point of view.

The simulation results in Chapter 5 showed that the power consumption of the proposed game solution is close to the global solution with equal preference to multiple optimisation objectives discussed above. Given sufficient network capacity, individual energy optimisation objectives are aligned with the global optimisation objective due to the linear characteristic of power consumption for individual network equipment. We demonstrated that the centralised approach adopted by GreenTouch^{TM} to address energy efficiency of communications networks is a valid option for proper planed and provisioned networks. Energy consumption of cloud-based communication networks is dominated by the idle power of data centres. Improving energy-proportional processing for network resources such as data entres can significantly improve the energy efficiency

of the whole system.

We also showed that the Nash equilibrium (NE) of the proposed game displayed a rich diversity of outcomes depending upon their local behaviour for different user preference and network conditions. Unequally weighted non-linear user specific objectives and asymmetric network resource allocation cast profound impacts on network resource utilisation and traffic routing for the game solution. The game solution with inadequate capacity provisioning and fail over for a few links could resulting significant system performance degradation such as system power consumption and traffic load balance.

In order to improve the system performance for multiple objectives, network operators need to understand the optimisation objectives of individual network users. It is unlikly "selfish" end customers will cooperate to achieve the global optimum without proper incentives. Without the central information, end customers are unable to align their individual interests to the global optimisation objective. To mitigate the so called Price of Anarchy (PoA), network operators need to plan, design and operate communication networks in a way that all users are motivated to adopt global optimal traffic distribution strategies rather than individual optimal traffic distribution strategies, which could lead to suboptimal solutions for the whole system.

7.1.3 Power consumption minimisation for optical core networks by using SDN

With the rapid growth of real-time multimedia traffic and the proliferation of cloud service, the power consumption of the core network will soon exceed the sum of the power consumed by the access network and the metro network. Technology advances improving energy efficiency of core networks generally require dynamic network configuration, network-wide coordination, fast traffic adaptation, optical-IP cross layer optimisation, rapid connection establishment and agile traffic control. However current core network configuration and operation are rather static and lack of agility. These limitations gave rise the third research problem in this dissertation: Power consumption minimisation for optical core networks by using SDN.

We developed a general SDN based core network model on Mininet platform hosted

in a Linux virtual machine, which encompassing a centralised POX controller. To demonstrate the agility and flexibility of the model, we implemented a multi-objective optimisation scheme considering energy efficiency, server load balance and user defined traffic delay QoS. By leveraging the SDN architecture, we showed that network functions such as statistical switching, multi-path routing and QoS-energy-aware traffic distribution can be customised and implemented in a systematic manner.

The simulation results for the system power consumption showed different "jumps" in terms of power consumption regarding different weights. The sudden changes are due to different "bottlenecks" of the network topology with different configurations on system power consumption and server load balance. The variation of system power consumption over a diurnal cycle is different for the same network with different weights. With high service performance requirements such as server load balance, small changes of input traffic could cause significant system power consumption variations. In contrast, the system power consumption may experience small changes over a diurnal cycle for a low level of service performance requirements.

User specific QoS requirements have significant impacts not only on network latency but also on system power consumption and server load balance. The challenge for the network operator is to learn not only the dynamic range and the pattern of the traffic to be handled but also the associated user specific QoS requirements. Unintended customer service level agreement (SLA) could result in significant system power consumption and server load balance performance degradation. Users with "aggressive" performance objectives may only improve their own application performance at the cost of degrading the system performance and rendering other users' performance much worse-off.

The Mininet simulation results showed challenges for energy efficient network plan, design and operation. Network planning needs to consider all network elements rather than elements with high power consumption only. The proposed SDN-based framework enables individual traffic QoS manipulation in an end-to-end manner, which entitles end customers more control on their data traffic. However, unregulated user defined QoS requirements could have significant negative impacts on the system performance such as system power consumption and server load balance. Also the QoS of other user's

traffic could be degraded due to the "aggressive" nature of QoS requirements from a clique of end users. Network operators need to balance the tradeoff of providing customised traffic control and managing system performance such as power consumption. It is necessary for network operators to choose judicious QoS rules for end users such that potential impacts on system performance are foreseeable and controllable.

7.2 Future Research Directions

Improving energy efficiency of communication networks are becoming increasingly important to sustain the growth of global IP traffic. The associated research covers a wide range of topics and is gaining attraction from the communication network community. The research presented in this dissertation can be extended in several directions. In this section, we endeavour to provide insight into open issues and future research directions.

In Chapter 4, we proposed a distributed algorithm to improve the energy efficiency of heterogeneous backhaul networks by optimising traffic distribution over allocated backhaul routes. A natural extension of this work could consider an end-to-end analysis of mobile networks where radio access networks (RANs) are taken into account. The algorithm described in this chapter requires communication between S-GWs, MUXs and eNodeBs to support updates for traffic distribution variables and Lagrangian multipliers. It would be worth investigating the impacts of asynchronous information exchange between those nodes on the system performance in terms of total power consumption and server load balance. In addition, this work can be extended by applying advanced gradient methods to improve the convergence. This in turn creates new research opportunities on stability and convergence performance analyses for advanced gradient methods. In Chapter 4, we assumed ideal utilisation ratio of each network equipment is given, which is derived from the global optimal solution. A sensitivity analysis could be performed to test the robustness of the proposed algorithm with non-ideal network equipment utilisation ratios. This analysis could provide network operators important information on network equipment deployment and capacity provisioning.

In Chapter 5, a non-cooperative game theoretical analysis was conducted to anal-

yse the impacts of rational behaviour of end users on energy efficiency of cloud-based communication networks. We demonstrated the performance gap between the proposed game solution and the global optimal solution in terms of data entre load balance, transport network delay and system power consumption. In order to close the gap, one possible option would be mechanism design, by which a network operator as a "principle" constructing a game to influence end users to act the way to achieve global optimum. Network operators could use different prices as signals to implicitly prevent end users from adopting selfish strategies, which result in system performance degradation . For example, if an end user's decision is against the global optimal solution, network operator could charge more from that user for using network resources in an global inefficient way. Another option would be applying the learning game theory such that all end users can learn the game over time by observing the outcome of each round of interaction. End users could use history of the game to form expectations and beliefs about other users such that they can make agreement to achieve the global optimum.

In Chapter 6, we showed that complex traffic engineering for core networks can be achieved with the help of OpenFlow protocol. Traditional traffic congestion avoidance mechanisms such as Random Early Detection (RED) and TCP congestion window are in general reactive. Only when congestion occurs at intermediate routers or switches, responses such as dropping packets or reducing sliding window will be taken. This framework can be extended to support proactive congestion avoidance. With the global network traffic information, edge nodes could decide to drop packets or distribute packets over the calculated routes by energising required network elements. Then traffic congestion could be effectively avoided in intermediate nodes, which would otherwise require complex congestion avoidance intelligence implemented in intermediate nodes.

Chapter 8

Appendix

Route index	Sources	Route	Destination
1	$E1$	$M1 \rightarrow M2 \rightarrow M3 \rightarrow M4$	$S1$
2	$E1$	$M1 \rightarrow M6 \rightarrow M7 \rightarrow M4$	$S1$
3	$E1$	$M1 \rightarrow M2 \rightarrow M3 \rightarrow M5 \rightarrow M4$	$S1$
4	$E1$	$M1 \rightarrow M2 \rightarrow M3 \rightarrow M7 \rightarrow M4$	$S1$
5	$E1$	$M1 \rightarrow M2 \rightarrow M6 \rightarrow M7 \rightarrow M4$	$S1$
6	$E1$	$M1 \rightarrow M6 \rightarrow M2 \rightarrow M3 \rightarrow M4$	$S1$
7	$E1$	$M1 \rightarrow M6 \rightarrow M3 \rightarrow M8$	$S2$
8	$E1$	$M1 \rightarrow M2 \rightarrow M3 \rightarrow M5 \rightarrow M8$	$S2$
9	$E1$	$M1 \rightarrow M6 \rightarrow M9 \rightarrow M10 \rightarrow M8$	$S2$
10	$E1$	$M1 \rightarrow M2 \rightarrow M3 \rightarrow M7 \rightarrow M8$	$S2$
11	$E1$	$M1 \rightarrow M6 \rightarrow M9 \rightarrow M7 \rightarrow M8$	$S2$
12	$E1$	$M1 \rightarrow M6 \rightarrow M11$	$S3$
13	$E1$	$M1 \rightarrow M6 \rightarrow M9 \rightarrow M11$	$S3$
14	$E1$	$M1 \rightarrow M2 \rightarrow M6 \rightarrow M11$	$S3$
15	$E1$	$M1 \rightarrow M6 \rightarrow M9 \rightarrow M12 \rightarrow M11$	$S3$
16	$E1$	$M1 \rightarrow M2 \rightarrow M6 \rightarrow M9 \rightarrow M11$	$S3$
17	$E1$	$M1 \rightarrow M6 \rightarrow M9 \rightarrow M10 \rightarrow M14$	$S4$
18	$E1$	$M1 \rightarrow M6 \rightarrow M7 \rightarrow M8 \rightarrow M10 \rightarrow M14$	$S4$
19	$E1$	$M1 \rightarrow M6 \rightarrow M11 \rightarrow M12 \rightarrow M13 \rightarrow M14$	$S4$
20	$E1$	$M1 \rightarrow M2 \rightarrow M3 \rightarrow M5 \rightarrow M8 \rightarrow M10 \rightarrow M14$	$S4$
21	$E1$	$M1 \rightarrow M2 \rightarrow M6 \rightarrow M7 \rightarrow M8 \rightarrow M10 \rightarrow M14$	$S4$

22	$E1$	$M1 \rightarrow M2 \rightarrow M3 \rightarrow M7 \rightarrow M8 \rightarrow M10 \rightarrow M14$	$S4$
23	$E2$	$M5 \rightarrow M4$	$S1$
24	$E2$	$M5 \rightarrow M3 \rightarrow M4$	$S1$
25	$E2$	$M5 \rightarrow M8 \rightarrow M7 \rightarrow M4$	$S1$
26	$E2$	$M5 \rightarrow M3 \rightarrow M7 \rightarrow M4$	$S1$
27	$E2$	$M5 \rightarrow M8$	$S2$
28	$E2$	$M5 \rightarrow M4 \rightarrow M7 \rightarrow M8$	$S2$
29	$E2$	$M5 \rightarrow M3 \rightarrow M7 \rightarrow M8$	$S2$
30	$E2$	$M5 \rightarrow M8 \rightarrow M10 \rightarrow M14$	$S4$
31	$E2$	$M5 \rightarrow M8 \rightarrow M10 \rightarrow M13 \rightarrow M14$	$S4$
32	$E2$	$M5 \rightarrow M3 \rightarrow M7 \rightarrow M8 \rightarrow M10 \rightarrow M14$	$S4$
33	$E2$	$M5 \rightarrow M4 \rightarrow M7 \rightarrow M9 \rightarrow M10 \rightarrow M14$	$S4$
34	$E2$	$M5 \rightarrow M4 \rightarrow M7 \rightarrow M9 \rightarrow M12 \rightarrow M13 \rightarrow M14$	$S4$
35	$E3$	$M9 \rightarrow M7 \rightarrow M4$	$S1$
36	$E3$	$M9 \rightarrow M7 \rightarrow M3 \rightarrow M4$	$S1$
37	$E3$	$M9 \rightarrow M7 \rightarrow M8$	$S2$
38	$E3$	$M9 \rightarrow M10 \rightarrow M8$	$S2$
39	$E3$	$M9 \rightarrow M11$	$S3$
40	$E3$	$M9 \rightarrow M12 \rightarrow M11$	$S3$
41	$E3$	$M9 \rightarrow M6 \rightarrow M11$	$S3$
42	$E3$	$M9 \rightarrow M10 \rightarrow M11$	$S4$
43	$E3$	$M9 \rightarrow M12 \rightarrow M13 \rightarrow M14$	$S4$
44	$E3$	$M9 \rightarrow M10 \rightarrow M13 \rightarrow M14$	$S4$
45	$E4$	$M13 \rightarrow M10 \rightarrow M8$	$S2$
46	$E4$	$M13 \rightarrow M12 \rightarrow M11$	$S3$
47	$E4$	$M13 \rightarrow M12 \rightarrow M9 \rightarrow M11$	$S3$
48	$E4$	$M13 \rightarrow M10 \rightarrow M9 \rightarrow M11$	$S3$
49	$E4$	$M13 \rightarrow M14$	$S4$
50	$E4$	$M13 \rightarrow M10 \rightarrow M14$	$S4$

Table 8.1: Routing table for asymmetric data enctre allocation

Route index	Sources	Route	Destination
51	$E2$	$M5 \rightarrow M3 \rightarrow M2 \rightarrow M6 \rightarrow M11$	$S3$
52	$E2$	$M5 \rightarrow M4 \rightarrow M7 \rightarrow M9 \rightarrow M11$	$S3$
53	$E2$	$M5 \rightarrow M8 \rightarrow M10 \rightarrow M13 \rightarrow M12 \rightarrow M11$	$S3$
54	$E2$	$M13 \rightarrow M10 \rightarrow M8 \rightarrow M5 \rightarrow M4$	$S1$
55	$E2$	$M13 \rightarrow M10 \rightarrow M9 \rightarrow M7 \rightarrow M4$	$S1$
56	$E2$	$M13 \rightarrow M12 \rightarrow M9 \rightarrow M7 \rightarrow M4$	$S1$

Table 8.2: Extra routing table for symmetric data enctre allocation

Bibliography

[1] "The zettabyte era – trends and analysis," White Paper, Cisco, June 2014.

[2] "Cisco visual networking index: Forecast and methodology, 2013-2018," White Paper, Cisco, May 2013.

[3] "GreenTouch green meter research study: Reducing the net energy consumption in communications networks by up to 90% by 2020," White Paper, GreenTouch, January 2013.

[4] "Cisco visual networking index: Global mobile data traffic forecast update, 2013-2018," White Paper, Cisco, February 2014.

[5] K. David, D. Dixit, and N. Jefferies, "2020 vision," *Vehicular Technology Magazine, IEEE*, vol. 5, no. 3, pp. 22 –29, September 2010.

[6] "Machine-to-machine communications: Connecting billions of devices," *OECD Digital Economy Papers*, no. 192, Jan. 2012. [Online]. Available: http://dx.doi.org/10.1787/5k9gsh2gp043-en

[7] L. Atzori, A. Iera, and G. Morabito, "The internet of things: A survey," *Comput. Netw.*, vol. 54, no. 15, pp. 2787–2805, October 2010. [Online]. Available: http://dx.doi.org/10.1016/j.comnet.2010.05.010

[8] "Gartner says the internet of things installed base will grow to 26 billion units by 2020," Gartner, December 2013. [Online]. Available: http://www.gartner.com/newsroom/id/2636073

[9] J. Baker, M. Mitchell, and F. Dalke, *The Power of IP Video: Unleashing Productivity with Visual Networking*, ser. Network business series. Cisco Press, 2009. [Online]. Available: https://books.google.com.au/books?id=6erGmAEACAAJ

[10] J. Wortham, "Customers angered as iphones overload AT&T," *The New York Times*, September 2009.

[11] J. Baliga, R. Ayre, K. Hinton, and R. Tucker, "Energy consumption in wired and wireless access networks," *Communications Magazine, IEEE*, vol. 49, no. 6, pp. 70 –77, June 2011.

[12] Z. Hasan, H. Boostanimehr, and V. Bhargava, "Green cellular networks: A survey, some research issues and challenges," *Communications Surveys Tutorials, IEEE*, vol. 13, no. 4, pp. 524 –540, November 2011.

[13] "Energy aware radio and network technologies (EARTH)." [Online]. Available: https://www.ict-earth.eu/

[14] J. Malmodin, A. Moberg, D. Lunden, G. Finnveden, and N. Lovehagen, "Greenhouse gas emissions and operational electricity use in the ICT and entertainment & media sectors," *Journal of Industrial Ecology*, vol. 14, no. 5, pp. 770 –790, October 2010.

[15] E. Ariwa, *Green Technology Applications for Enterprise and Academic Innovation*, ser. Advances in Environmental Engineering and Green Technologies:. IGI Global, February 2014. [Online]. Available: https://books.google.com.au/books?id=cwKXBQAAQBAJ

[16] S. Aleksic, "Analysis of power consumption in future high-capacity network nodes," *Optical Communications and Networking, IEEE/OSA Journal of*, vol. 1, no. 3, pp. 245–258, August 2009.

[17] D. Kilper, G. Atkinson, S. Korotky, S. Goyal, P. Vetter, D. Suvakovic, and O. Blume, "Power trends in communication networks," *Selected Topics in Quantum Electronics, IEEE Journal of*, vol. 17, no. 2, pp. 275–284, March 2011.

[18] GeSI, "Gesi smarter 2020: The role of ICT in driving a sustainable future," Global e-Sustainability Initiative aisbl and The Boston Consulting Group, December 2012.

[19] D. Feng, C. Jiang, G. Lim, L. Cimini, Jr., G. Feng, and G. Li, "A survey of energy-efficient wireless communications," *Communications Surveys Tutorials, IEEE*, vol. PP, no. 99, pp. 1 –12, February 2012.

[20] O. Tipmongkolsilp, S. Zaghloul, and A. Jukan, "The evolution of cellular backhaul technologies: Current issues and future trends," *Communications Surveys Tutorials, IEEE*, vol. 13, no. 1, pp. 97 –113, February 2011.

[21] G. Shen and R. Tucker, "Energy-minimized design for ip over wdm networks," *Optical Communications and Networking, IEEE/OSA Journal of*, vol. 1, no. 1, pp. 176–186, June 2009.

[22] X. Dong, T. El-Gorashi, and J. Elmirghani, "Green IP over WDM networks with data centers," *Lightwave Technology, Journal of*, vol. 29, no. 12, pp. 1861–1880, June 2011.

[23] A. Ephremides and S. Verdu, "Control and optimization methods in communication network problems," *Automatic Control, IEEE Transactions on*, vol. 34, no. 9, pp. 930–942, September 1989.

[24] A. Kelly, F.P. Maulloo and D. Tan, "Rate control for communication networks: shadow prices, proportional fairness and stability," *Journal of Operations Research Society*, vol. 49, no. 3, pp. 237–252, March 1998.

[25] X.-H. Jia, D.-Z. Du, X.-D. Hu, M.-K. Lee, and J. Gu, "Optimization of wavelength assignment for qos multicast in wdm networks," *Communications, IEEE Transactions on*, vol. 49, no. 2, pp. 341–350, February 2001.

[26] L. Xiao, M. Johansson, H. Hindi, S. Boyd, and A. Goldsmith, "Joint optimization of communication rates and linear systems," *Automatic Control, IEEE Transactions on*, vol. 48, no. 1, pp. 148–153, January 2003.

[27] C. A. Oliveira and P. M. Pardalos, "A survey of combinatorial optimization problems in multicast routing," *Computers & Operations Research*, vol. 32, no. 8, pp. 1953–1981, August 2005.

[28] X. Lin, N. Shroff, and R. Srikant, "A tutorial on cross-layer optimization in wireless networks," *Selected Areas in Communications, IEEE Journal on*, vol. 24, no. 8, pp. 1452–1463, August 2006.

[29] W. C. Cheung, T. Quek, and M. Kountouris, "Throughput optimization, spectrum allocation, and access control in two-tier femtocell networks," *Selected Areas in Communications, IEEE Journal on*, vol. 30, no. 3, pp. 561–574, April 2012.

[30] A. Bley, M. Grötschel, and R. Wessäly, "Design of broadband virtual private networks: Model and heuristics for the B-WiN," in *Robust communication networks: Interconnection and survivability, volume 53 of DIMACS Series in Discrete Mathematics and Theoretical Computer Science*. American Mathematical Society, 1998, pp. 1–16.

[31] A. Bley and T. Koch, *Integer programming approaches to access and backbone IP network planning*. Springer, 2008.

[32] M. X. Cheng, Y. Li, and D.-Z. Du, *Combinatorial optimization in communication networks*. Springer Science & Business Media, 2006, vol. 18.

[33] L. Lobjois and M. Lemaitre, "Branch and bound algorithm selection by performance prediction," in *In AAAI*. Citeseer, 1998.

[34] S. Boyd and L. Vandenberghe, *Convex Optimization*. Cambridge, UK: Cambridge University Press, March 2004.

[35] Z.-Q. Luo and W. Yu, "An introduction to convex optimization for communications and signal processing," *Selected Areas in Communications, IEEE Journal on*, vol. 24, no. 8, pp. 1426–1438, August 2006.

[36] S. Cui, R. Madan, A. J. Goldsmith, and S. Lall, "Cross-layer energy and delay optimization in small-scale sensor networks," *Wireless Communications, IEEE Transactions on*, vol. 6, no. 10, pp. 3688–3699, October 2007.

[37] S. Maleki, A. Pandharipande, and G. Leus, "Energy-efficient distributed spectrum sensing for cognitive sensor networks," *Sensors Journal, IEEE*, vol. 11, no. 3, pp. 565–573, January 2011.

[38] S. Wang, Y. Wang, J. Coon, and A. Doufexi, "Energy-efficient spectrum sensing and access for cognitive radio networks," *Vehicular Technology, IEEE Transactions on*, vol. 61, no. 2, pp. 906–912, February 2012.

[39] D. Palomar and M. Chiang, "A tutorial on decomposition methods for network utility maximization," *Selected Areas in Communications, IEEE Journal on*, vol. 24, no. 8, pp. 1439 –1451, August 2006.

[40] S. Low and D. Lapsley, "Optimization flow control. I. basic algorithm and convergence," *Networking, IEEE/ACM Transactions on*, vol. 7, no. 6, pp. 861 –874, December 1999.

[41] D. P. Bertsekas, *Nonlinear Programming*. Belmont, MA: Athena Scientific, September 1999.

[42] X. Dong, T. El-Gorashi, and J. Elmirghani, "On the energy efficiency of physical topology design for IP over WDM networks," *Lightwave Technology, Journal of*, vol. 30, no. 12, pp. 1931–1942, June 2012.

[43] R. T. Marler and J. S. Arora, "Survey of multi-objective optimization methods for engineering," *Structural and multidisciplinary optimization*, vol. 26, no. 6, pp. 369–395, April 2004.

[44] D. Fudenberg and J. Tirole, *Game Theory*. The MIT Press, August 1991.

[45] J. Von Neumann and O. Morgenstern, *Theory of games and economic behavior*, ser. Science: Economics. Princeton University Press, 1944.

[46] J. F. Nash *et al.*, "Equilibrium points in n-person games," in *Proceedings of the national academy of sciences*, vol. 36, no. 1, January 1950, pp. 48–49.

[47] J. F. Nash Jr, "The bargaining problem," *Econometrica: Journal of the Econometric Society*, pp. 155–162, April 1950.

[48] J. Nash, "Non-cooperative games," *Annals of mathematics*, pp. 286–295, September 1951.

[49] M. Osborne and A. Rubinstein, *A Course in Game Theory*. MIT Press, July 1994. [Online]. Available: http://books.google.com.au/books?id=5ntdaYX4LPkC

[50] T. Basar and G. Olsder, *Dynamic Noncooperative Game Theory, 2nd Edition*. Society for Industrial and Applied Mathematics, January 1998.

[51] K. Ritzberger, *Foundations of Non-cooperative Game Theory*. Oxford University Press, April 2002.

[52] Z. Han, *Game Theory in Wireless and Communication Networks: Theory, Models, and Applications*, ser. Cambridge books online. Cambridge University Press, January 2012.

[53] N. Nisan, T. Roughgarden, E. Tardos, and V. V. Vazirani, *Algorithmic game theory*. Cambridge University Press Cambridge, September 2007, vol. 1.

[54] J. Watson, *Strategy: An Introduction to Game Theory (Third Edition)*. W. W. Norton, May 2013. [Online]. Available: http://books.google.com.au/books?id=BK7nLwEACAAJ

[55] E. Stein, *Without Good Reason: The Rationality Debate in Philosophy and Cognitive Science*, ser. Clarendon library of logic and philosophy. Clarendon Press, January 1996. [Online]. Available: http://books.google.com.au/books?id=_3CymAEACAAJ

[56] J. Nash, "Two-person cooperative games," *Econometrica: Journal of the Econometric Society*, pp. 128–140, January 1953.

[57] E. Altman, T. Boulogne, R. El-Azouzi, T. Jiménez, and L. Wynter, "A survey on networking games in telecommunications," *Computers & Operations Research*, vol. 33, no. 2, pp. 286–311, February 2006.

[58] S. Kakutani, "A generalization of brouwers fixed point theorem," *Duke Mathematical Journal*, vol. 8, no. 3, pp. 457 – 459, 1941.

[59] P. J. Reny, "Non-cooperative games: Equilibrium existence," *The New Palgrave Dictionary of Economics*,, August 2005.

[60] P. Dubey, "Inefficiency of nash equilibria," *Mathematics of Operations Research*, vol. 11, no. 1, pp. 1–8, Feburary 1986.

[61] E. Koutsoupias and C. Papadimitriou, "Worst-case equilibria," in *Proceedings of The 16Th Annual Symposium on Theoretical Aspects of Computer Science*, May 1999, pp. 404–413.

[62] Á. L. Valdivieso Caraguay, A. Benito Peral, L. I. Barona López, and L. J. García Villalba, "SDN: Evolution and opportunities in the development IoT applications," *International Journal of Distributed Sensor Networks*, vol. 2014, May 2014.

[63] N. Feamster, J. Rexford, and E. Zegura, "The road to SDN," *Queue*, vol. 11, no. 12, p. 20, December 2013.

[64] H. J. Chao and B. Liu, *High performance switches and routers*. John Wiley & Sons, April 2007.

[65] A. Bletsas, "Physical limitations on the expansion of internet," MIT Media Lab, Tech. Rep., December 1999. [Online]. Available: http://web.media.mit.edu/~aggelos/861.html

[66] J. S. Turner and D. E. Taylor, "Diversifying the internet," in *Global Telecommunications Conference, 2005. GLOBECOM'05. IEEE*, vol. 2. St. Louis, Missouri, USA: IEEE, November 2005, pp. 6–pp.

[67] J. Pan, S. Paul, and R. Jain, "A survey of the research on future internet architectures," *Communications Magazine, IEEE*, vol. 49, no. 7, pp. 26–36, July 2011.

[68] T. Zahariadis, D. Papadimitriou, H. Tschofenig, S. Haller, P. Daras, G. D. Stamoulis, and M. Hauswirth, *Towards a future internet architecture*. Springer, January 2011.

[69] S. Shenker *et al.*, "The future of networking, and the past of protocols," October 2011.

[70] J. H. Saltzer, D. P. Reed, and D. D. Clark, "End-to-end arguments in system design," *ACM Transactions on Computer Systems (TOCS)*, vol. 2, no. 4, pp. 277–288, November 1984.

[71] ONF, "Software-defined networking: The new norm for networks," https://www.opennetworking.org/images/stories/downloads/sdn-resources/white-papers/wp-sdn-newnorm.pdf, Open Networking Foundation, April 2012.

[72] N. Handigol, M. Flajslik, and S. Seetharaman, "Aster* x: Load-balancing as a network primitive," in *Proceedings of the 9th GENI Engineering Conference (Plenary)*, 2010, pp. 1–2.

[73] S. Sharma, D. Staessens, D. Colle, D. Palma, J. Goncalves, R. Figueiredo, D. Morris, M. Pickavet, and P. Demeester, "Implementing quality of service for the software defined networking enabled future internet," in *Software Defined Networks (EWSDN), 2014 Third European Workshop on*, Budapest, Hungary, September 2014, pp. 49–54.

[74] J. Schulz-Zander, L. Suresh, N. Sarrar, A. Feldmann, T. Hühn, and R. Merz, "Programmatic orchestration of wifi networks," in *Proceedings of the 2014 USENIX conference on USENIX Annual Technical Conference*. Philadelphia, PA, USA: USENIX Association, June 2014, pp. 347–358.

[75] D. Kreutz, F. Ramos, P. Esteves Verissimo, C. Esteve Rothenberg, S. Azodolmolky, and S. Uhlig, "Software-defined networking: A comprehensive survey," *Proceedings of the IEEE*, vol. 103, no. 1, pp. 14–76, January 2015.

[76] "Open networking foundation," https://www.opennetworking.org/, ONF, 2014.

[77] N. McKeown, T. Anderson, H. Balakrishnan, G. Parulkar, L. Peterson, J. Rexford, S. Shenker, and J. Turner, "Openflow: enabling innovation in campus networks," *ACM SIGCOMM Computer Communication Review*, vol. 38, no. 2, pp. 69–74, March 2008.

[78] M. Channegowda, R. Nejabati, M. Rashidi Fard, S. Peng, N. Amaya, G. Zervas, D. Simeonidou, R. Vilalta, R. Casellas, R. Martínez *et al.*, "Experimental demonstration of an openflow based software-defined optical network employing packet, fixed and flexible dwdm grid technologies on an international multi-domain testbed," *Optics express*, vol. 21, no. 5, pp. 5487–5498, March 2013.

[79] M. Channegowda, R. Nejabati, and D. Simeonidou, "Software-defined optical networks technology and infrastructure: Enabling software-defined optical network operations [invited]," *Optical Communications and Networking, IEEE/OSA Journal of*, vol. 5, no. 10, pp. A274–A282, October 2013.

[80] ONF, "Openflow switch specification, version 1.4.0," https://www.opennetworking.org/images/stories/downloads/sdn-resources/onf-specifications/openflow/openflow-spec-v1.4.0.pdf, Oct 2014.

[81] B. Lantz, B. Heller, and N. McKeown, "A network in a laptop: rapid prototyping for software-defined networks," in *Proceedings of the 9th ACM SIGCOMM Workshop on Hot Topics in Networks*. Monterey, CA, USA: ACM, October 2010, p. 19.

[82] N. Handigol, B. Heller, V. Jeyakumar, B. Lantz, and N. McKeown, "Reproducible network experiments using container-based emulation," in *Proceedings of the 8th international conference on Emerging networking experiments and technologies*. Nice, France: ACM, December 2012, pp. 253–264.

[83] J. Salina and P. Salina, *Next Generation Networks: Perspectives and Potentials*. Wiley, January 2008. [Online]. Available: https://books.google.com.au/books?id=T1zFNAEACAAJ

[84] F. Mattern, T. Staake, and M. Weiss, "ICT for green: how computers can help us to conserve energy," in *Proceedings of the 1st international conference on energy-efficient computing and networking*. Passau, Germany: ACM, April 2010, pp. 1–10.

[85] B. Aebischer and L. M. Hilty, "The energy demand of ict: a historical perspective and current methodological challenges," in *ICT Innovations for Sustainability*. Springer, August 2015, pp. 71–103.

[86] S. Lambert, W. Van Heddeghem, W. Vereecken, B. Lannoo, D. Colle, and M. Pickavet, "Worldwide electricity consumption of communication networks," *Optics express*, vol. 20, no. 26, pp. B513–B524, December 2012.

[87] T. Kelly and S. Head, "ICTs and climate change," *ITU-T Technology, Tech. Rep*, 2007.

[88] J. G. Koomey *et al.*, "Estimating total power consumption by servers in the US and the world," February 2007.

[89] R. Tucker, R. Parthiban, J. Baliga, K. Hinton, R. Ayre, and W. Sorin, "Evolution of wdm optical ip networks: A cost and energy perspective," *Lightwave Technology, Journal of*, vol. 27, no. 3, pp. 243–252, February 2009.

[90] P. Monti, S. Tombaz, L. Wosinska, and J. Zander, "Mobile backhaul in heterogeneous network deployments: Technology options and power consumption," in *Transparent Optical Networks (ICTON), 2012 14th International Conference on*, Coventry, England, July 2012, pp. 1 –7.

[91] "Mobile backhaul - The power behind LTE," http://networks.nokia.com/sites/default/files/mobilebackhaul_executive_summary.pdf, Nokia Siemens Networks, 2009.

[92] T. Nakamura, "3GPP radio access networks LTE-Advanced status," 3GPP, Tech. Rep., September 2011.

[93] "Easy small cell backhaul an analysis of small backhaul requirement and comparision of solutions," http://www.academia.edu/4402938/Easy_Small_Cell_Backhaul_v0_9_5, Cambridge Broadband Networks, White Paper, February 2012.

[94] CERAGON, "Wireless backhaul solutions for small cells," Application Note.

[95] G. Li, Z. Xu, C. Xiong, C. Yang, S. Zhang, Y. Chen, and S. Xu, "Energy-efficient wireless communications: tutorial, survey, and open issues," *Wireless Communications, IEEE*, vol. 18, no. 6, pp. 28 –35, December 2011.

[96] G. Auer, V. Giannini, C. Desset, I. Godor, P. Skillermark, M. Olsson, M. Imran, D. Sabella, M. Gonzalez, O. Blume, and A. Fehske, "How much energy is needed

to run a wireless network?" *Wireless Communications, IEEE*, vol. 18, no. 5, pp. 40–49, October 2011.

[97] J. Segel and M. Weldon, "Lightradio portfolio: White paper 1," http://www.siliconrepublic.com/download/fs/doc/reports/lightradio-1-tech-overview.pdf, Alcatel-Lucent, 2011.

[98] S. Sesia, I. Toufik, and M. Baker, *LTE–The UMTS Long Term Evolution: From Theory to Practice*. John Wiley and Sons, February 2009.

[99] D. Grosu and A. Chronopoulos, "Noncooperative load balancing in distributed systems," *Journal of Parallel and Distributed Computing*, vol. 65, no. 9, pp. 1022 –1034, September 2005.

[100] R. Subrata, A. Zomaya, and B. Landfeldt, "Game-theoretic approach for load balancing in computational grids," *Parallel and Distributed Systems, IEEE Transactions on*, vol. 19, no. 1, pp. 66 –76, January 2008.

[101] Y. Liu, F. Lo Presti, V. Misra, D. Towsley, and Y. Gu, "Fluid models and solutions for large-scale ip networks," in *Proceedings of the 2003 ACM SIGMETRICS International Conference on Measurement and Modeling of Computer Systems*, ser. SIGMETRICS '03. San Diego, CA, USA: ACM, June 2003, pp. 91–101. [Online]. Available: http://doi.acm.org/10.1145/781027.781039

[102] F. Kelly and R. Williams, "Fluid model for a network operating under a fair bandwidth-sharing policy," *Annals of Applied Probability*, pp. 1055–1083, February 2004.

[103] A. Orda, R. Rom, and N. Shimkin, "Competitive routing in multiuser communication networks," *IEEE/ACM Transactions on Networking (ToN)*, vol. 1, no. 5, pp. 510–521, October 1993.

[104] T. Alpcan, T. Başar, R. Srikant, and E. Altman, "CDMA uplink power control as a noncooperative game," *Wireless Networks*, vol. 8, no. 6, pp. 659–670, November 2002.

[105] C. Saraydar, N. B. Mandayam, and D. Goodman, "Pricing and power control in a multicell wireless data network," *Selected Areas in Communications, IEEE Journal on*, vol. 19, no. 10, pp. 1883–1892, October 2001.

[106] C. Papadimitriou, "Algorithms, games, and the internet," in *Proceedings of the Thirty-third Annual ACM Symposium on Theory of Computing*, ser. STOC '01. Heraklion, Crete, Greece: ACM, July 2001, pp. 749–753.

[107] T. Roughgarden and E. Tardos, "How bad is selfish routing?" *J. ACM*, vol. 49, no. 2, pp. 236–259, March 2002.

[108] T. Roughgarden, "The price of anarchy is independent of the network topology," *Journal of Computer and System Sciences*, vol. 67, no. 2, pp. 341–364, 2003.

[109] G. Christodoulou and E. Koutsoupias, "The price of anarchy of finite congestion games," in *Proceedings of the Thirty-seventh Annual ACM Symposium on Theory of Computing*, ser. STOC '05. Hunt Valley, MD, USA: ACM, May 2005, pp. 67–73.

[110] B. Awerbuch, Y. Azar, and A. Epstein, "The price of routing unsplittable flow," in *Proceedings of the thirty-seventh annual ACM symposium on Theory of computing*. Hunt Valley, MD, USA: ACM, May 2005, pp. 57–66.

[111] M. Armbrust, A. Fox, R. Griffith, A. D. Joseph, R. H. Katz, A. Konwinski, G. Lee, D. A. Patterson, A. Rabkin, and M. Zaharia, "Above the clouds: A berkeley view of cloud computing," University of California at Berkeley, Tech. Rep., 2009.

[112] S. Srikantaiah, A. Kansal, and F. Zhao, "Energy aware consolidation for cloud computing," in *Proceedings of the 2008 Conference on Power Aware Computing and Systems*, ser. HotPower'08. Berkeley, CA, USA: USENIX Association, December 2008, pp. 10–10.

[113] J. Baliga, R. Ayre, K. Hinton, and R. Tucker, "Green cloud computing: Balancing energy in processing, storage, and transport," *Proceedings of the IEEE*, vol. 99, no. 1, pp. 149–167, January 2011.

[114] Y. C. Lee and A. Y. Zomaya, "Energy efficient utilization of resources in cloud computing systems," *The Journal of Supercomputing*, vol. 60, no. 2, pp. 268–280, May 2012.

[115] A. Beloglazov, J. Abawajy, and R. Buyya, "Energy-aware resource allocation heuristics for efficient management of data centers for cloud computing," *Future generation computer systems*, vol. 28, no. 5, pp. 755–768, May 2012.

[116] A. Saleh and J. M. Simmons, "Evolution toward the next-generation core optical network," *Lightwave Technology, Journal of*, vol. 24, no. 9, pp. 3303–3321, September 2006.

[117] ——, "All-optical networking-evolution, benefits, challenges, and future vision," *Proceedings of the IEEE*, vol. 100, no. 5, pp. 1105–1117, May 2012.

[118] E. Le Rouzic, E. Bonetto, L. Chiaraviglio, F. Giroire, F. Idzikowski, F. Jimenez, C. Lange, J. Montalvo, F. Musumeci, I. Tahiri, A. Valenti, W. Van Heddeghem, Y. Ye, A. Bianco, and A. Pattavina, "Trend towards more energy-efficient optical networks," in *Optical Network Design and Modeling (ONDM), 2013 17th International Conference on*, April 2013, pp. 211–216.

[119] A. Lawey, T. El-Gorashi, and J. Elmirghani, "Distributed energy efficient clouds over core networks," *Lightwave Technology, Journal of*, vol. 32, no. 7, pp. 1261–1281, April 2014.

[120] VERDANTIX, "Cloud computing – The IT solution for the 21st century," White Paper, CDP, June 2011.

[121] M. P. Mills, "The cloud begins with coal: Big data, big networks, big infrastructure and big power," White Paper, Digital Power Group, August 2013.

[122] "How clean is your cloud?" White Paper, greenpeace.org, April 2012.

[123] Y. Zhang, P. Chowdhury, M. Tornatore, and B. Mukherjee, "Energy efficiency in telecom optical networks," *Communications Surveys Tutorials, IEEE*, vol. 12, no. 4, pp. 441–458, July 2010.

[124] M. Dharmaweera, R. Parthiban, and Y. Sekercioglu, "Toward a power-efficient backbone network: The state of research," *Communications Surveys Tutorials, IEEE*, vol. 17, no. 1, pp. 198–227, March 2014.

[125] J. Baliga, R. Ayre, K. Hinton, W. Sorin, and R. Tucker, "Energy consumption in optical ip networks," *Lightwave Technology, Journal of*, vol. 27, no. 13, pp. 2391–2403, July 2009.

[126] J. Buysse, K. Georgakilas, A. Tzanakaki, M. De Leenheer, B. Dhoedt, and C. Develder, "Energy-efficient resource-provisioning algorithms for optical clouds," *Optical Communications and Networking, IEEE/OSA Journal of*, vol. 5, no. 3, pp. 226–239, March 2013.

[127] J. Wang, Y. Yan, and L. Dittmann, "Design of energy efficient optical networks with software enabled integrated control plane," *Networks, IET*, vol. 4, no. 1, pp. 30–36, December 2014.

[128] B. Heller, S. Seetharaman, P. Mahadevan, Y. Yiakoumis, P. Sharma, S. Banerjee, and N. McKeown, "Elastictree: Saving energy in data center networks," in *Proceedings of the 7th USENIX Conference on Networked Systems Design and Implementation*, ser. NSDI'10. Berkeley, CA, USA: USENIX Association, April 2010, pp. 17–17.

[129] D. Staessens, S. Sharma, D. Colle, M. Pickavet, and P. Demeester, "Software defined networking: Meeting carrier grade requirements," in *Local Metropolitan Area Networks (LANMAN), 2011 18th IEEE Workshop on*, Chapel Hill, NC, USA, October 2011, pp. 1–6.

[130] R. Wang, Z. Jiang, S. Gao, W. Yang, Y. Xia, and M. Zhu, "Energy-aware routing algorithms in software-defined networks," in *A World of Wireless, Mobile and Multimedia Networks (WoWMoM), 2014 IEEE 15th International Symposium on*, Sydney, Australia, June 2014, pp. 1–6.

[131] E. Mannie, "Generalized multi-protocol label switching GMPLS architecture," *Interface*, vol. 501, p. 19, 2004.

[132] S. Das, G. Parulkar, and N. McKeown, "Why openflow/SDN can succeed where GMPLS failed," in *European Conference and Exhibition on Optical Communication*. Amsterdam,Holland: Optical Society of America, September 2012, pp. 1–3.

[133] ——, "Rethinking IP core networks," *Optical Communications and Networking, IEEE/OSA Journal of*, vol. 5, no. 12, pp. 1431–1442, December 2013.

[134] A. Vishwanath, J. Zhu, K. Hinton, R. Ayre, and R. Tucker, "Estimating the energy consumption for packet processing, storage and switching in optical-IP routers," in *Optical Fiber Communication Conference and Exposition and the National Fiber Optic Engineers Conference (OFC/NFOEC), 2013*, Anaheim, CA, USA, March 2013, pp. 1–3.

[135] D. Abts, M. R. Marty, P. M. Wells, P. Klausler, and H. Liu, "Energy proportional datacenter networks," vol. 38, no. 3. New York, NY, USA: ACM, June 2010, pp. 338–347.

[136] Y. Wu, B. Guo, Y. Shen, J. Wang, and X. Liu, "Toward energy-proportional internet core networks: an energy-minimized routing and virtual topology design for internet protocol layer," *International Journal of Communication Systems*, vol. 28, no. 3, pp. 513–533, February 2015.

[137] H. Zimmermann, "Osi reference model–the iso model of architecture for open systems interconnection," *Communications, IEEE Transactions on*, vol. 28, no. 4, pp. 425–432, April 1980.

[138] A. Leon-Garcia and I. Widjaja, *Communication networks*. McGraw-Hill, Inc., July 2003.

[139] I. Vogelsang, "The relationship between mobile and fixed-line communications: A survey," *Information Economics and Policy*, vol. 22, no. 1, pp. 4–17, March 2010.

[140] D. Livengood, J. Lin, C. Vaishnav, T. D. Whitney, J. Moses, and C. Magee, "Public switched telephone networks: A network analysis of emerging networks."

[141] D. Abts and B. Felderman, "A guided tour through data-center networking," *Queue*, vol. 10, no. 5, pp. 10:10–10:23, May 2012.

[142] G. Held, "Internetworking LANs and WANs: Concepts, techniques and methods," June 1993.

[143] R. Sharma, *Network topology optimization: the art and science of network design*, ser. VNR computer library. Van Nostrand Reinhold, 1990. [Online]. Available: http://books.google.com.au/books?id=PeVrAAAAIAAJ

[144] M. Van Steen, *Graph Theory and Complex Networks: An Introduction*. Maarten van Steen, April 2010.

[145] E. W. Dijkstra, "A note on two problems in connexion with graphs," *Numerische mathematik*, vol. 1, no. 1, pp. 269–271, 1959.

[146] R. C. Prim, "Shortest connection networks and some generalizations," *Bell system technical journal*, vol. 36, no. 6, pp. 1389–1401, 1957.

[147] R. Banner and A. Orda, "Multipath routing algorithms for congestion minimization," *Networking, IEEE/ACM Transactions on*, vol. 15, no. 2, pp. 413–424, April 2007.

[148] W. Milliken, T. Mendez, and C. Partridge, "RFC 1546 - host anycasting service," 1993.

[149] J. He and J. Rexford, "Toward internet-wide multipath routing," *Network, IEEE*, vol. 22, no. 2, pp. 16–21, March 2008.

[150] W. Jia, D. Xuan, W. Tu, L. Lin, and W. Zhao, "Distributed admission control for anycast flows," *Parallel and Distributed Systems, IEEE Transactions on*, vol. 15, no. 8, pp. 673–686, August 2004.

[151] A. Adas, "Traffic models in broadband networks," *Communications Magazine, IEEE*, vol. 35, no. 7, pp. 82–89, July 1997.

[152] V. Frost and B. Melamed, "Traffic modeling for telecommunications networks," *Communications Magazine, IEEE*, vol. 32, no. 3, pp. 70–81, March 1994.

[153] A. Erlang, "The theory of probabilities and telephone conversations," *Nyt Tidsskrift for Matematik*, vol. 20, no. B, pp. 33–39, 1909.

[154] J. Kolbusz, S. Paszczynski, and B. Wilamowski, "Network traffic model for industrial environment," *Industrial Informatics, IEEE Transactions on*, vol. 2, no. 4, pp. 213–220, November 2006.

[155] Y. Guo, "On fluid modeling of networks and queues," Ph.D. dissertation, University of Massachusetts Amherst, January 2000.

[156] A. Yan and W.-B. Gong, "Time-driven fluid simulation for high-speed networks," *Information Theory, IEEE Transactions on*, vol. 45, no. 5, pp. 1588–1599, July 1999.

[157] D. Nicol, "Discrete event fluid modeling of TCP," in *Simulation Conference, 2001. Proceedings of the Winter*, vol. 2, Arlington, VA, USA, December 2001, pp. 1291–1299 vol.2.

[158] B. Liu, D. Figueiredo, Y. Guo, J. Kurose, and D. Towsley, "A study of networks simulation efficiency: fluid simulation vs. packet-level simulation," in *INFOCOM 2001. Twentieth Annual Joint Conference of the IEEE Computer and Communications Societies. Proceedings. IEEE*, vol. 3, Anchorage, AK, USA, April 2001, pp. 1244–1253 vol.3.

[159] Y. Gu, Y. Liu, and D. Towsley, "On integrating fluid models with packet simulation," in *INFOCOM 2004. Twenty-third AnnualJoint Conference of the IEEE Computer and Communications Societies*, vol. 4, HongKong, China, March 2004, pp. 2856–2866 vol.4.

[160] J. S. Vandergraft, "A fluid flow model of networks of queues," *Management Science*, vol. 29, no. 10, pp. 1198–1208, October 1983.

[161] V. Misra, W.-B. Gong, and D. Towsley, "Fluid-based analysis of a network of AQM routers supporting TCP flows with an application to RED," in *Proceedings of the Conference on Applications, Technologies, Architectures, and Protocols for Computer Communication*, ser. SIGCOMM '00. Stockholm, Sweden: ACM, August 2000, pp. 151–160.

[162] P. Mahadevan, P. Sharma, S. Banerjee, and P. Ranganathan, "A power benchmarking framework for network devices," in *NETWORKING 2009*. Springer, May 2009, pp. 795–808.

[163] P. Reviriego, V. Sivaraman, Z. Zhao, J. Maestro, A. Vishwanath, A. Sanchez-Macian, and C. Russell, "An energy consumption model for energy efficient ethernet switches," in *High Performance Computing and Simulation (HPCS), 2012 International Conference on*, Madrid, Spain, July 2012, pp. 98–104.

[164] B. Sedighi, J. Li, K.-L. Lee, S. Gambini, H. Chow, and R. Tucker, "Energy-efficient optical links: Optimal launch power," *Photonics Technology Letters, IEEE*, vol. 25, no. 17, pp. 1715–1718, September 2013.

[165] M. Murakami, "Analyzing power consumption in optical cross-connect equipment for future large-capacity optical networks," *Journal of Networks*, vol. 5, no. 11, pp. 1254–1259, November 2010.

[166] A. Vishwanath, F. Jalali, R. Ayre, T. Alpcan, K. Hinton, and R. Tucker, "Energy consumption of interactive cloud-based document processing applications," in *Communications (ICC), 2013 IEEE International Conference on*, Budapest, Hungary, June 2013, pp. 4212–4216.

[167] W. Van Heddeghem, F. Idzikowski, W. Vereecken, D. Colle, M. Pickavet, and P. Demeester, "Power consumption modeling in optical multilayer networks," *Photonic Network Communications*, vol. 24, no. 2, pp. 86–102, October 2012.

[168] L. A. Barroso and U. Hölzle, "The case for energy-proportional computing," *Computer*, no. 12, pp. 33–37, December 2007.

[169] "Cisco IOS network management command reference," White Paper, Cisco, December 2010.

[170] G. Auer et al., "Efficiency Analysis of the Reference Systems, Areas of Improvements and Target Breakdown, Deliverable 2.3, *Energy Aware Radio and*

neTwork tecHnologies (EARTH)," https://bscw.ict-earth.eu/pub/bscw.cgi/d71252/EARTH_WP2_D2.3_v2.pdf, 2010.

[171] J. Hoydis, M. Kobayashi, and M. Debbah, "Green small-cell networks," *Vehicular Technology Magazine, IEEE*, vol. 6, no. 1, pp. 37 –43, March 2011.

[172] "C-RAN the road towards green RAN," http://labs.chinamobile.com/cran/wp-content/uploads/CRAN_white_paper_v2_5_EN.pdf, China Mobile, White Paper, October 2011.

[173] "Energy efficiency analysis of the reference systems, areas of improvements and target breakdown," White Paper, EARTH, January 2012.

[174] Z. Niu, "TANGO: traffic-aware network planning and green operation," *Wireless Communications, IEEE*, vol. 18, no. 5, pp. 25 –29, October 2011.

[175] 3G Americas, "The benefits of SON in LTE," http://www.4gamericas.org/documents/2009_%203GA_LTE_SON_white_paper_12_15_09_Final.pdf, 3G Americas, December 2009.

[176] D. Bertsekas, *Nolinear Programming, 2nd edition*. Belmon, MA: Athena Scientific, September 1999.

[177] L. Xiao, M. Johansson, and S. Boyd, "Simultaneous routing and resource allocation via dual decomposition," *Communications, IEEE Transactions on*, vol. 52, no. 7, pp. 1136–1144, July 2004.

[178] M. Benaim, "A dynamical system approach to stochastic approximations," *SIAM Journal on Control and Optimization*, vol. 34, no. 2, pp. 437–472, 1996.

[179] H. Khalil, *Nonlinear Systems (Third Edition)*. Prentice Hall, December 2001.

[180] "Cisco ASR 5000 series product overview," Cisco, January 2013.

[181] "Ericsson microwave networks portfolio." [Online]. Available: http://www.ericsson.com/ourportfolio/products/microwave-networks

[182] S. Prabhavat, H. Nishiyama, N. Ansari, and N. Kato, "On load distribution over multipath networks," *Communications Surveys Tutorials, IEEE*, vol. 14, no. 3, pp. 662–680, July 2012.

[183] A. Economides and J. Silvester, "Multi-objective routing in integrated services networks: A game theory approach," in *INFOCOM '91. Proceedings. Tenth Annual Joint Conference of the IEEE Computer and Communications Societies. Networking in the 90s., IEEE*, April 1991, pp. 1220–1227 vol.3.

[184] S. Sotiriadis, N. Bessis, and N. Antonopoulos, "Towards inter-cloud schedulers: A survey of meta-scheduling approaches," in *P2P, Parallel, Grid, Cloud and Internet Computing (3PGCIC), 2011 International Conference on*, Barcelona, Spain, October 2011, pp. 59–66.

[185] B. A. Shirazi, K. M. Kavi, and A. R. Hurson, Eds., *Scheduling and Load Balancing in Parallel and Distributed Systems*. Los Alamitos, CA, USA: IEEE Computer Society Press, April 1995.

[186] D. Gross, J. F. Shortle, J. M. Thompson, and C. M. Harris, *Fundamentals of Queueing Theory*, 4th ed. New York, NY, USA: Wiley-Interscience, August 2008.

[187] T. Alpcan, "Noncooperative games for control of networkes systems," Ph.D. dissertation, University of Illinois at Urbana-Champaign, 2006.

[188] A. Beck, A. Nedic, A. Ozdaglar, and M. Teboulle, "Optimal distributed gradient methods for network resource allocation problems," *Submitted for publication*, 2013.

[189] D. Abts, M. R. Marty, P. M. Wells, P. Klausler, and H. Liu, "Energy proportional datacenter networks," *SIGARCH Comput. Archit. News*, vol. 38, no. 3, pp. 338–347, June 2010.

[190] Y. Zhang, P. Chowdhury, M. Tornatore, and B. Mukherjee, "Energy efficiency in telecom optical networks," *Communications Surveys Tutorials, IEEE*, vol. 12, no. 4, pp. 441–458, November 2010.

[191] R. Tucker, "Green optical networking," in *Quantum Electronics Conference Lasers and Electro-Optics (CLEO/IQEC/PACIFIC RIM), 2011*, August 2011, pp. 781–781.

[192] ONF, "Software-defined networking: The new norm for networks," https://www.opennetworking.org/images/stories/downloads/sdn-resources/white-papers/wp-sdn-newnorm.pdf, August 2013.

[193] MININET, "Mininet an instant virtual network on your laptop (or other pc)," http://mininet.org/, 2015.

[194] M. McCauley, "The pox controller," http://www.noxrepo.org/pox/about-pox/.

[195] M. Roughan, A. Greenberg, C. Kalmanek, M. Rumsewicz, J. Yates, and Y. Zhang, "Experience in measuring backbone traffic variability: Models, metrics, measurements and meaning," in *Proceedings of the 2Nd ACM SIGCOMM Workshop on Internet Measurment*, ser. IMW '02. Marseille, France: ACM, November 2002, pp. 91–92.

[196] G. Sakellari, C. Morfopoulou, and E. Gelenbe, "Investigating the tradeoffs between power consumption and quality of service in a backbone network," *Future Internet*, vol. 5, no. 2, pp. 268–281, May 2013.

[197] K. Salchow Jr, "Load balancing 101: The evolution to application delivery controllers," http://www.f5.com/pdf/white-papers/evolution-adc-wp.pdf, F5.

[198] B. Briscoe, A. Brunstrom, A. Petlund, D. Hayes, D. Ros, I.-J. Tsang, S. Gjessing, G. Fairhurst, C. Griwodz, and M. Welzl, "Reducing internet latency: A survey of techniques and their merits," *Communications Surveys Tutorials, IEEE*, vol. PP, no. 99, pp. 1–1, November 2014.

[199] J. Jay, "Low signal latency in optical fiber networks," in *Corning Optical Fiber, Proceedings of the 60th IWCS Conference on*, November 2011, pp. 6 – 9.

[200] SIEMENS, "Latency on a switched ethernet network," http://w3.siemens.com/mcms/industrial-communication/en/rugged-communication/Documents/AN8.pdf.

[201] V. Gropp, "bwm-ng (bandwidth monitor ng)," http://www.gropp.org/?id=projects&sub=bwm-ng.

[202] A. Dixit, F. Hao, S. Mukherjee, T. Lakshman, and R. Kompella, "Towards an elastic distributed SDN controller," in *Proceedings of the Second ACM SIGCOMM Workshop on Hot Topics in Software Defined Networking*, ser. HotSDN '13. Helsinki, Finland: ACM, August 2013, pp. 7–12.

Author/s:
LIN, TAO

Title:
Optimisation of energy efficiency in communication networks

Date:
2015

Persistent Link:
http://hdl.handle.net/11343/56530

File Description:
Optimisation of Energy Efficiency in Communication Networks